REPORT DOCUMENTATION PAGE

Form Approved
OMB No. 0704-0188

1. AGENCY USE ONLY (Leave Blank)	2. REPORT DATE	3. REPORT TYPE AND DATES COVERED
	February 1995	Scientific and Technical Report April 1993 - March 1994

4. TITLE AND SUBTITLE

Surface Towed Ordnance Locator System Scientific and Technical Report

5. FUNDING NUMBERS

6. AUTHOR(S)

7. PERFORMING ORGANIZATION NAME(S) AND ADDRESS(ES)

Naval Explosive Ordnance Disposal Technology Division
Project Manager: Gerard Snyder 301/743-6855
2008 Stump Neck Road
Indian Head, Maryland 20640-5070

8. PERFORMING ORGANIZATION REPORT NUMBER

9. SPONSORING / MONITORING AGENCY NAME(S) AND ADDRESS(ES)

U.S. Army Environmental Center
Project Officer: Kelly Rigano 410/612-6868
SFIM-AEC-ETP
Aberdeen Proving Ground, Maryland 21010-5401

10. SPONSORING / MONITORING AGENCY REPORT NUMBER

SFIM-AEC-ET-CR-95042

11. SUPPLEMENTARY NOTES

Supporting Contractor: PRC, Inc.
801 North Strauss Avenue
Indian Head, Maryland 20640-1807

Contract Number N00600-88-D-3717

12a. DISTRIBUTION / AVAILABILITY STATEMENT	12b. DISTRIBUTION CODE
Unlimited Distribution	"A"

13. ABSTRACT (Maximum 200 words)

This report presents the results of an evaluation of the capabilities and performance of the prototype Surface Towed Ordnance Locator System. The system includes a cesium vapor magnetometer array towed by a man-operated, all-terrain vehicle. Data processing and navigation subsystems are utilized to recognize targets and chart their locations. The evaluation was based on surveys for unexploded ordnance at the Marine Corps Air-Ground Combat Center, Twenty-nine Palms, CA and Jefferson Proving Ground, Madison, IN. The results showed that the Surface Towed Ordnance Locator System is capable of detecting and accurately charting the locations of ferrous targets, but that self-magnetic noise limited the detection capability. Additional efforts are necessary to give the system an ordnance/non-ordnance discrimination capability.

14. SUBJECT TERMS

Navigation, Magnetometer, Search Systems, Unexploded Ordnance

15. NUMBER OF PAGES

16. PRICE CODE

17. SECURITY CLASSIFICATION OF REPORT	18. SECURITY CLASSIFICATION OF THIS PAGE	19. SECURITY CLASSIFICATION OF ABSTRACT	20. LIMITATION OF ABSTRACT
Unclassified	Unclassified	Unclassified	Unlimited

U.S. Army
Environmental
Center

Report No. SFIM-AEC-ET-CR-95042

Surface Towed Ordnance Locator System Scientific and Technical Report

February 1995

Prepared by PRC Inc.

Distribution Unlimited; Approved for Public Release

SURFACE TOWED ORDNANCE LOCATOR SYSTEM SCIENTIFIC AND TECHNICAL REPORT

FEBRUARY 1995

EXECUTIVE SUMMARY

This report presents the results of an evaluation of the capabilities and performance of the prototype Surface Towed Ordnance Locator System (STOLS). The evaluation was based on data obtained during demonstration surveys conducted under operational conditions at the Marine Corps Air-Ground Combat Center (MCAGCC), Twentynine Palms, California, and the Jefferson Proving Ground (JPG), Madison, Indiana.

Public Law 98-212 provided resources for a program to demonstrate and evaluate advanced technologies and systems that can be used to characterize and remediate active and formerly used defense sites. The resulting program was established in June 1993 by the U.S. Army Environmental Center (USAEC), with the U.S. Naval Explosive Ordnance Disposal Technology Division (NAVEODTECHDIV) as the technical lead. The USAEC has tasked the NAVEODTECHDIV to develop and demonstrate advanced technology systems that are capable of detecting, locating, and classifying buried Unexploded Ordnance (UXO).

A prototype of the STOLS was developed for the NAVEODTECHDIV beginning in October 1986 under an advanced technology demonstration contract to Geo-Centers, Inc. The STOLS utilizes an array of seven cesium-vapor, total-field magnetometers, towed by an all-terrain vehicle, to detect and map magnetic anomalies. The magnetometer data collected by STOLS are downloaded to a data processing system in the STOLS Command Center and displayed for the operator in the form of color or gray-scale maps of magnetic field strength. The operator must tag potential UXO on the display for analysis by the STOLS software, which matches the magnetic anomaly to a known set of magnetic signatures. The software estimates the location, size, and depth of the detected anomaly, and provides this information to the user in the form of a target map and a tabular report. During fiscal year 1992, the NAVEODTECHDIV incorporated a differential global positioning system (DGPS) to replace the original microwave navigation system, and upgraded the data analysis system from the original Force minicomputer to a Unix-based, Silicon Graphics Workstation.

The MCAGCC survey, conducted during May and July 1993, covered 50 of the 74 acres of an Ammunition Supply Point (ASP 20B) where future construction plans required characterization of the level of UXO contamination. The NAVEODTECHDIV used the STOLS to detect and map magnetic anomalies and the Marine Corps provided data validation by excavating selected targets. The STOLS identified 1,223 anomalies and 264 were classified as targets. MCAGCC personnel excavated 71 targets to assess the STOLS detection capability, false alarm rate, size and depth prediction, and location accuracy. These 71 targets consisted of 31 ferrous, non-ordnance objects and 40 false alarms where no objects were found. The majority of the false alarms were caused by compacted minerals that produce a magnetic anomaly that disappears when the soil is broken up. The STOLS achieved a mean position accuracy of 1.7 m for targets relocated using the microwave navigation system, and 1.1 m using DGPS navigation. Mean depth accuracy was 0.7 m. No probability of detection could be computed because there was no prior knowledge of targets present at the site. A planned survey of a second site was not accomplished due to a failure of the STOLS data acquisition subsystem.

The JPG survey was conducted in March 1994 on a 40 acre controlled test site being developed for demonstration of ground-based UXO detection, identification, and remediation technologies. The 40 acre site contains controlled targets consisting of inert ordnance, non-ordnance, and debris carefully emplaced at depths and orientations typically found in UXO contaminated areas. The target positions were optically surveyed after emplacement to provide a baseline target set. The STOLS team surveyed 22.5 acres of the 40 acre area during target emplacement operations and identified 76 anomalies. The STOLS achieved an overall probability of detection of 0.08 for small targets, 1.00 for medium targets, and 0.86 for large targets, or 0.48 overall. The STOLS correctly classified the target size 50 percent of the time. Position accuracy was 0.9 m, and depth accuracy was 0.7 m.

The data collected by the STOLS during the two field surveys were subjected to statistical analyses to characterize system noise and detection capabilities and assess the performance of the STOLS technology. Noise in the STOLS data consists of system-induced noise, magnetic background noise, and noise from external magnetic or electromagnetic sources. The average standard deviations for noise in the STOLS data at the MCAGCC and JPG were 29.28 gamma

and 22.15 gamma, respectively. Characterization of system-induced noise revealed significant noise contributions from the sensors and electronics (1.7 to 2.4 gamma), sensor motion as the array is towed over rough terrain (4 gamma), and the STOLS tow vehicle engine (5 to 8 gamma when running). An accepted threshold for good detection capability (95 percent probability of detection) is 10 times the standard deviation for noise, or 221.5 gamma using the STOLS JPG average. Comparison of this threshold to the magnetic signatures of typical ordnance items (60 mm mortar round, 105 mm and 155 mm projectiles) indicates a detection capability for the STOLS of less than 1 m in depth for all three items.

The STOLS was operated for approximately 190 hours during the two surveys. Aside from frequent magnetometer failures, which resulted in degradation of system performance but did not prohibit operation, the STOLS experienced 10 system failures, resulting in approximately 393.5 hours of down time and a mean time between failures of 19 hours. Many of the system failures were attributable to the fact that the prototype system was not sufficiently ruggedized for field operations.

Evaluation of the STOLS performance at the MCAGCC and JPG resulted in the following conclusions:

- The STOLS was incapable of distinguishing between ordnance targets and ferrous debris, including ferrous non-ordnance objects and compacted mineral deposits.

- The current noise levels of the STOLS are too high to detect the desired ordnance (60 mm, 105 mm, and 155 mm shells) to the desired probability of detections and false alarms, and to the maximum penetration depths (2 feet, 8.5 feet, and 12.5 feet, respectively).

- To achieve the desired performance at the maximum penetration depths (155 mm shell at 12.5 feet), the final noise level of the processed output should be 0.3 gamma, which is equivalent to a noise reduction of 37 dB.

- Approximately 90 to 98 percent of the STOLS noise is due to irregular sensor motion in the earth's magnetic field while being towed over the ground. This motion-induced noise is Gaussian in nature.

- The direction of towing introduces a positive or negative shift of 5 gamma dependent on the orientation of the sensors and tow vehicle relative to the earth's magnetic field.

- The current data compression algorithm does not have sufficient dynamic range to handle noisy sensors. It may also distort very strong magnetic signals, which would impair the STOLS ability to characterize the UXO.

- The DGPS navigation system has an absolute positioning accuracy to within 1 m 95 percent of the time. The original microwave navigation system had an absolute positioning accuracy to within 1.7 m 95 percent of the time.

The following recommendations are made to improve the performance of the current STOLS or future systems:

- To reduce the motion induced noise from the magnetometers, three axis accelerometers should be mounted on each sensor in the array and processed with some form of an adaptive noise cancellation technique.

- Techniques to remove the large scale fluctuation in the magnetometers (engine induced, tow direction, background clutter, etc.) should be investigated to further reduce the noise. Some of the techniques could include adaptive mean removal filters, adaptive median filters, two dimensional filters, etc.

- More robust data compression techniques with greater dynamic ranges should be investigated, or the full digitized information should be recorded and stored in uncompressed form.

- Since UXO size and depth primarily determine the strength of the magnetic signature, design goals for future systems should be stated in terms of specific UXO types and maximum penetration depths of interest.

- Since estimation of the size and depth of the ordnance requires accurate calibration of the magnetometer sensor array, techniques for checking the calibration of the magnetometers in the field should be developed.

This page is intentionally left blank

TABLE OF CONTENTS

This page is intentionally left blank

LIST OF FIGURES

LIST OF TABLES

SECTION 1 - INTRODUCTION

1.1 Objective

This report presents the results of an evaluation of the capabilities and performance of the prototype Surface Towed Ordnance Locator System (STOLS) in an operational environment. The evaluation covered all aspects of the STOLS technology demonstrated during two field surveys. The first survey was a joint project conducted in 1993 by the Naval Explosive Ordnance Disposal Technology Division (NAVEODTECHDIV) and the Marine Corps Air-Ground Combat Center (MCAGCC) at Twentynine Palms, California. The second survey was a project conducted in 1994 at a controlled test site then being developed by the NAVEODTECHDIV at Jefferson Proving Ground (JPG), Madison, Indiana.

1.2 Background

The NAVEODTECHDIV, in support of the U.S. Army Environmental Center (USAEC), conducts demonstrations of advanced technology systems for the detection of buried ordnance. Public Law 98-212 provided resources to the DoD for environmental restoration programs to clear military ranges and other areas contaminated with unexploded ordnance (UXO) and related hazardous materials. The U.S. Army Corps of Engineers, as the cognizant DoD activity, requested that the NAVEODTECHDIV develop and demonstrate advanced technology systems capable of detecting, locating, and classifying buried UXO.

Design and development of the STOLS began in October 1986 under a NAVEODTECHDIV Advanced Technology Demonstration (ATD) contract with Geo-Centers, Inc., of Newton Centre, Massachusetts. The goal of the STOLS ATD project was to develop a magnetometer-based survey system that could rapidly search large areas. Computer-aided sensor data analysis would be used to improve detection probabilities and determine the positions of anomalies. The initial system configuration was approved on 17 February 1987 and consisted of a tow vehicle, towed sensor platform, navigation subsystem, and data processing center.

The contractor conducted initial field trial and integration tests in June 1988, and acceptance tests in August 1988, at Ft. Devens, Massachusetts. In September 1988, the contractor delivered the STOLS prototype to the NAVEODTECHDIV, where additional tests of hardware and software were completed at the Magnetometer Test Range (MTR). These tests showed the utility of conducting a rapid magnetometer search and then remediating targets based on position data. The NAVEODTECHDIV conducted a system demonstration for the U.S. Army Corps of Engineers in April 1989, and performed field tests at the MCAGCC, Twentynine Palms, in June and December 1989. From January through September 1990, the NAVEODTECHDIV conducted field exercises to evaluate upgrades, perform system stress tests, and validate equipment manual data. These exercises introduced wear and tear on the STOLS hardware. The advent of differential Global Positioning System (DGPS) and advancements in computer technology led to a program to improve STOLS subsystem performance.

1.3 Report Organization

Section 2 of this report describes the prototype STOLS demonstrated during the MCAGCC and JPG surveys. Section 3 documents the methods, assumptions, and procedures used in the evaluation of the STOLS technology. Section 4 contains the results of the evaluation, including both survey data and system performance data. Section 5 provides further analyses of the data contained in Section 4. Section 6 presents conclusions related to the project objective defined above. Section 7 lists documents referenced in the text of sections 2 through 6. The appendices contain detailed survey data and a description of the analysis methodology.

SECTION 2 - STOLS SYSTEM DESCRIPTION

2.1 System Function

The STOLS is a prototype system capable of surveying large areas contaminated with UXO at a rate of up to 15 acres per day by detecting, locating, and categorizing magnetic anomalies up to 4.5 m deep (reference 1). The STOLS uses an array of seven cesium vapor, total field magnetometers mounted on a platform that is towed by an all terrain vehicle (see Figure 1). The STOLS Tow Vehicle (STV) houses a data collection subsystem and a position-fixing navigation subsystem, either microwave or DGPS. The sensor and navigation data stored on the STV is periodically transferred to the command center computer. That computer, a graphics workstation, processes the data to estimate each anomaly's relative size (i.e., small, medium, or large), depth (to within 0.5 m), and location (to within 1.0 m). The processed data is then presented, in both graphic and tabular form, as target maps and target tables.

2.2 STOLS Subsystems

2.2.1 **Tow Vehicle.** The STV is a Recreative Industries Buffalo Max II six-wheel, all terrain vehicle, modified so it has a low magnetic signature (see figure 2). Modifications included retrofitting the STV with stainless steel frame, axles, wheels, nuts, bolts, and washers. The vehicle serves as a platform for the data acquisition system, navigational equipment, and power supply.

2.2.2 **Tow Platform.** The STOLS tow platform (STP) is a four-wheel tandem trailer that serves as a platform for the sensors, cables, and compass (see figure 3). It is constructed of aluminum, brass, fiberglass, and stainless steel to produce a low magnetic signature. The STP supports a magnetometer array, an electronic compass, a cable junction box, and a breakaway system to protect the outboard magnetometers.

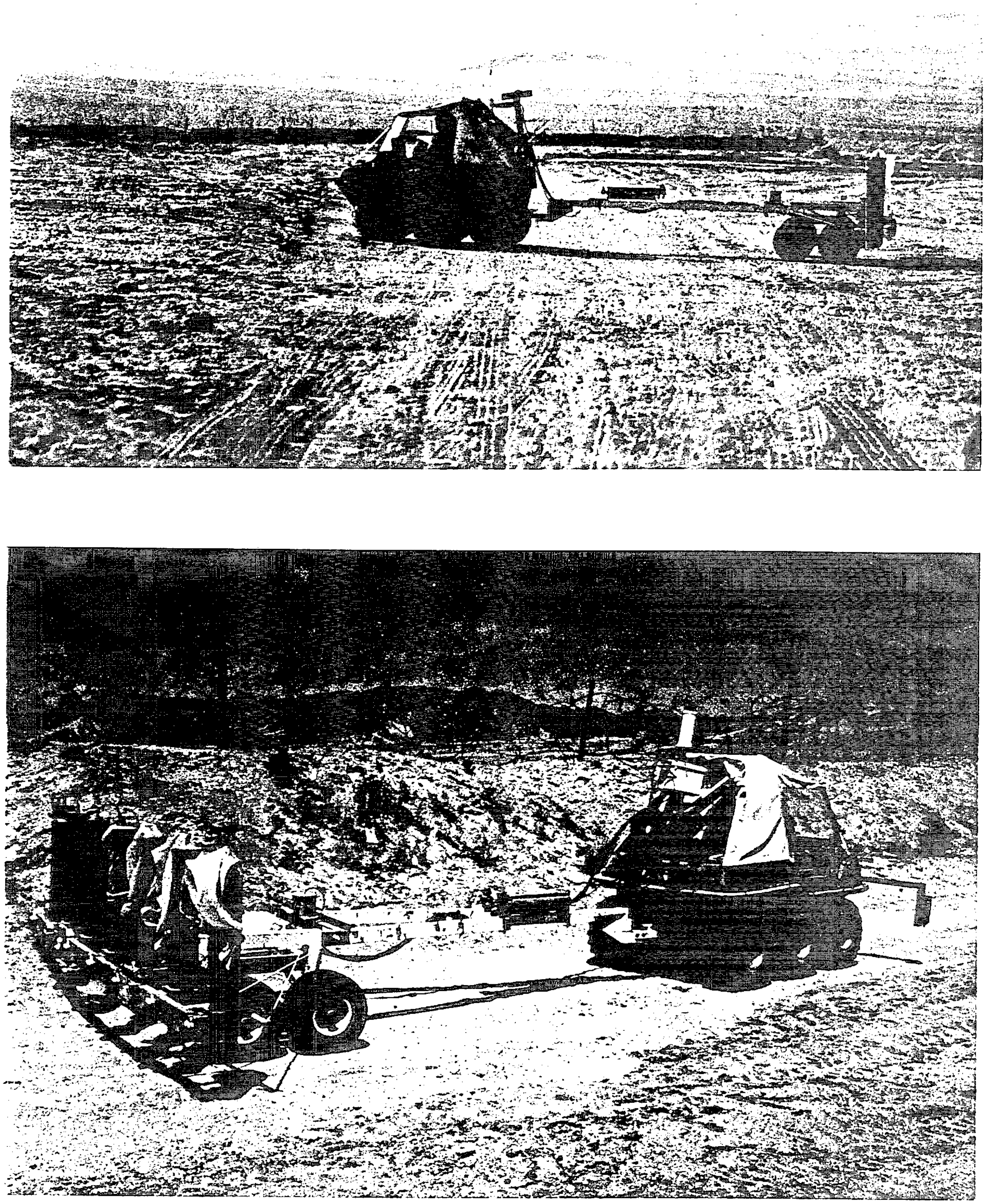

Figure 1. Surface Towed Ordnance Locator System (STOLS)

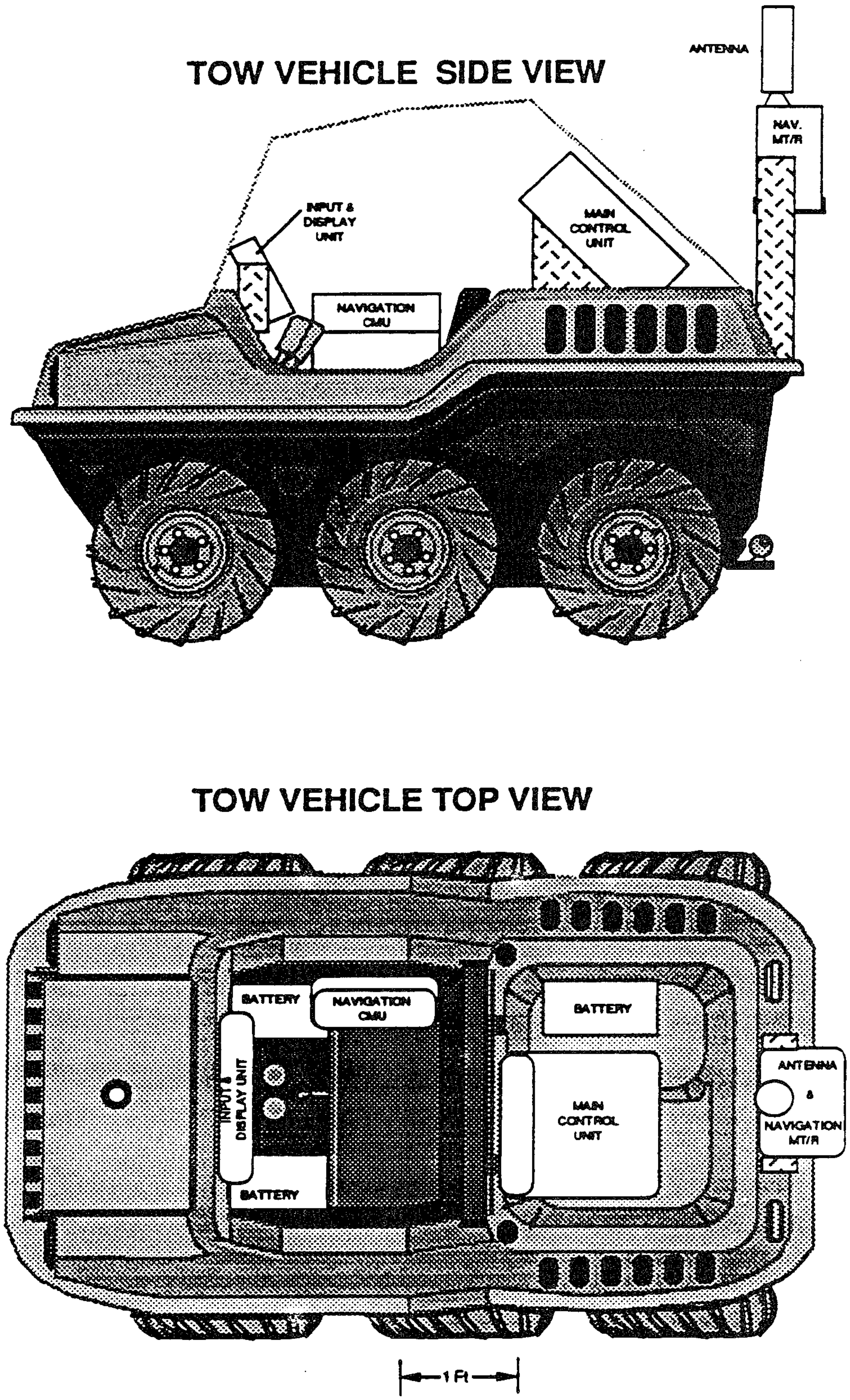

MICROWAVE NAVIGATION CONFIGURATION

Figure 2. STOLS Tow Vehicle (Sheet 1 of 2)

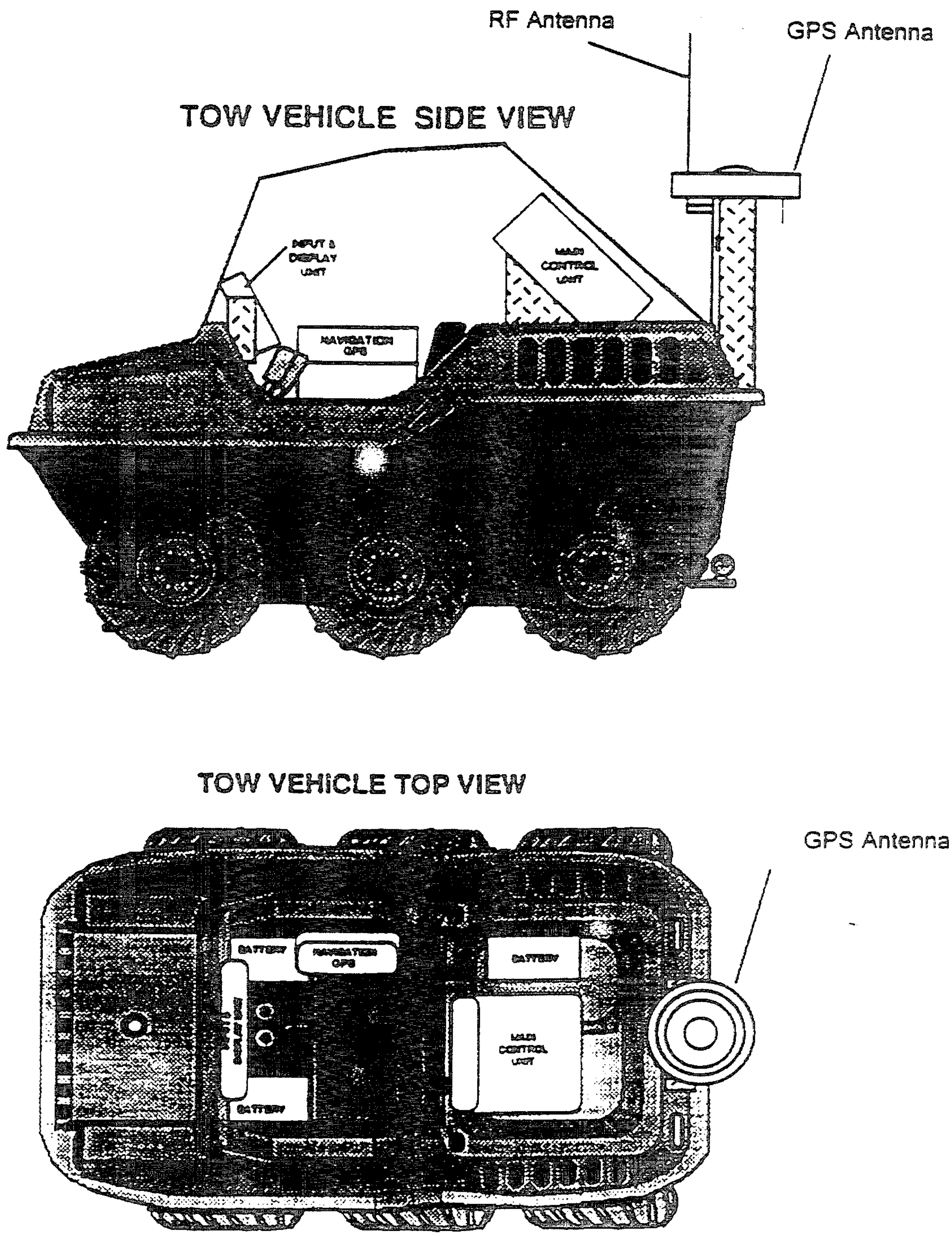

DGPS NAVIGATION CONFIGURATION

Figure 2. STOLS Tow Vehicle (Sheet 2)

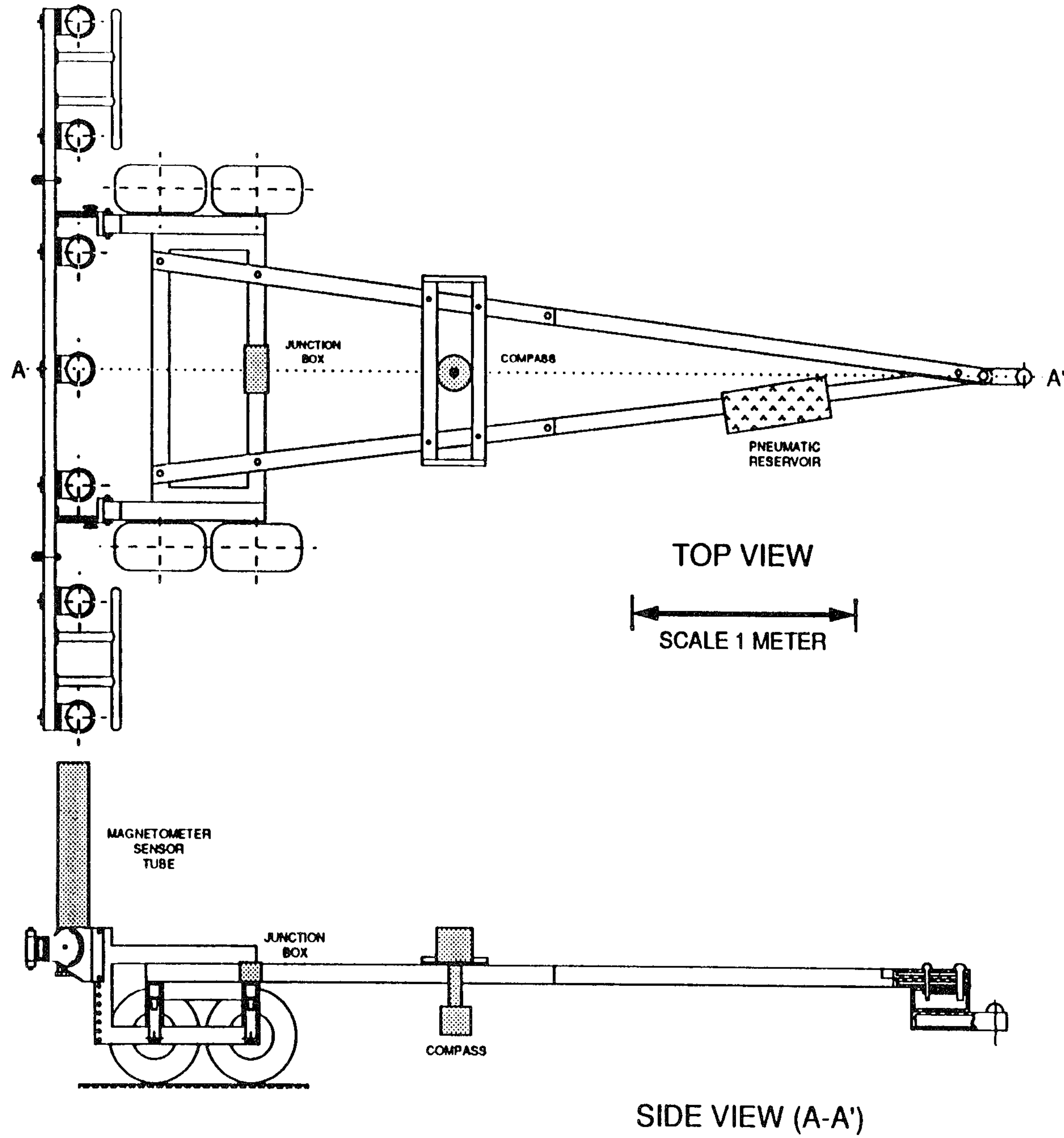

Figure 3. STOLS Towed Platform

2.2.3 **Sensors.** Seven Scintrex Model VIW2321J1 cesium vapor total field magnetometers serve as the magnetic field sensors on the STOLS. These magnetometers measure the total field over the range 20,000 to 100,000 gamma with an accuracy of $\pm$ 0.1 gamma. The VIW2321J1 is a special order ultra-low magnetic signature (0.1 gamma at 0.1 m) magnetometer specifically designed for simultaneous operation in close proximity to other magnetometers in the seven sensor array (see figure 4). The array can be set to various heights between 6 inches and 18 inches above the ground.

A separate remote cesium vapor total field magnetometer (see figure 5) records the earth's local magnetic field once per second for use as a background reference in data processing. Time tagging is used to correlate data from the reference magnetometer with the sensor platform data. Diurnal variations of the earth's magnetic field are removed from the sensor platform data during data processing.

2.2.4 **Data Acquisition System.** The data acquisition system consists of the Main Control Unit (MCU) and Input and Display Unit (IDU) mounted on the STV, and a portable battery-operated storage device, referred to as a data mop, used to download survey data periodically during a mission.

The MCU contains a microprocessor that serves as the master controller for the STV and STP systems, and 8 megabytes of dynamic random access memory (RAM) used to store data from the magnetometers, compass, and navigation system. Magnetometer data is recorded at 20 Hz for each sensor; navigation data is recorded at 1 Hz. The RAM can store up to 4.5 hours of survey data before downloading is required. An internal battery can maintain the data in the volatile RAM for up to 2.5 hours in case of STV main battery failure. The MCU front panel includes a data cartridge slot for uploading reference magnetometer data, and a data transfer port for downloading survey data into the data mop. The MCU front panel also contains circuit breaker switches and indicators for control of power to the sensor and navigation systems.

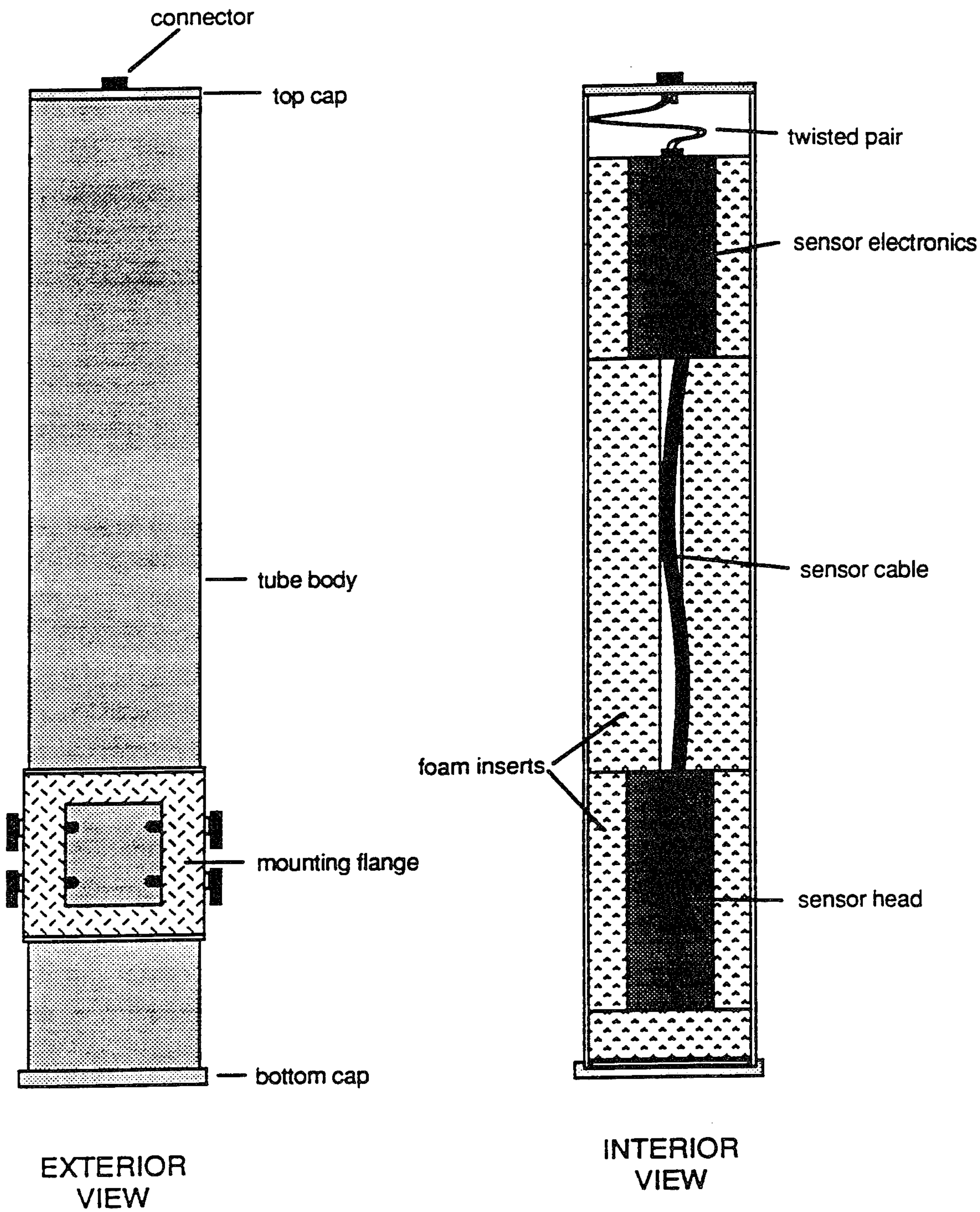

Figure 4. STOLS Sensor

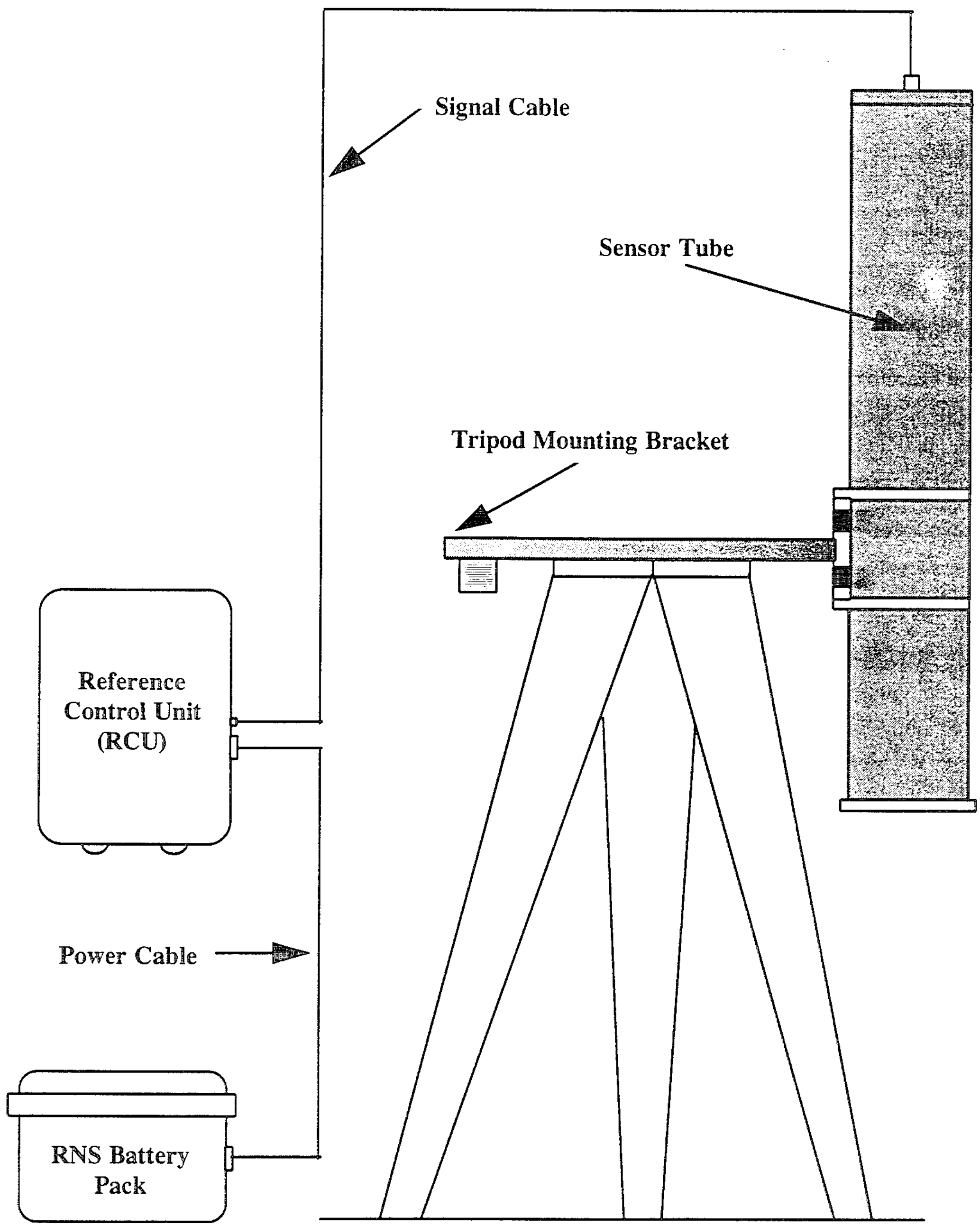

Figure 5. Reference Sensor

The IDU provides the operator interface for the data acquisition system. The IDU front panel includes a display for track and guidance information, system condition/failure indicators (trouble lights and an audible alarm), and a system control keypad and message display. The IDU is controlled by a microprocessor slaved to the master controller in the MCU.

The data mop is a hand-held device connected to the data transfer port on the MCU front panel and an I/O port on the laptop PC by umbilical cables during survey data download operations. All data mop operations are controlled from the laptop PC.

2.2.5 **Navigation System.** The STOLS is capable of using either a RACAL Microwave Navigation System or a NOVATEL Differential Global Position System (DGPS).

RACAL Microwave Navigation System. The RACAL system is a range-range microwave navigation system that operates at 5 Ghz. It consists of four remote navigation beacons deployed in known positions around the survey area and a master transmitter/receiver (T/R) on the STV (see figure 6). Each remote beacon T/R is a stand-alone station that operates on battery power. The master T/R on the STV must maintain line-of-sight to at least three remote beacons in order to compute an accurate position (nominally 1 m to 2 m). This requirement restricts the use of the RACAL system to sites where topography, foliage, and other obstructions do not interfere with line-of-sight operations.

NOVATEL DGPS Navigation System. The NOVATEL DGPS relies on the NAVSTAR Global Positioning System (GPS) satellite navigation system developed by the GPS Joint Program Office. The NOVATEL DGPS uses a differential mode of operation that requires a stationary remote GPS base station and a mobile GPS station on the STV (see figure 7). The base station is powered by a small Honda generator. Both the stationary and mobile GPS receivers require line-of-sight visibility to at least four satellites of the overhead NAVSTAR constellation. An Esteem Model 96F VHF wireless modem transmits GPS data from the remote station to the mobile station, allowing the mobile station to remove much of the error associated with

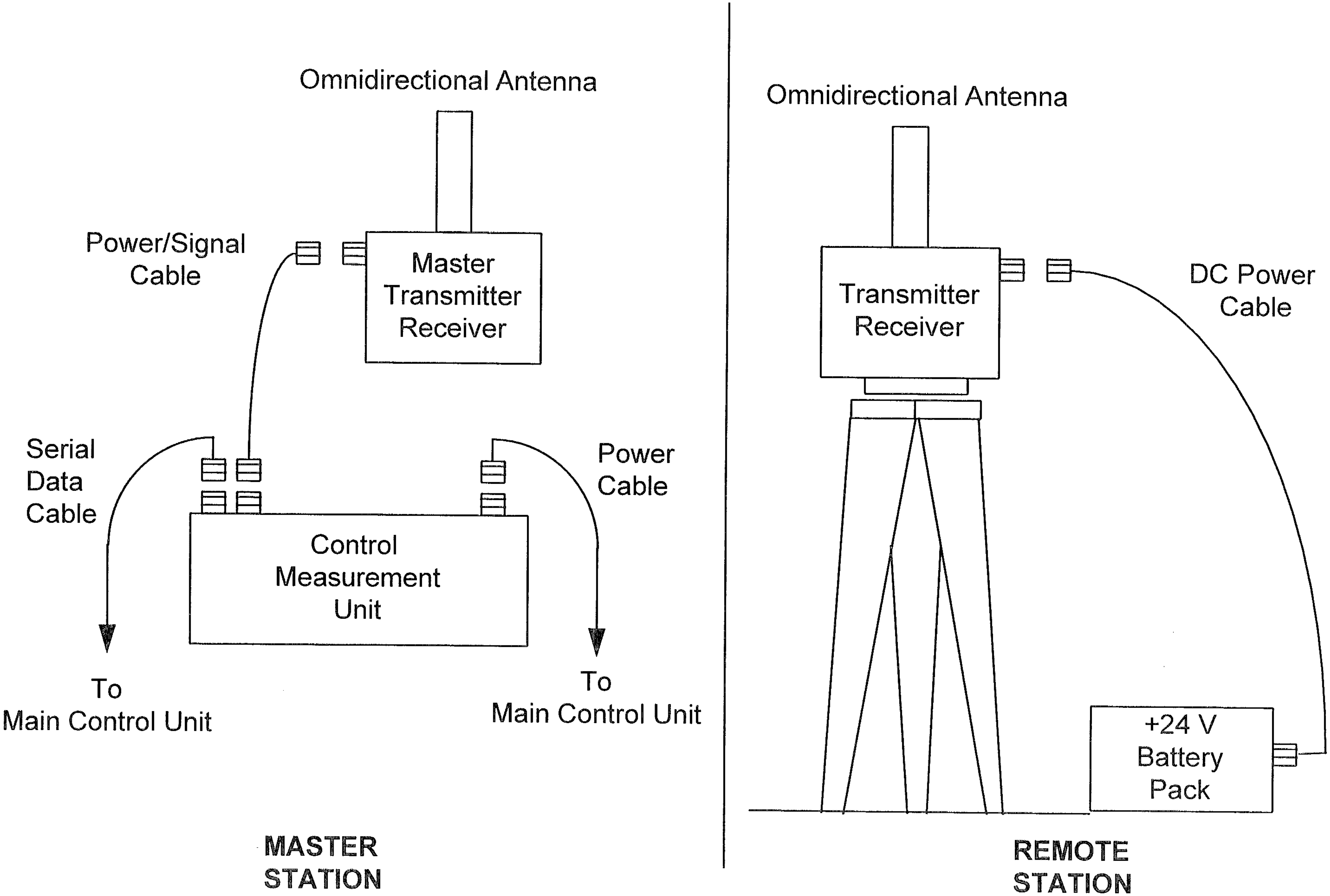

Figure 6. Microwave Navigation System

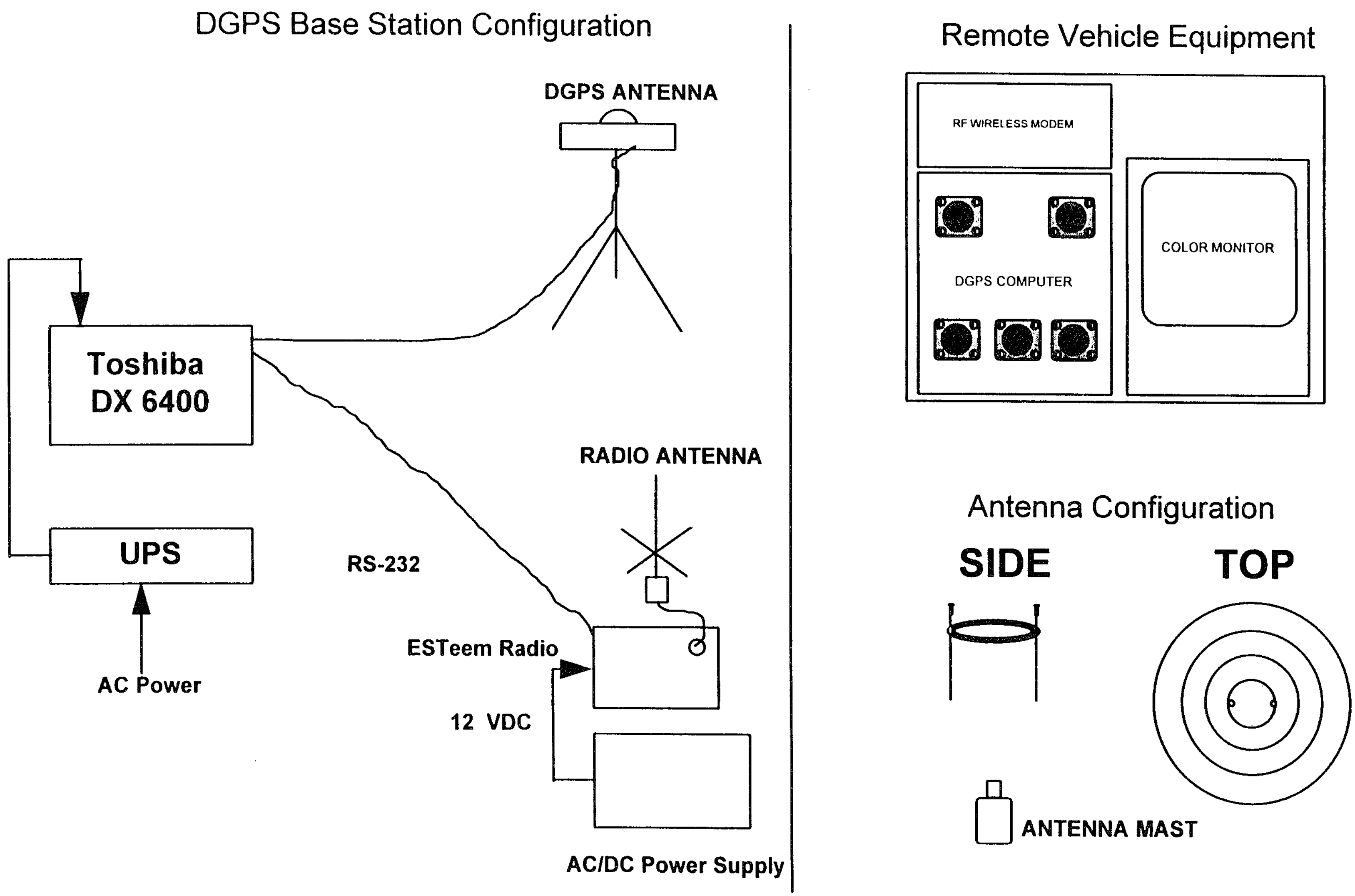

Figure 7. DGPS System

standard (autonomous C/A Code) GPS positioning. This approach reduces position error from 100 m (with Selective Availability on) to approximately 1 m. The NOVATEL DGPS provides geodetic positions in Universal Transverse Mercator (UTM) grid coordinates for compatibility with STOLS data processing. This system is suitable for any site where foliage and topographic features do not limit satellite visibility.

2.2.6 **Data Processing System.** The data processing system includes a Silicon Graphics IRIS Indigo workstation, Hewlett Packard Laserjet printer, Seiko CH034 color printer, power line conditioner, and an uninterruptable power supply. The workstation contains 64 megabytes of RAM, two 1.2 gigabyte hard drives, internal tape and 3.5 inch diskette drives, external QIC 150 megabyte tape drive, external CD-ROM drive, and a 19 inch color monitor and operates at 33 Mhz.

2.2.7 **STOLS Command Center.** The STOLS command center (SCC), which doubles as the system transport trailer, is partitioned into two work areas (see figure 8). The area in the front of the trailer contains the data processing system and office workspace. The rear area is a workshop/storage space for STOLS maintenance and tool/equipment storage and transportation. The end of the trailer has a fold-down gate for loading/unloading STOLS equipment.

2.3 STOLS Procedures

2.3.1 **Mission Planning.** Prior to starting a STOLS survey of a potentially UXO-contaminated area, survey personnel visit the area to conduct a site assessment, identify local regulations and operating procedures, and arrange local logistical support.

Site assessment includes identification of relevant site characteristics, including site boundaries, benchmarks, landmarks, topography, geology, environmental data, weather, historical uses of the site, and the types of ordnance and other items that may have been stored or used there.

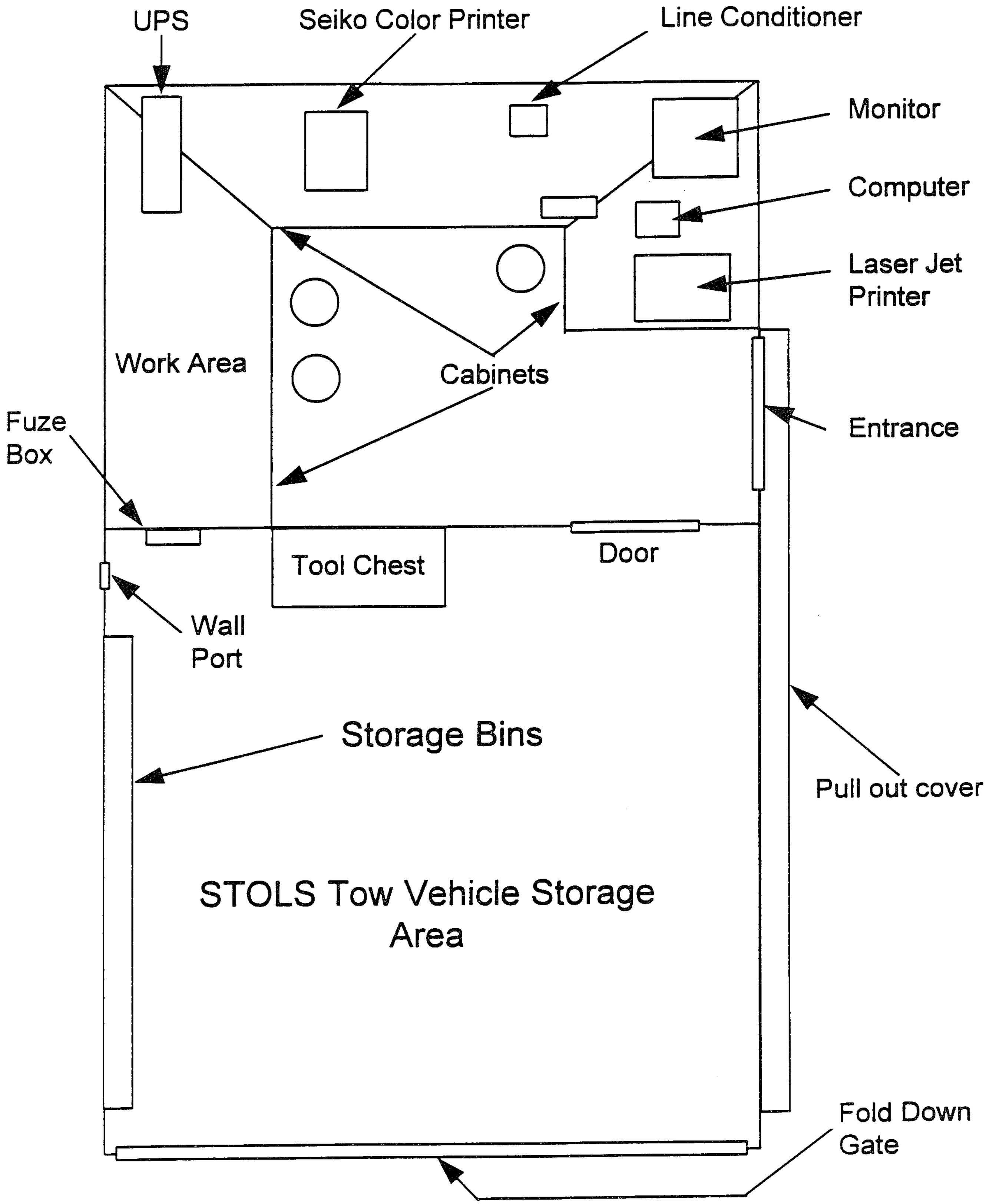

Figure 8. STOLS Command Center

During the pre-survey visit, survey personnel also contact administrative, environmental, EOD, safety, security, and medical personnel at the local command or activity, and receive from them local directives, regulations, and procedures applicable to survey operations.

Based on the data compiled during the pre-survey site visit, an Operational Plan, a Safety, Health, and Emergency Response Plan (SHERP), and a Site Assessment Report are prepared. These documents define the survey objective, establish procedures that will be followed during survey operations, and document the site characteristics.

2.3.2 **Site Setup.** Prior to commencing survey operations, the SCC must be prepared for operation in a staging area outside the boundaries of the survey area. The STV and STP must undergo inspection, self-test, and servicing as specified in the STOLS Operation and Maintenance Manual (ref. 1). The Reference Sensor must be set up in a "magnetically quiet" area, and the reference station(s) for the navigation system must be set up as follows:

(1) **Microwave Navigation System.** Four beacon transmitter/receivers must be set up outside the survey boundaries in either a box or L-shaped pattern. Beacons must be located so that at least three will be in a direct line-of-sight from the master transmitter/receiver on the STV from every point inside the survey area.

(2) **DGPS System.** A single DGPS base station must be set up at or near the site, preferably directly over a U.S. Geological Survey (USGS) or Defense Mapping Agency (DMA) monument.

The command center system operator must also run a site setup routine on the computer. The setup routine is used to identify the survey site and the magnetometer array height setting to be used. The STOLS software creates an artificial grid over the survey area based on 45 m by 45 m (approximately 1/2 acre) quadrants. The software partitions the survey site into missions, which represent the maximum survey area that can be processed by the computer at one time (up to 20 acres), and sections, which consist of 10 quadrants.

2.3.3 **Survey Procedure.** A survey is performed by driving the STV along parallel tracks until 100 percent of the area is covered. The magnetometer array covers a 3 m wide swath. If the surface conditions at the site do not result in visible STV tracks, then the vehicle's tracks must be marked with paint, flags, or stakes. The preferred orientation of the traverse lines is north-south.

2.3.4 **Data Collection.** During the survey, magnetometer data from the sensor array and position data from the on-board navigation system are recorded in the volatile solid-state memory of the MCU. Magnetometer data is acquired at 20 Hz and stored in individual data records, each record containing the data collected from one magnetometer in 1 second. Navigation data is recorded at 1 Hz. In order to increase effective storage capacity, magnetometer data is compressed using a standard delta compression technique. The first two bytes of each record contain an actual magnetic field amplitude reading, but the next 19 bytes contain only the amplitude differences (delta) between the next 19 readings and the first reading.

Data initially stored in volatile solid state memory is periodically (every 2 hours) downloaded to the data mop. The data is then transferred into a laptop PC and uploaded into the STOLS data processing workstation. Vehicle File Test (VFT) software in the laptop PC can be used to perform a quick-look analysis of the data to determine whether any areas were missed. A block diagram of STOLS data acquisition and processing is shown in figure 9.

2.3.5 **Data Processing.** After the unprocessed data from the sensor and navigation systems are uploaded to the command center Silicon Graphics workstation, the STOLS data processing system uses the magnetometer and position data to generate either a color or gray scale raster image of the area surveyed. The image is displayed within a 45 m by 45 m grid. The images are keyed to the field strength of magnetic anomalies, which are variations from the local magnetic reference caused by ferrous objects modifying the local earth's magnetic field. The color, or gray scale, of the display is used to indicate the magnitude and polarity of the variation, with blue (or darkest gray) representing the largest negative variation, and red (or

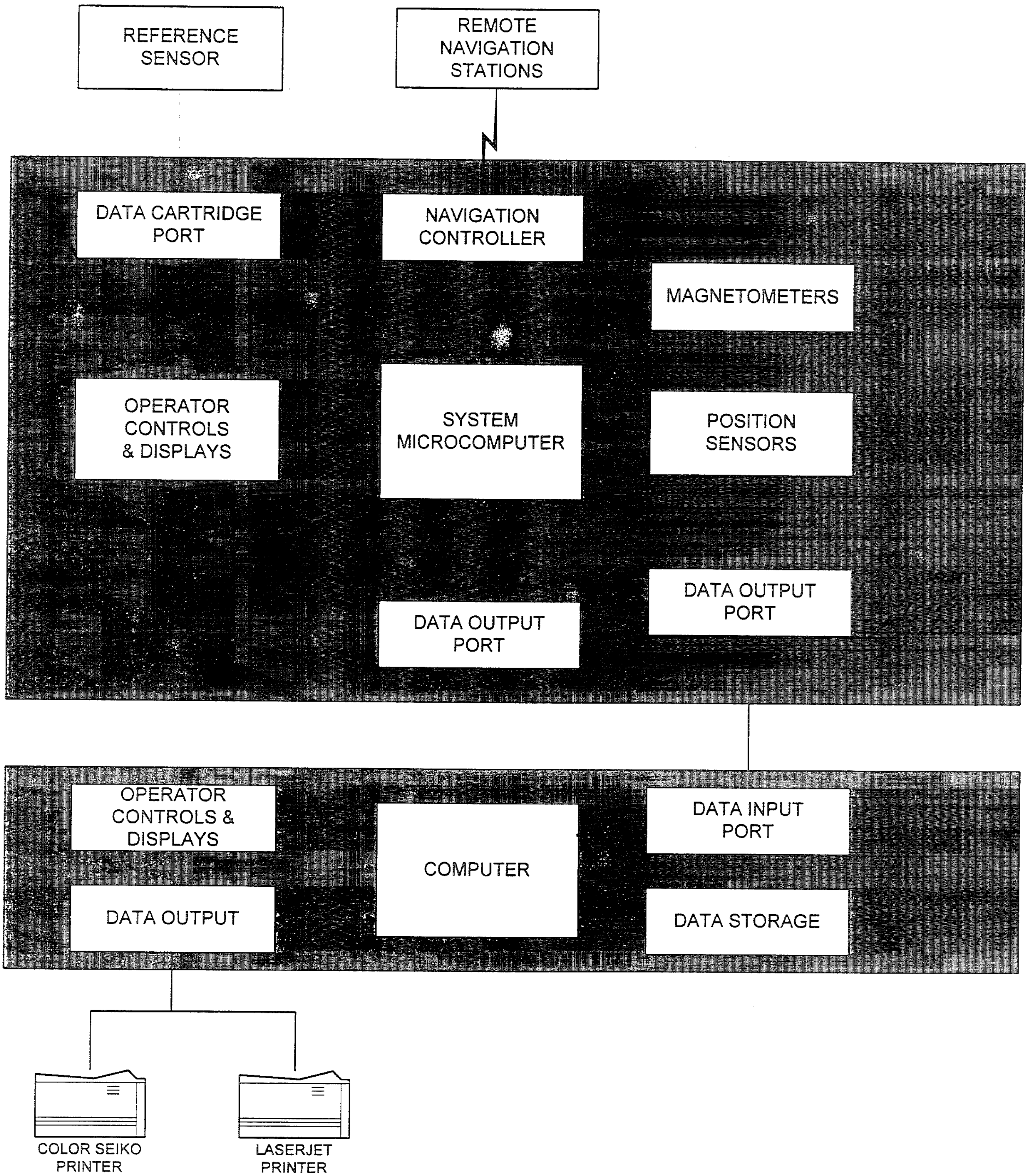

Figure 9. Data Acquisition/Processing Block Diagram

lightest gray) representing the largest positive variation. Thus a ferrous object that forms a magnetic dipole would appear as adjacent blue and red (or light and dark) anomalies. Missed areas (areas not surveyed) appear in the background color.

Preliminary evaluation of the magnetic anomalies is performed by the system operator. The operator selects an intensity threshold based on background noise and/or target signature, then visually identifies potential targets and marks them on the display with an "area of interest" box. The potential targets selected by the operator are then processed by the STOLS software using three algorithms to determine the size (small, medium, or large), depth, and grid location of the detected anomaly. Targets classified as small are the size of an 81 mm mortar shell or smaller. A medium target varies in size from the 81 mm mortar shell to a 250 pound bomb, and large targets are anything larger than a 250 pound bomb. Computer aided classification helps the operator estimate the depth, size, and location of detected anomalies.

A depth algorithm provides an estimate of the depth of the target. This algorithm assumes that the depth of a dipole target is approximately equal to the width of the magnetic anomaly at half its maximum level, as measured along a straight line between its poles. This rule of thumb is referred to as the "full-width-half-maximum" algorithm. Another algorithm, developed specifically for the STOLS application, uses mathematical curve fitting to establish a model match based on the 14 models (known ordnance magnetic signatures) in the processor. The curve fitting technique used by the STOLS software is based on a form of the least-squares regression method. Finally, a third algorithm calculates target location taking into account the magnitude and inclination of the earth's magnetic field at the target's position. The processed target data is displayed for operator approval as small, medium, or large. If the STOLS software is unable to converge on a reliable estimate, the target is displayed with a "?" (for unknown). The operator may accept the target classification assigned by the software, or cancel it and reprocess the data.

2.4 STOLS Data Output

When target analysis is completed, the computer builds a report file of "detected, localized, and classified targets." The file includes the following information about each target:

(1) Target ID number

(2) Quadrant the item is located in

(3) X/Y or UTM coordinates of the target

(4) Estimated target depth, in meters

(5) Target size classification (small, medium, large, or undetermined)

(6) Any comments that were entered by the system operator

The STOLS is also capable of producing output data in the form of raster image maps. The maps may be printed in full color or gray-scale images similar to the displays generated during data processing. The STOLS software can produce a site map (which shows the site boundaries, mission areas, and landmarks overlaid with the software-generated grid), missed area maps (which highlight unsurveyed areas), and target maps (which show the magnetic anomalies detected by STOLS during the survey). Target maps may be produced at a variety of scales, with the data scaled to fit the entire site, a single mission, a single section, or a single quadrant on a letter-size page. The software can also produce a beacon map showing the locations of beacon T/Rs if the microwave navigation system is being used.

For examples of the STOLS data output products, refer to the MCAGCC and JPG survey data in Appendices A and B.

SECTION 3 - TECHNICAL APPROACH

3.1 Surveys

The prototype STOLS technology was demonstrated during surveys conducted at two separate locations. During each survey, STOLS sensor data was collected and processed, and system performance data was recorded. The data collected during the surveys was the basis for evaluation of the STOLS technology.

3.1.1 **MCAGCC Survey.** The MCAGCC survey (reference 2) was performed with the dual purpose of evaluating STOLS performance and assessing the level of UXO contamination at a proposed construction site. The MCAGCC is located in southern California approximately 138 miles east of Los Angeles. The survey site consisted of two ordnance/ammunition storage sites, designated Ammunition Supply Points (ASPs) 20A and 20B, that had been in use since 1976. Site conditions were typical of those found in the desert southwest; that is, relatively flat terrain with sandy soil, sparse vegetation, and a hot, dry climate. Detailed site descriptions and characteristics are contained in appendix A. The STOLS sensor array was set at the "A" (lowest) setting during the first MCAGCC survey period to facilitate detection of individual small arms (20 mm) targets. The objective was to locate, identify, and mark all potential UXO of 20 mm diameter and larger. The minimum target size changed as the survey progressed, first to targets larger than a 60 mm mortar, and then to 105 mm rounds and larger or smaller targets located deeper than 1 m. These changes were dictated by operational considerations and the high magnetic field background noise at the site. An additional parameter in the MCAGCC survey was the navigation system used to determine target position. Both microwave and DGPS navigation systems were used to determine comparative navigation accuracies for target reacquisition.

3.1.2 **JPG Survey.** The JPG survey (reference 3) was performed with the dual purpose of evaluating STOLS performance and characterizing a controlled test area to be used for advanced technology demonstrations of ground-based systems. The JPG is located in southeastern

Indiana approximately 65 miles southeast of Indianapolis. The survey area consisted of 40 acres of indeterminate historical usage. Existing records indicated that the site had not been used as a firing line, impact range, exercise area, or ordnance/ammunition storage site. Site conditions were typical of those found in the Midwest; that is, rolling, uneven terrain with a thin topsoil over clay subsoil and bedrock; mixed vegetation; and a humid climate with seasonal extreme temperatures. Detailed site descriptions and characteristics are contained in appendix B. The STOLS sensor array was set at the "D" setting (next to the highest) during the JPG survey period to reduce the effects of ferrous surface clutter noise. The objective was to detect, locate, and classify inert ordnance targets that had been emplaced as controlled targets, and to characterize the site after target emplacement and prior to the start of advanced technology demonstrations. Emplaced inert ordnance ranged from 20 mm rounds emplaced in patterns or clusters, up to 2,000 pound bombs. The DGPS navigation system was used during the JPG survey.

3.2 Target Data Processing

Data processing and target analysis were performed concurrent with surveying operations. All survey data was collected, processed, and stored at the site using the command center workstation and standard STOLS procedures as described in paragraphs 2.3.4 and 2.3.5. Target analyses were performed after each mission to produce target and missed area maps and a target list that showed the estimated position (in UTM coordinates), depth, and size (small, medium, large, or undetermined) of each detected target.

3.3 Performance Analyses

The data collected during the surveys were subjected to additional analyses in order to provide a means of assessing the system's capabilities, limitations, and performance in operational situations. Three sets of analysis criteria were used in evaluating STOLS performance: operational availability, mission effectiveness, and detection capability. These criteria are defined in the following paragraphs.

3.3.1 **Availability.** Operational availability (A_o) is a measure of the percentage of time a system is capable of performing its intended mission, and includes scheduled and corrective

maintenance "down time" and administrative and logistic delays. Operational availability is a realistic prediction of the level of system readiness that will be experienced by field users of the system. However, because STOLS was a prototype system, statistical availability calculations would not be appropriate. Other assessments were conducted in the form of evaluations of demonstrated reliability, maintainability, and human factors characteristics of the system.

3.3.2 **Mission Effectiveness.** The primary mission of the STOLS is to detect, locate, and classify UXO. The following measures of effectiveness were developed to assess STOLS performance, capabilities, and limitations in accomplishing that mission:

a. **Detection Ratio.** The detection ratio (P_D) is the ratio of the number of targets detected by the system to the total number of targets within the area surveyed. This ratio is representative of the system's overall detection capability.

b. **Classification Ratio.** The classification ratio (P_{Size}) is the ratio of the detected targets correctly classified by size to the total number of detected targets of that size. The ratio can be calculated for each of the target size classifications (small, medium, and large). This ratio is representative of the system's ability to discriminate between targets of various sizes.

c. **Position Accuracy.** Position accuracy is the average distance between a detected target's position (referenced to its center of mass) and the position estimated by STOLS. Location accuracy is calculated for the horizontal position and depth accuracy for the target depth. A probable detection radius was also calculated. This radius is the radius from the STOLS position for a detected target that contains the actual or surveyed target center of mass 95 percent of the time. Position accuracy is representative of the composite precision of the sensors, navigation system, and target analysis software.

Application of the measures of effectiveness differed for the MCAGCC and JPG because of the nature of the two surveys. All targets identified at the MCAGCC were unknowns, and a

limited number of the detected targets, those judged by the NAVEODTECHDIV as the most likely to be UXO, were investigated by excavation. The target positions were relocated using the STOLS, and the measured distance between the STOLS position and the actual position of the excavated target was the position accuracy. The excavated targets became the baseline target set for the measures of effectiveness. At JPG, the controlled targets that had been emplaced at the time of the STOLS survey made up the baseline target set. These were known inert ordnance items with accurately surveyed X-Y coordinates and depths. Location and depth accuracies were determined by calculating the difference between the surveyed UTM coordinates and depths and those estimated by the STOLS.

3.3.3 **Detection Capability.** In order to assess the inherent detection capability of the STOLS prototype, statistical analyses of the raw magnetometer data were performed. The data from each of the seven magnetometers in the array were plotted on a raster time scale and evaluated by inspection to identify and eliminate any non-functioning or malfunctioning magnetometers and other obvious anomalies; those data were excluded from the statistical analyses to prevent contamination of the analysis results. The means of the ambient noise were removed from the magnetometer data in the raster plots and in subsequent analyses. To obtain reasonable noise estimates, a preliminary mean and standard deviation from each magnetometer were computed. Signals whose levels were greater than ± 2 standard deviations from the mean were truncated at ± 2 standard deviations. Final estimates of the mean and standard deviation were then computed from the magnetometer data. The magnetometer noise data were then analyzed for frequency content and coherence between sensors to determine possible sources, such as magnetic background noise characteristic of the survey area, magnetic or electronic noise inherent in the STOLS sensors or other system hardware, ambient electromagnetic interference (EMI), and artificial noise created by the STOLS sensor data compression technique. The results from these analyses were compared to three-dimensional models of the magnetic anomalies created by 60 mm, 105 mm, and 155 mm projectiles to assess the probable detection capability and range of the prototype STOLS system. A detailed discussion of the analysis methodology is contained in appendix C.

SECTION 4 - RESULTS

4.1 Survey Results

4.1.1 **MCAGCC Survey.** The MCAGCC survey was broken into two survey periods because of training exercises scheduled for the survey area. Surveys were conducted from 14 to 26 May 1993 and 19 July to 2 August 1993 at ASP 20B. The survey covered 50 of the 74 acres of ASP 20B. The STOLS detected a total of 1,223 magnetic anomalies, and 264 of these were picked out by the system operator and marked for further processing and target analysis. The microwave navigation system was used to mark 36 targets for investigation. All 36 were excavated, finding no UXO and 20 ferrous (non-ordnance) objects such as metal stakes, wire, and Marsden matting. For the remaining targets excavated no objects were found; these targets were believed to be compacted hematite and limonite. When compacted, these minerals cause a magnetic anomaly that disappears when the soil is broken up. During the second survey period, the DGPS navigation system was used to mark 72 previously detected targets. Only 50 were selected for investigation; the remainder were located in high-traffic/road areas and were assumed to be mineral concentrations. EOD personnel excavated 35 targets, finding no ordnance and 11 ferrous objects. The remaining targets consisted of compacted mineral deposits. Appendix A contains the detailed survey results, including the target lists, target maps, and missed area maps for the MCAGCC survey.

4.1.2 **JPG Survey.** The STOLS survey at JPG was conducted from 7 to 16 March 1994. The STOLS team surveyed 22.5 acres of the 40 acre ground-based system test area during ordnance emplacement operations. The purpose of the survey was to establish the practicality of a large scale test before demonstrations began. The STOLS survey team independently verified the location of selected targets and confirmed the presence of some of the anomalies found in a prior site characterization survey by the 75th Explosive Ordnance Detachment using hand-held magnetometers. The STOLS survey detected a total of 76 anomalies. Appendix B contains the detailed survey results, including the target lists, target maps, and missed area maps for the JPG survey. Some of the target data has been purposely omitted from this report in order to prevent disclosure of the numbers and locations of emplaced targets at the controlled test site.

4.2 Target Data Analysis Results

A preliminary analysis of the STOLS target data was performed in order to correlate STOLS target data with actual target data. For the MCAGCC survey, the analysis was accomplished using the target validation data from the excavated targets. Tables 1 and 2 list the results of the MCAGCC analysis effort, for targets located with the microwave and DGPS navigation systems, respectively. For the JPG survey, the analysis was accomplished using the target data surveyed and recorded during controlled target emplacement. Table 3 shows the results of a comparison of the STOLS target data from the JPG survey with baseline target data surveyed and recorded for controlled targets.

Table 1. MCAGCC Target Analysis Results using Microwave Navigation

Quadrant No.	Target I.D. No.	STOLS Predicted Size	Object Excavated	STOLS Depth Accuracy (m)	STOLS Location Accuracy (m)
B-13	23	L	Compacted Soil	Undetermined	Undetermined
B-13	12	M	Compacted Soil	Undetermined	Undetermined
B-13	11	L	Engineer Stake	1.4	3.0 from marker
B-13	52	L	Compacted Soil	Undetermined	Undetermined
B-8	262	L	Engineer Stake	1.5	1.0 from marker
C-7	66	L	Engineer Stake	0.8	Kicked up by grader
C-7	64	L	Matting	0	2.0 from marker
C-7	69	L	Matting & 2 Engineer Stakes	0.2	1.5 from marker
D-2	174	L	4 ft X 10 ft Matting	1.2	0.3 from marker
D-7	46	L	Matting & Pylon	0.4	1.5 from marker
D-7	61	Undetermined	Pylon	0.2	4.0 from marker
D-7	63	Undetermined	Engineer Stake	0.8	Under marker
D-7	39	M	Matting	0.2	0.5 from target
D-7	46	L	Matting	0.4	2.0 from marker
D-7	69	L	Conduit	Undetermined	2.0 from marker
D-7	45	Undetermined	Engineer Stake	0.5	1.0 from marker
D-7	44	Undetermined	Pylon	0.6	4.0 from marker
E-7	34	M	Engineer Stake	1.7	5.0 from marker

Table 1. MCAGCC Target Analysis Results using Microwave Navigation (Continued)

Quadrant No.	Target I.D. No.	STOLS Predicted Size	Object Excavated	STOLS Depth Accuracy (m)	STOLS Location Accuracy (m)
G-3	230	L	Engineer Stake	0.4	0.3 from marker
G-3	229	M	Engineer Stake	0.4	0.3 from marker
G-4	232	L	1/3 Engineer Stake	1.0	2.0 from marker
G-4	233	L	Engineer Stake	0.8	0.0 from marker
G-7	29	L	Magnetic Rock	Undetermined	Undetermined
G-7	28	M	Engineer Stake	0.1	1.2 From Marker
H-3	234	M	Compacted Soil	Undetermined	Undetermined
H-3	236	Undetermined	Compacted Soil	Undetermined	Undetermined
H-6	210	L	Magnetic Rock	Undetermined	Undetermined
B-13	51	L	Engineer Stake	0.9	Undetermined
D-2	220	L	Undetermined	Undetermined	Undetermined
F-2	221	L	Undetermined	Undetermined	Undetermined
E-6	527	L	Magnetic Rock	Undetermined	Undetermined
E-6	521	L	Conductive Soil	1.1	No Reading
D-6	492	L	Conductive Soil	1.0	No Reading
D-6	495	M	Culvert	0.5	No Reading
D-6	494	M	Conductive Soil	0.3	No Reading
A-6	457	L	Conductive Soil	0.2	No Reading

Table 2. MCAGCC Target Analysis Results using DGPS Navigation

Quadrant No.	Target I.D.	STOLS Predicted Size	Object Excavated	STOLS Depth Accuracy (m)	STOLS Location Accuracy (m)
E-5	1	L	Conductive Soil	Undetermined	Undetermined
E-5	2	L	Conductive Soil	Undetermined	Undetermined
F-8	35	L	Conductive Soil	Undetermined	Undetermined
F-7	43	M	Conductive Soil	Undetermined	Undetermined
G-6	87	L	Conductive Soil	Undetermined	Undetermined
G-6	89	M	Conductive Soil	Undetermined	Undetermined
H-5	105	L	Conductive Soil	Undetermined	Undetermined
G-5	107	L	Conductive Soil	Undetermined	Undetermined
F-6	121	M	Conductive Soil	Undetermined	Undetermined
F-6	122	M	Conductive Soil	Undetermined	Undetermined
F-6	123	M	Comm Wire/Bailing Wire	Undetermined	Undetermined
F-6	124	M	Comm Wire	Undetermined	5.5 - 6.0 (between 123 & 124)
F-6	126	M	Conductive Soil	Undetermined	Undetermined
E-5	148	L	Conductive Soil	Undetermined	Undetermined
D-1	165	L	Engineer Stake	Undetermined	1.0
D-2	171	M	Engineer Stake	Undetermined	0.5
D-2	180	M	Engineer Stake	Undetermined	1.0
D-2	181	L	Engineer Stake	Undetermined	0.5
D-2	187	M	Conductive Soil	Undetermined	Undetermined
D-3	194	M	Strapping Bands & EMR Shields	Undetermined	2.0
D-3	197	M	Strapping Bands & EMR Shields	Undetermined	2.0
D-3	198	M	Strapping Bands & EMR Shields	Undetermined	Undetermined
D-3	200	L	Conductive Soil, Padlock, Small Wire	Undetermined	Right on Mark
D-5	206	L	Conductive Soil	Undetermined	Undetermined
D-7	212	L	Conductive Soil	Undetermined	Undetermined
C-4	222	L	Conductive Soil	Undetermined	Undetermined
C-4	223	L	Conductive Soil	Undetermined	Undetermined
C-5	225	M	Conductive Soil	Undetermined	Undetermined
B-11	271	M	Conductive Soil	Undetermined	Undetermined
B-11	273	M	Conductive Soil	Undetermined	Undetermined

Table 2. MCAGCC Target Analysis Results using DGPS Navigation (Continued)

Quadrant No.	Target I.D.	STOLS Predicted Size	Object Excavated	STOLS Depth Accuracy (m)	STOLS Location Accuracy (m)
F-7	284	M	35 inches of Strapping Band	Undetermined	Undetermined
D-4	288	L	Conductive Soil	Undetermined	0.5
D-5	289	L	Conductive Soil	Undetermined	Undetermined
G-5	291	M	Conductive Soil	Undetermined	Undetermined
G-6	292	M	Conductive Soil	Undetermined	Undetermined

Table 3. JPG Target Analysis Results

Quadrant No.[1]	Target I.D.[1]	STOLS Predicted Size	Actual Object[2]	STOLS Depth Accuracy (m)	STOLS Location Accuracy (m)
--	1	L	L	0.9	0.6
--	2	L	L	0.4	0.1
--	3	L	L	0.7	0.7
--	4	L	S	2.0	1.6
--	5	S	L	1.7	2.4
--	6	M	L	1.0	1.2
--	7	S	M	0.3	1.1
--	8	S	M	0.3	0.3
--	9	S	M	0.2	0.9
--	10	M	M	0.5	1.3
--	11	L	L	0.7	0.6
--	12	S	M	0.2	1.8
--	13	M	M	1.1	0.9
--	14	S	L	0.8	0.6
--	15	M	L	0.1	0.3
--	16	L	M	0.0	1.1
--	17	L	L	0.6	0.3
--	18	L	L	1.0	1.0
--	19	L	L	0.8	0.4
--	20	L	L	0.4	0.4
--	21	L	L	1.5	0.4
--	22	L	L	0.6	1.2
--	23	S	L	--[3]	0.9
--	24	S	M	0.9	0.7

NOTES:

1 The quadrant in which the target was located, as well as the I.D. No. assigned by the STOLS have been omitted to prevent disclosure of data that could be used to determine controlled target locations.

2 The emplaced ordnance items are part of the baseline target data for the controlled test area. Equivalent STOLS size classifications are shown in place of an actual object description to prevent disclosure of sensitive controlled site target data.

3 Actual depth for this target was undefined due to the nature of the target.

4.3 Performance Analysis Results

4.3.1 **Availability.** The STOLS experienced a variety of hardware and software problems throughout both survey periods that affected the amount and quality of survey data collected. The following paragraphs summarize significant results:

a. **System.**

Data collected during the Twentynine Palms survey indicate that a survey rate of approximately 10 acres per day was achieved. Although the topography at the survey site was relatively flat, the system was not able to achieve the desired capability of 15 acres per day.

The IDU on the STV failed to initialize on the first day of the second survey period. A systematic diagnostic process was performed, but the team was unable to repair the STOLS in the field. As a result, no surveying was performed during the period of 19 July to 2 August 1993.

b. **Navigation Systems.**

The wireless modems for the DGPS failed to communicate at the start of the first day of surveying at the MCAGCC. This problem was caused by an improper modem frequency change. The microwave system was used in place of the DGPS while personnel worked on correcting the problem. The re-configuration resulted in a time loss of approximately 5 hours.

Once the problem with the modems was corrected, the DGPS was used for 3 days. On the fourth day, the DGPS failed to operate. Ambient temperatures in excess of 120 °F were suspected of causing the failure.

The antenna on the STV serving the wireless modem broke off at the base on two separate occasions. The failures were caused by metal fatigue due to the whipping action of the antenna as the STV traversed the rough terrain. Repairs were quick and time loss was minor. Further failures were avoided by slowing the speed of the STV.

c. **Software and Data Processing.**

Using the Silicon Graphics workstation, STOLS operators were able to process mission data and produce target reports in about 2 hours. During previous surveys, processing the same volume of data on the Force minicomputer system normally required a full day or more. It is estimated that the new workstation reduces processing time by approximately 90 percent.

The STOLS approach to Target Analysis is strongly dependent on the user interface. Targets are manually selected based on the visual proximity of blue and red blotches of color on the display. The addition of large amounts of ferrous surface clutter and conductive soil makes the selection of a target more difficult. It is likely that no two operators will select the same targets, and this would result in significant subjectivity in the target report.

Another data processing problem encountered was temporary loss of data due to software error. On two separate occasions while target analysis was in progress the target files were overwritten by the STOLS software and all target analysis was lost for that day. This occurred with two different target operators performing target analysis. The areas covered by the lost data had to be reprocessed, resulting in 12 hours of lost processing time.

d. **Electrical and Mechanical Systems.**

Two support rods used to maintain the navigation antenna mount upright broke during operations. Two new support rods, made from scrap wood, were field improvised to repair the problem. This failure resulted in approximately 30 minutes of downtime.

The battery for the STV became discharged necessitating hand starting. Diagnosis revealed the power requirement for an engine cooling fan installed as an enhancement was greater than the power produced by the STV's alternator. The cooling fan was removed and a new battery was bought and installed. The discharged battery was placed on charge. Estimated down time was 1 hour.

The trailer ball on the STV came loose when the retaining bolt fell out. This placed the full towing load on the interconnecting cables, causing strain on the cables and inflicting minor damage to the cable junction box. Approximate time lost was 1 hour.

Upon return to the MCAGCC for the second survey period, batteries on the command center tow vehicle were found to be fully discharged, and one tire was deflated. One tire on the command center trailer was also deflated. Time lost was approximately 2 hours.

4.3.2 **Mission Effectiveness Analysis Results.** Measures of effectiveness for STOLS mission performance during the two surveys were computed as follows:

a. **Detection Ratio.** Calculation of a meaningful detection ratio requires knowledge of actual targets located within the survey area. Because no ordnance was found during excavation of detected targets at the MCAGCC, no detection ratio was calculated for that site. The requisite data were available for the controlled test

area at JPG, and the detection ratios calculated for that survey are shown in table 4.

b. **Classification Ratio.** No classification ratios could be calculated for the MCAGCC survey. The classification ratios calculated for the JPG survey are listed in table 4.

Table 4. JPG Mission Effectiveness Results

Size	Detected	Correctly Classified	Total	P_D	P_{Size}
Small	2	1	24	0.08	0.50
Medium	8	2	8	1.00	0.25
Large	12	8	14	0.86	0.67
Overall	22[1]	11	46	0.48	0.50

NOTES:
1 Two targets were detected that could not be classified as small, medium, or large.

c. **Position Accuracy.** The mean position accuracies and standard deviations calculated for each survey are listed in table 5. The probable detection radius shown in the table is the radius within which a detected target will be found 95 percent of the time.

Table 5. STOLS Location Accuracy

Survey	Position Accuracy		Depth Accuracy		Probable Detection Radius (m)
	Mean (m)	Std Deviation (m)	Mean (m)	Std Deviation (m)	
MCAGCC (Microwave)	1.7	1.4	0.7	0.5	2.8
MCAGCC (DGPS)	1.1	0.7	Undetermined	Undetermined	1.4
JPG	0.9	1.0	0.7	0.9	2.0

4.3.3 **Detection Capability Analysis Results.** The detection capability for the STOLS is directly related to the amplitude of the noise component of the recorded sensor data. Table 6 lists noise statistics for the MCAGCC survey; table 7 lists statistics for the JPG survey. The standard deviations for each of the magnetometers are listed for each survey file.

Table 6. MCAGCC Survey Noise Statistics

STOLS Noise (Standard Deviation) (gamma)								
File No.	Magnetometer							File Average
	1	2	3[1]	4	5	6	7	
1	31.32	34.33	167.88	32.55	34.30	36.06	35.86	34.07
2	26.63	24.42	132.65	25.66	28.40	93.24	24.85	37.20
4	19.53	19.18	91.21	18.67	25.01	20.23	18.03	30.27
6	17.46	18.37	45.13	18.38	22.30	29.48	18.35	24.21
8	15.36	15.90	77.60	15.47	20.57	15.96	15.19	25.15
9	14.76	16.15	26.72	15.58	19.27	16.25	14.83	17.65
12	12.77	13.92	51.98	13.23	19.55	13.55	12.62	19.66
13[2]	103.30	107.82	146.92	126.64	139.76	161.47	174.40	137.19
Sensor Average	30.14	31.26	92.51	33.27	38.65	48.28	39.27	29.28

Notes:
1 Measurements over 100 for this magnetometer were used in computing averages only for sensor # 3 and File # 13.
2 The magnetometers stopped working during the last 3 minutes of data collection for this file.

Statistical Summary		
Parameter	By Magnetometer	By File
Lowest Standard Deviation	12.62	17.65
Average Standard Deviation	29.28	29.28
Highest Standard Deviation	174.40	137.19

Table 7. JPG Survey Noise Statistics

STOLS Noise (Standard Deviation) (gamma)								
File No.	Magnetometer							File Average[1]
	1	2	3	4	5	6	7	
1	34.63	228.68	4519.13	129.64	10.21	212.57	13.47	19.44
2	3278.96	228.44	1868.49	68.38	13.11	13.52	13.37	27.10
3	4942.26	10.87	67.88	173.89	10.87	14.74	1061.02	26.09
4	0.00	63.26	91.66	9.52	19.37	10.02	739.75	38.77
5	4724.55	155.47	45.98	8.81	72.94	13.34	1251.01	35.27
6	4361.14	31.46	159.88	11.74	17.09	11.41	942.58	17.93
7	4151.86	32.73	163.00	9.60	31.44	21.87	22468.89	23.91
8	5133.63	15.87	17.50	15.23	18.28	15.36	0.00	16.45
9	3833.53	10.98	26.20	10.36	12.20	10.54	0.00	14.06
10	3167.25	22.38	121.52	10.52	11.91	8.77	0.00	13.40
11	3625.26	9.57	73.61	9.11	11.90	8.78	0.00	22.59
12	3814.95	9.82	51.61	8.95	11.72	8.86	0.00	18.19
13	4209.15	687.72	83.50	10.76	12.81	11.94	23641.46	29.75
14	4029.93	69.50	164.14	12.76	14.84	9.92	0.00	26.76
15	3135.27	17.07	117.35	21.76	453.20	8.40	6487.16	15.74
16	1788.50	20.44	13.81	9.93	731.42	11.41	7864.64	13.90
17	0.00	10.36	15.78	9.38	42.84	9.44	0.00	17.56
Sensor Average	4136.90	95.56	447.12	31.19	88.00	23.58	3793.10	22.15

Notes:
1 Magnetometer measurements over 100 were not used in computing file and overall averages.

Statistical Summary		
Parameter	By Magnetometer	By File
Lowest Standard Deviation	8.81	13.40
Average Standard Deviation	22.15	22.15
Highest Standard Deviation	23641.46	38.77

SECTION 5 - DISCUSSION OF RESULTS

5.1 Mission Performance Assessment

In this section, the capability of the STOLS to detect the presence of UXO is assessed. Next the STOLS capability to position locate UXO and then to classify the size is discussed. Data from the two STOLS surveys (MCAGCC and JPG) was used.

The MCAGCC survey was an uncontrolled test in that the purpose of the STOLS was to detect and then identify the locations, size, and depths of potential buried UXO targets. The STOLS detected 1223 magnetic anomalies at the site. Of these 1223 anomalies, the STOLS operators identified 264 as potential targets, of which 71 were excavated. Upon excavation, 40 of the holes contained magnetized earth (natural clutter) and 31 of the holes contained metallic objects, none of which were UXO. Though no UXO were found, a live fuze and two inert 2.75 inch rocket warheads were found during the site preparation by NAVEODTECHDIV personnel.

The JPG survey was a controlled test since the locations, depths, and sizes of the UXO were known prior to the survey. From this test, it was possible to derive the performance accuracy of the STOLS in detecting, classifying, and locating the buried UXO. The STOLS detected 22 out of a possible 46 UXO targets, corresponding to an overall probability of ordnance detection of 0.48.

5.1.1 **Detection Capability.** An assessment of the STOLS detection capabilities was performed through detailed analyses of the target data files produced during the two surveys. The following paragraphs discuss the outcome of that assessment.

5.1.1.1 **Data Compression Anomalies.** Prior to performing an analysis of the STOLS sensors, a data quality assessment was performed on the STOLS data collected from the two surveys. In this assessment, the data from each file were decompressed and time series raster plots (signal vs. time) of each magnetometer were produced for each file. These plots were

visually examined for any data that seemed out of the ordinary. Figure 10 shows a sample raster plot of all seven magnetometers from the JPG test site. The sensor signal mean and standard deviation for each of the magnetometers are listed to the side of each plot. The mean value for each magnetometer was subtracted prior to plotting to normalize the graphs. In this sample, four of the magnetometers (numbers 2, 4, 5, and 6) appear to be operating normally. Two others (numbers 3 and 7) show no response and appear to be inoperative, while magnetometer number 1 exhibits a high noise level interrupted randomly by step-like signals uncharacteristic of the other magnetometers. The step-like signals were most probably due to the combination of a noisy sensor and inadequate dynamic range in the data compression algorithm. In the data compression algorithm, the first magnetometer value in a sequence of 20 values is represented by a 2 byte (16-bit) integer value. This corresponds to a maximum change between samples of $\pm$ 64 gamma. The next 19 are represented by single bytes (8-bits) which are the delta change in value from the previous value. If the delta change is greater than ± 127, a constant -127 is placed in the next 19 values of that record. When the data are decompressed, a constant value equal to the first value in the sequence is replicated. This causes the step-like characteristic observed in these raster plots.

To assess how prevalent this problem was during the surveys, the compressed data from all of the data files were examined, and the number of times the magnetometer signals exceeded the dynamic range of the system (i.e., the number of -127s observed) was determined for each sensor. These results were tabulated for each survey and then normalized by the total number of points in the survey to indicate the percentage of survey time the data are contaminated. Table 8 lists these percentages by sensor for each survey along with the total amount of survey time.

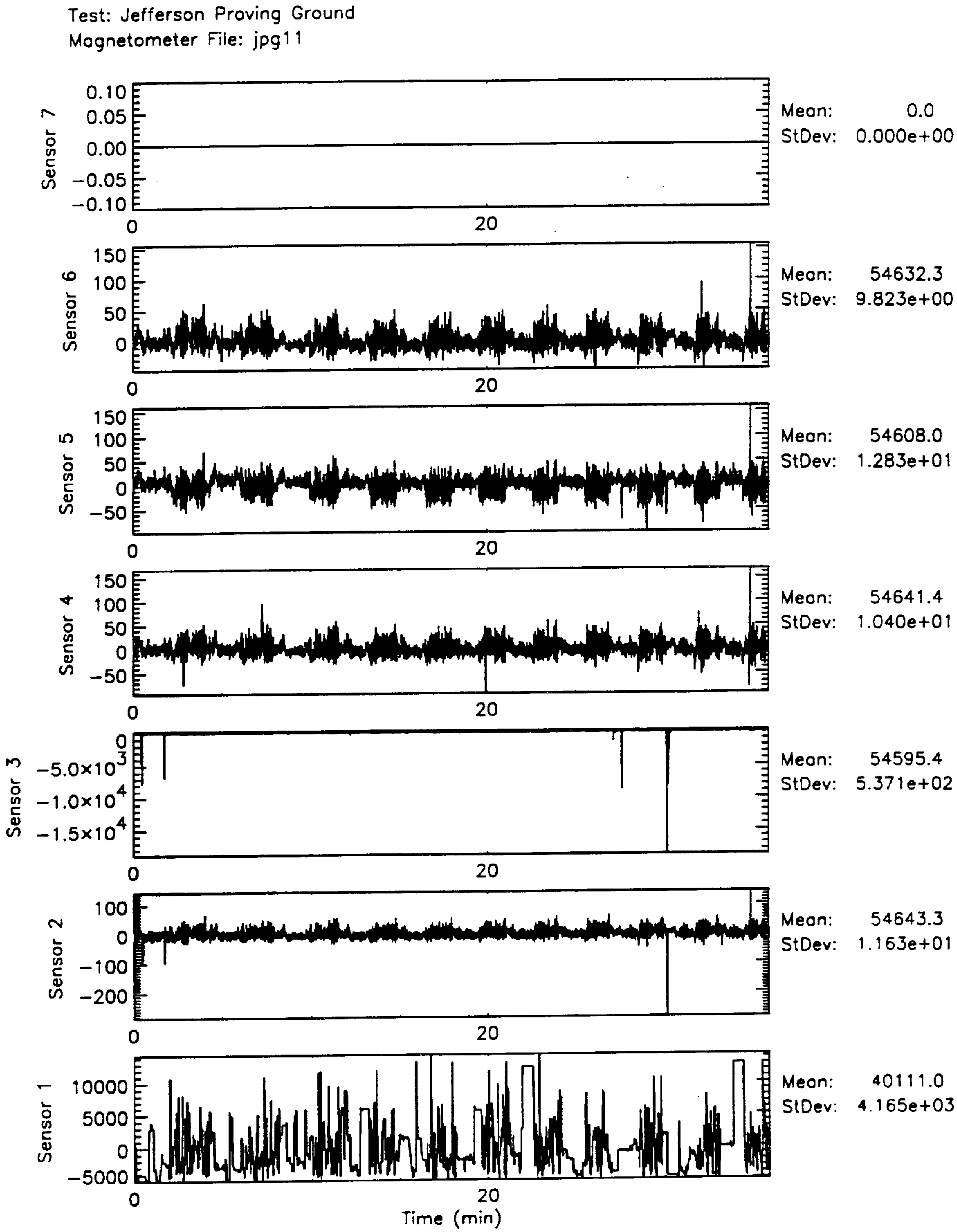

Figure 10. Magnetometer Raster Plots (JPG File 11)

Table 8. **Percentage of Data Contaminated by Compression Algorithm**

Test Name	Magnetometer (% contaminated)							Total Time (min)
	1	2	3	4	5	6	7	
MCAGCC	0.0	0.0	1.0	0.0	0.0	0.2	0.0	408.19
JPG	80.8	0.8	2.3	0.3	0.9	0.1	64.5	978.70

During the MCAGCC survey, the data contamination was 1 percent or less for all magnetometers. During the JPG survey, the magnetometers on either end of the array were contaminated a significant percentage of the survey time; the middle sensors were affected by contamination only 2 percent of the time or less. The lack of dynamic range is a limiting factor, particularly when a large target signal or a noisy magnetometer is encountered. This effect will be most troublesome when applying filters to the data, or, in the case of magnetic anomalies, trying to fit models to the magnetometer signature.

5.1.1.2 **Noisy/Inoperative Sensors.** Figures 11 and 12 are magnetometer raster plots from the MCAGCC survey and another JPG survey file, respectively. During the MCAGCC survey, raster plots from sensors 3 and 6 exhibited large negative-going spikes greater than 10,000 gamma below the mean value, while the other magnetometers appeared to exhibit normal behavior. These observations are also reflected in the standard deviations from each of the magnetometers (to the right of each raster). The standard deviations of magnetometers 3 and 6 are on the order of 500 to 600 gamma, while the other magnetometers have standard deviations less than 70 gamma. In the raster plot from JPG (figure 12), sensor 1 appeared to be extremely noisy while sensor 7 appeared to be inoperative. The other sensors appeared normal with the exception of sensor 3, which exhibited a few large negative spikes. Examination of other raster plots from JPG revealed other sensors with large negative spikes. In figure 13, almost all of the sensors exhibited these spikes.

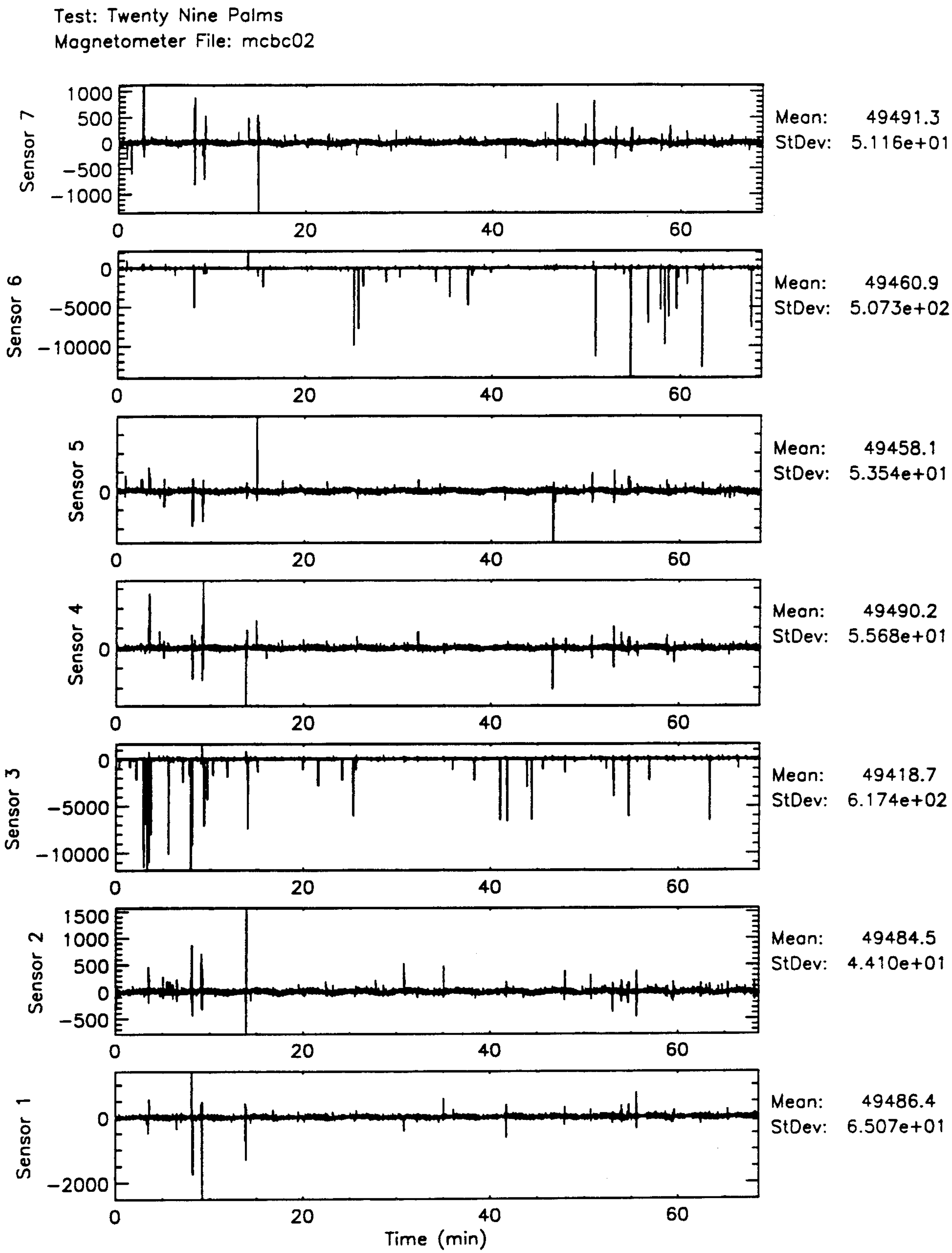

Figure 11. Magnetometer Raster Plots (MCAGCC File 02)

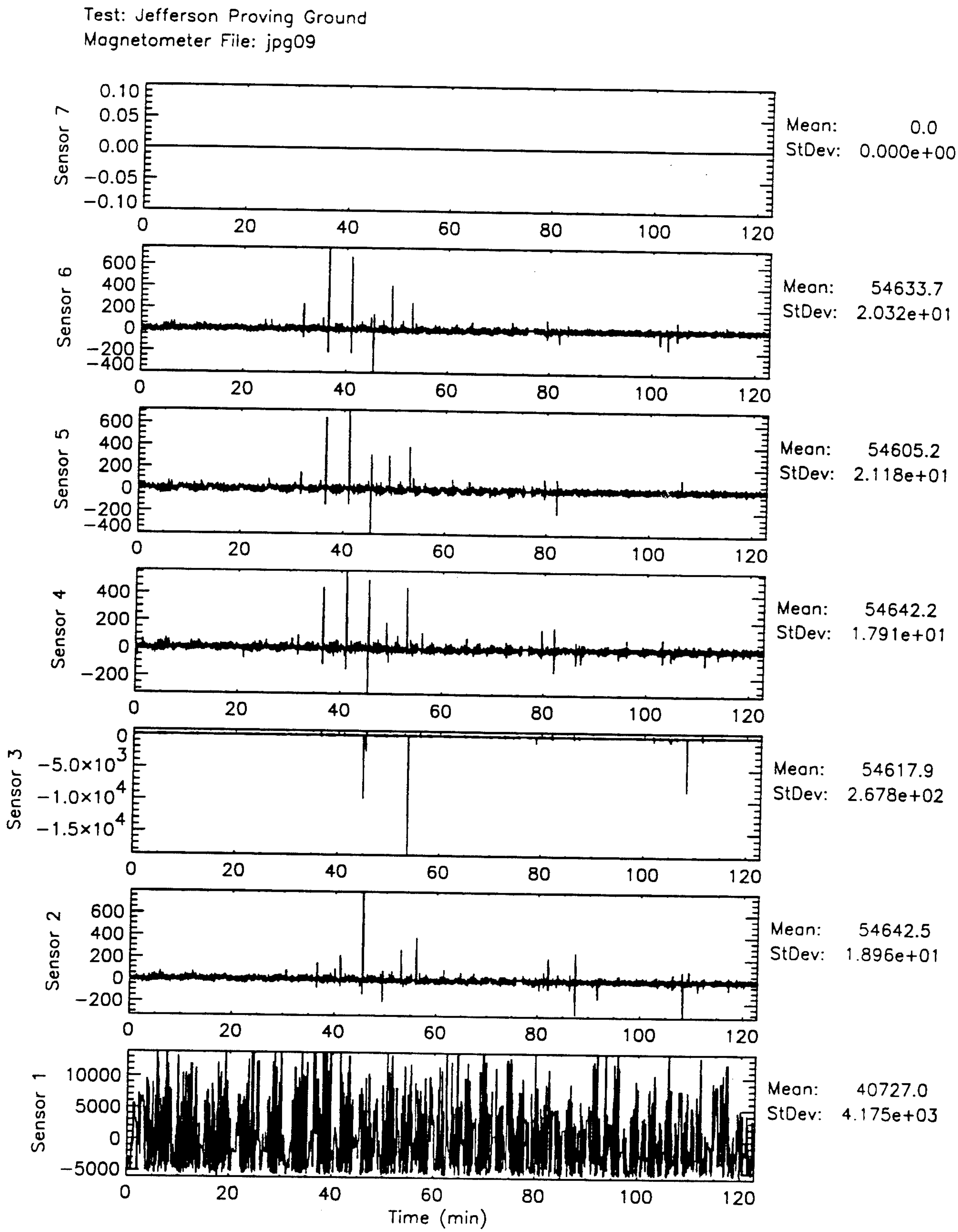

Figure 12. Magnetometer Raster Plots (JPG File 09)

In order to identify noisy or inoperative sensors, noise statistics (mean and standard deviation) from each of the sensors were computed using the method described in paragraph 3.3.3 and appendix C. The standard deviations, which form the basis for flagging noisy or inoperative sensors, are listed in tables 5 and 6 in section 4. From the noise statistics and an examination of the magnetometer raster plots, a standard deviation of 100 gamma was determined to be the threshold for flagging noisy or inoperative sensors for elimination from further detection analyses. The assessment of sensor operability is summarized as follows:

- During the MCAGCC survey, sensor 3 consistently had a noise level above the threshold (except for file 13 in which all of the sensors were above the threshold after apparently being turned off during the last 3 minutes of the file).

- For most of the JPG survey the number of usable sensors ranged from three to five. Sensors 1 and 7 were only usable during the early portion of the survey.

When sensors are inoperable during survey operations, there is less reliable magnetic anomaly data available for the STOLS to use in displaying the anomaly for operator selection, estimating location and depth, and attempting to match the anomaly to a signature model. The result is degraded detection capability and less likelihood that the detected targets will be properly classified.

5.1.1.3 **Noise Characterization.** In any detection system or signal processor, the performance is directly related to the ratio of signal levels to noise levels; in other words, the higher the signal amplitude relative to the noise amplitude, the better the detection performance. Since one typically does not have control over the characteristics of the signals encountered in the field, most of the effort in designing a detection system is concerned with reducing and characterizing system noise. Therefore, it is important to identify the various noise sources that affect the system and then to understand their respective characteristics so that effective noise reduction techniques might be applied.

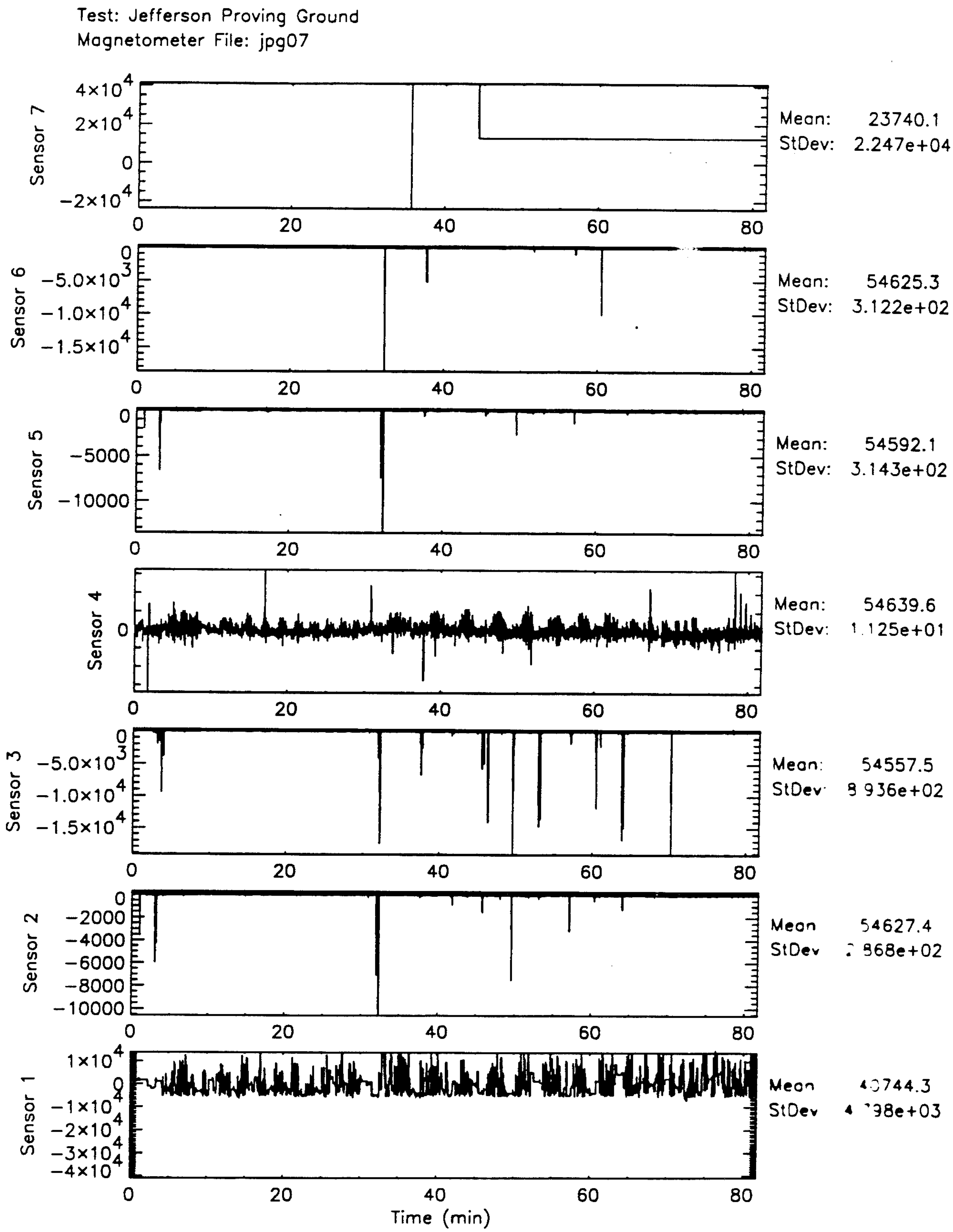

Figure 13. Magnetometer Raster Plots (JPG File 07)

In the case of the STOLS, the term noise applies to any signal fluctuation that is non-ordnance in origin. Using this definition, the STOLS noise arises from a combination of the following sources: sensor/electronic noise, sensor motion, EMI pickup, background clutter (both man-made and natural), digitization noise, variations in the local magnetic field, data compression/decompression, and absolute and relative sensor calibration accuracy. In this section, each of the above noise sources will be discussed; and, where possible, various techniques for reducing that noise will be discussed.

a. **Sensor/Electronic Noise.** In analyzing the noise of a sensor/system, it is useful to examine the power spectral density (PSD) functions of sensor data. (These functions are described in more detail in appendix C.) Figures 14 through 16 show plots of the PSDs as a function of frequency for sensor 6 from a typical MCAGCC data file and sensors 4 and 5 from a typical JPG data file, respectively. In these figures, the spectra are generally "red" starting at approximately 1000 to 2000 gamma^2/Hz, then decreasing with increasing frequency to values of 0.3 to 0.5 gamma^2/Hz at the Nyquist frequency (10 Hz). Examination of other PSD function across the two surveys revealed that all of the spectra tended to reach a white noise floor of 0.3 to 0.5 gamma^2/Hz at around 8 to 10 Hz. These levels are probably due to sensor/electronic noise, which is typically white (spectrally flat) in nature. For a digital resolution of 1 gamma, the corresponding noise floor would be 0.0083 gamma^2/Hz, which is approximately two orders of magnitude below the observed white noise floor for the STOLS.

From the Wiener-Khintchine theorem (reference 4), the integral of the PSD across the bandwidth of the system is equal to the variance. Integrating a white noise floor of 0.3 to 0.5 gamma^2/Hz yields a range of variances between 3 to 5 gamma^2, or a range of standard deviations between 1.7 and 2.4 gamma. During the JPG survey, data were collected with the sensor in a static condition (i.e., the array not moving and the STOLS engine not operating). The standard deviation of the magnetometer noise was approximately 1 gamma, which is within a factor of 2 to 3 of the white floor indicated by the PSDs.

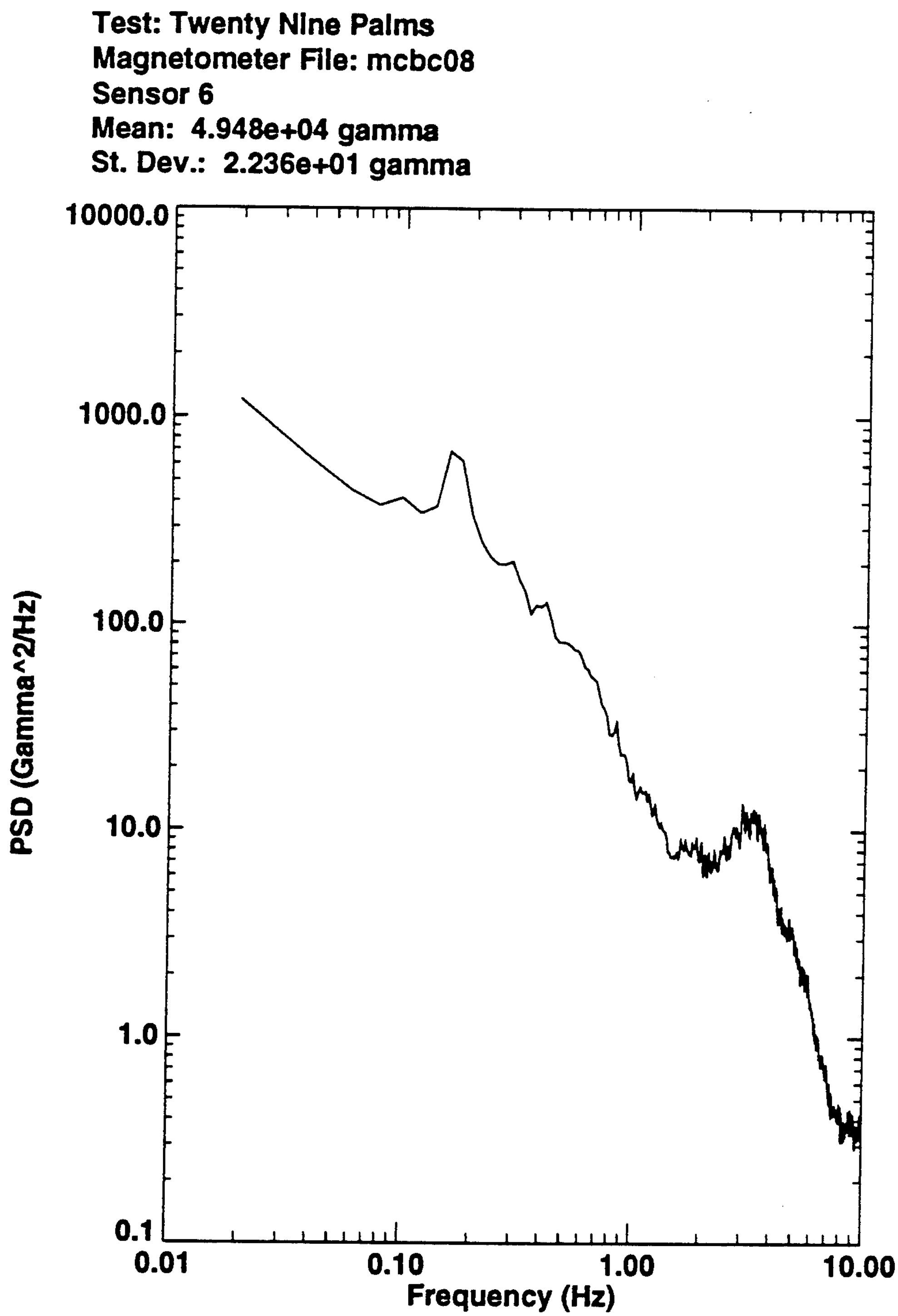

Figure 14. Magnetometer Power Spectral Density, Sensor 6 (MCAGCC File 08)

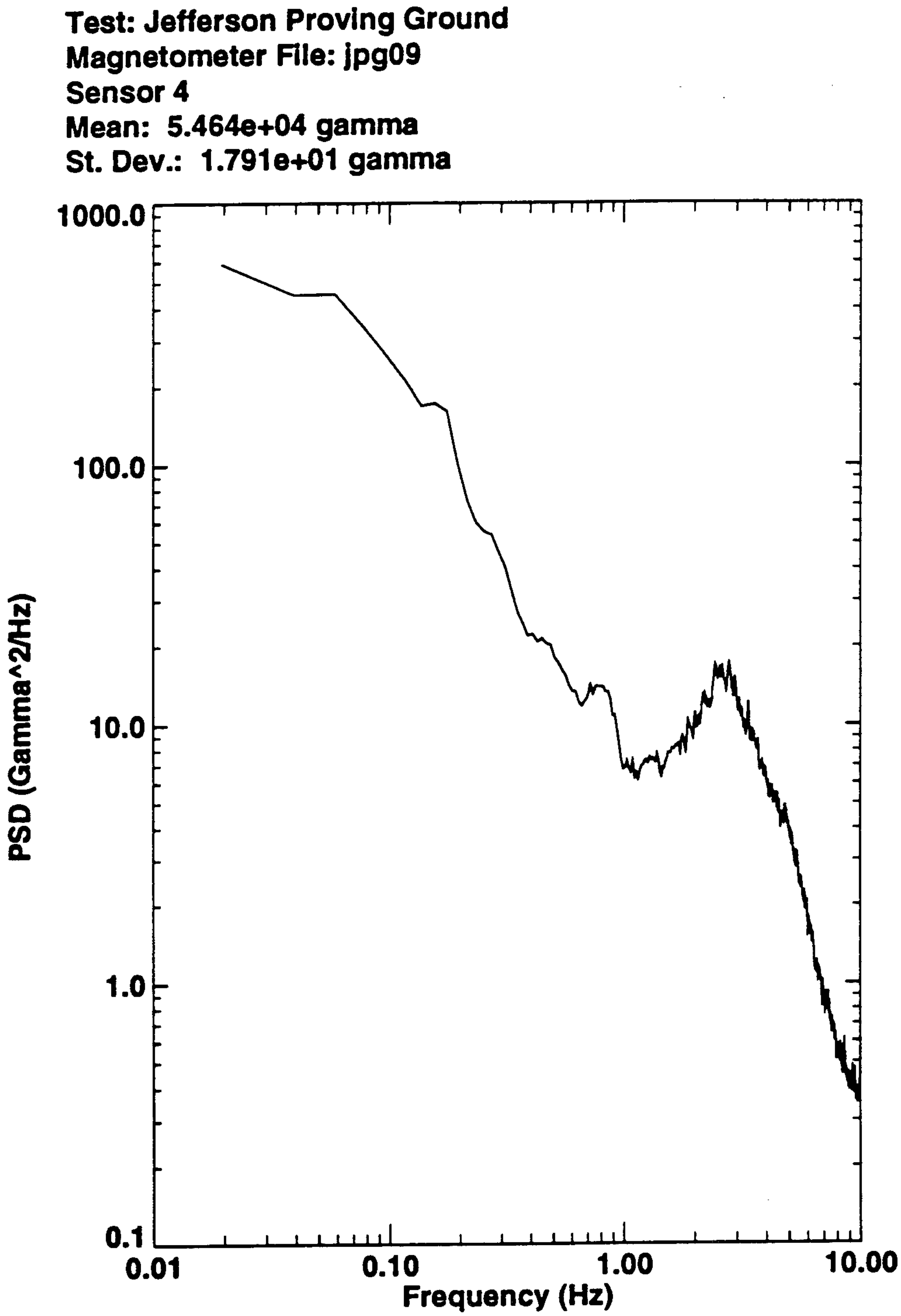

Figure 15. Magnetometer Power Spectral Density, Sensor 4 (JPG File 09)

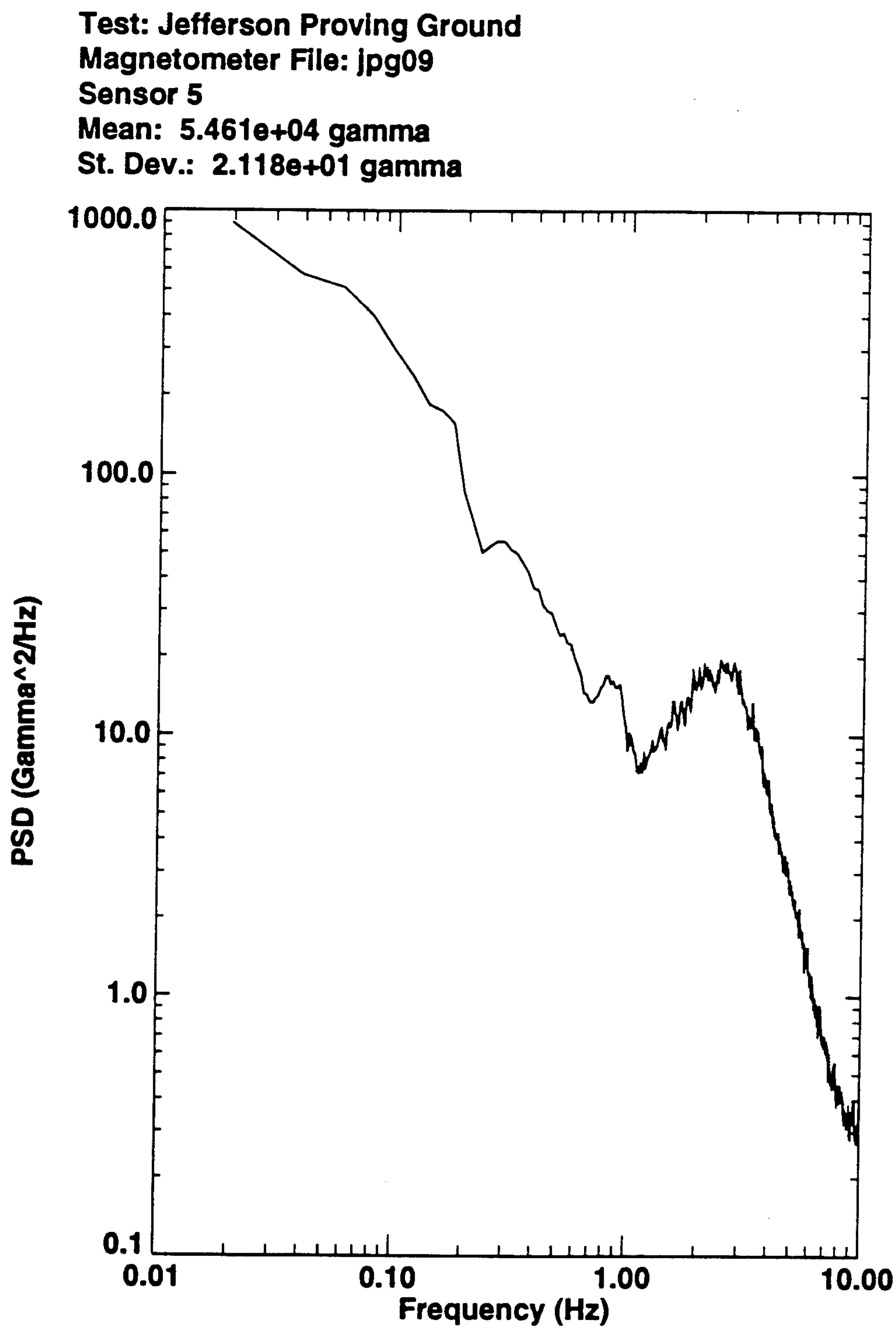

Figure 16. Magnetometer Power Spectral Density, Sensor 5 (JPG File 09)

b. **Magnetometer Motion.** The small peak in the PSDs around 2 to 3 Hz is probably due to irregular vertical and horizontal motion of the magnetometers in the earth's magnetic field. These irregular motions are induced in the sensor array as it is towed across rough terrain. As seen from the spectral coherence plots (figure 17), the energies within these bands are highly coherent (0.8) between sensors as well. Following the JPG static test mentioned previously, the tow platform, with the magnetometer array, was manually bounced up and down to provide vertical motion in the earth's magnetic field. The standard deviations of the magnetometers went from 1 gamma in the static mode to approximately 5 gamma when bounced.

This noise contamination could be removed by low-pass filtering. However, since most of the UXO targets are expected to fall within this band, filtering would reduce these signals as well. Since the contamination is proportional to the motion of the sensor in the earth's magnetic field, an independent measure of sensor motion would be required. Three-axis accelerometers mounted on each end of the magnetometers would provide this measure. Then, using the sensor motion computed from the accelerometers as system noise, standard adaptive techniques could be used to remove the effects of vertical motion in the magnetometer data (reference 5).

c. **Magnetic Environment.** In addition to the higher frequency noise, the energy at the lower frequency (less than 1.0 Hz) is probably due to large scale changes in the magnetic environment (nonuniformity in soil magnetization, change in the local magnetic field, etc.). Examination of the spectral coherence (figure 17), which plots spectral coherence between the same magnetometer sensors displayed in figures 15 and 16, indicates that the energies within this band are highly coherent (0.8) between these sensors. Based on examination of other spectral coherence plots, this observation is valid for all usable sensors from the two surveys. For

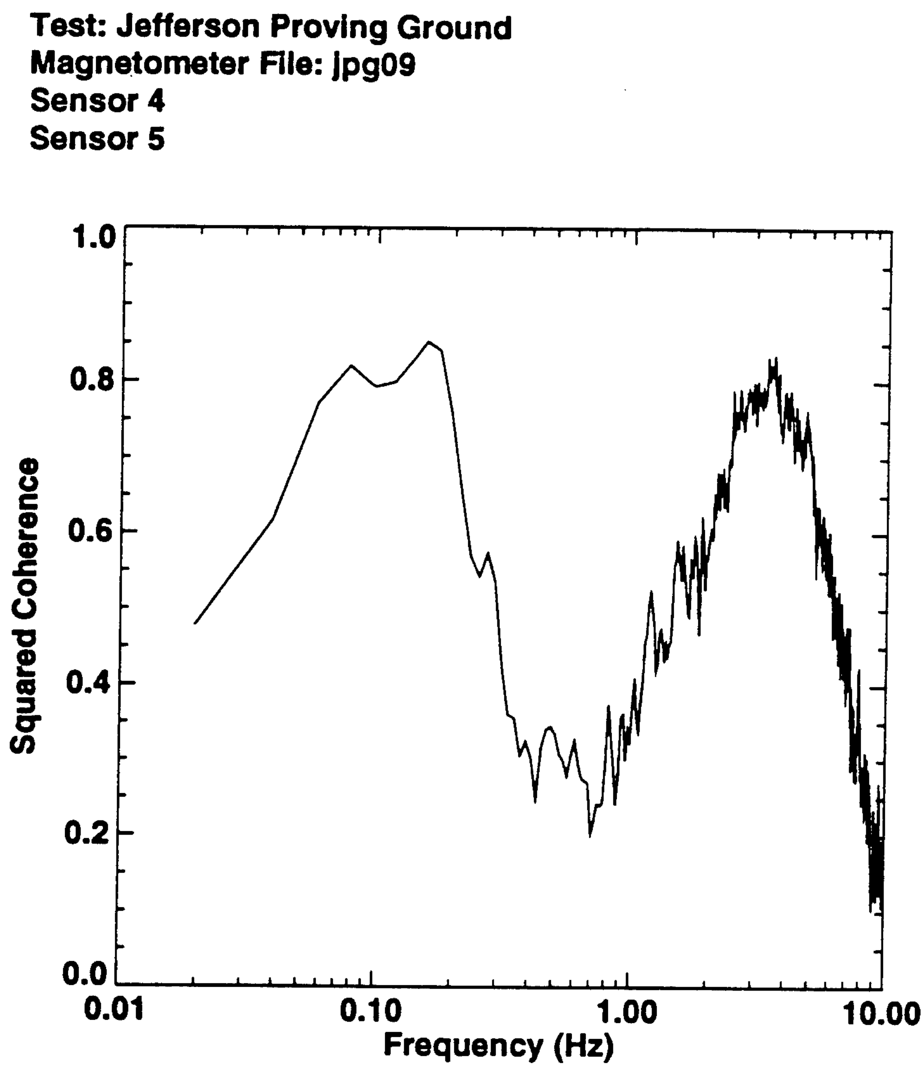

Figure 17. Magnetometer Squared Coherence, Sensors 4 and 5 (JPG File 09)

the PSD computations, the reference magnetometer readings (local background magnetic field strength) were not subtracted from the data.

Removal of the noise resulting from changes in the local earth's magnetic field is already accounted for by the reference magnetometer. Residual noise left from this process as well as fluctuations occurring over relatively large spatial scales (when compared to typical target sizes) can be removed from the data using adaptive mean or median removal filters. These filters can either be one or two dimensional in construction.

d. **Vehicle-Induced Noise.** Two other noise sources were observed in the magnetometers during the JPG survey. The first source was related to the direction in which the STOLS array was being towed. During the JPG survey, the STOLS array was towed in relatively straight legs oriented in alternating north-south/south-north directions. A shift in the mean levels of the magnetometer data was observed when the direction of towing was changed. At the end of each survey leg, when the STOLS was stopped, an increase of 5 gamma relative to the reference was observed when the STOLS tow vehicle and platform were pointed toward the north, while a 5 gamma decrease was observed when pointed south. It is believed that this artifact is due to modification of the earth's magnetic field by the magnetic dipole signature of the STOLS tow vehicle and platform.

The other noise source is related to the STOLS vehicle engine. When the STOLS was stopped at the end of each survey leg, the mean level of the magnetometer readings was observed to increase a positive 5 to 8 gamma when the engine was running relative to when the engine was off. This positive increase in mean level was observed regardless of the orientation of the STOLS tow vehicle and platform. This would seem to indicate that the engine of the STOLS generates a small but measurable magnetic field around the magnetometers. Both this artifact and the

one mentioned in the previous paragraph can be removed by employing some form of adaptive filtering.

5.1.1.4 **Detection Thresholds.** To assess the impact of these various noise sources on the magnetometer data, cumulative distribution functions (CDFs) and probability density functions (PDFs) were computed (see appendix C). In designing the optimum detection processor, as well as predicting its performance, the statistical distributions that describe both the signal and noise data were needed. Figure 18 contains plots of the PDF and CDF of magnetometer sensor data corresponding to the PSD in figure 15. In this figure, the bottom panel contains the PDF, and the top panel contains the CDF, which is plotted on a probability axis. On a probability axis, the CDF of a normal (Gaussian) distribution becomes a straight line. The dashed line in this figure indicates a normal distribution fit to the median of the data.

In this figure, approximately 95 percent of the magnetometer data can be characterized by a normal distribution. Examination of usable sensors from the other test indicates that this percentage ranges from 90 to 98 percent. Applying a Chi-Square Goodness of Fit test to the normal distribution fit revealed that the data can be characterized by a normal probability distribution with a 95 percent confidence level. The standard deviation of 9 gamma (from legend on the bottom of the figure) is approximately equal to the standard deviation obtained when the motion peak observed in the PSD plot (figure 15) was integrated. Therefore, approximately 90 to 98 percent of the magnetometer data is dominated by sensor motion, which is Gaussian in nature.

The tails of the distribution (the large positive and negative deviations from the mean) are due to a combination of actual UXO and geophysical magnetic clutter. Because the majority of the data were masked by the sensor motion-induced noise, it was impossible to determine the statistical distribution of the underlying clutter. However, since the background clutter is primarily due to geophysical processes, its distribution is probably not Gaussian.

Test: Jefferson Proving Ground
Magnetometer File: jpg09
Sensor 4
Chi Square Statistic: 1.605e+02
K-S Statistic: 0.0481
Degrees of Freedom: 141445

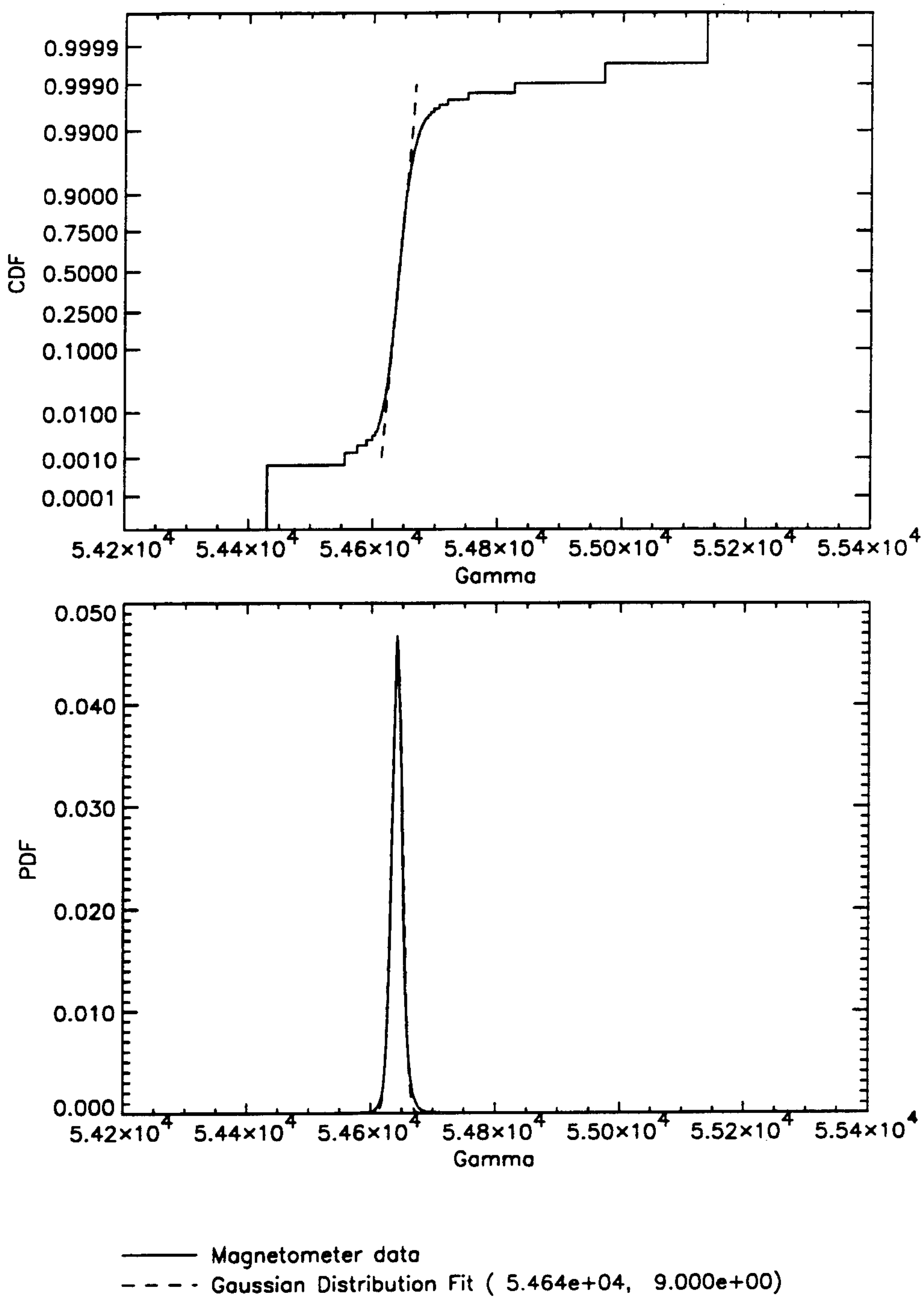

Figure 18. Magnetometer PDF and CDF, Sensor 4 (JPG File 09)

The relatively poor performance of the STOLS during the MCAGCC survey was due to system noise and the elevated background gamma readings caused by compacted ferrous minerals. From the data presented in tables 5 and 6 of section 4, the average standard deviations of the usable sensors (i.e., those with standard deviations less than 100 gamma) were 29.28 gamma at MCAGCC and 22.15 gamma at JPG.

Reference 6 states that the minimum threshold for declaring a UXO detection is 2 standard deviations above the mean value. If the statistical distribution of both the noise and signal are Gaussian, this threshold would yield a probability of detection of 55 percent at a 10 percent probability of false alarm. For a good detection (reference 4), the threshold rises to 10 standard deviations above the mean, which yields a probability of detection of 95 percent at a 5 percent probability of false alarm. Using the JPG statistics as representative of STOLS sensor noise, a nominal threshold for a good detection should be 221.5 gamma (10 times the standard deviation).

To estimate how effective the current STOLS is in detecting UXO, the magnitude of the magnetic signature for three standard UXO targets (the 60 mm, 105 mm, and 155 mm projectiles) were computed as a function of depth (distance below the surface). Using the formula specified in appendix C, the peak magnetometer signal strength is proportional to $1/r^3$ (where r is the radial distance from the sensor to the UXO) and the weight of ferrous material. The selected ordnance has the following ferrous weights:

60 mm:	2 lbs
105 mm:	20 lbs
155 mm:	45 lbs

From the formula, the expected magnetic signals from the three types of UXO were plotted as a function of depth at two sensor heights above the ground, 6 inches (figure 19) and 14 inches (figure 20). In figures 19 and 20, the nominal threshold for a good detection for the current STOLS is indicated by a dashed line. The threshold corresponding to a 25 dB reduction in the noise (factor of 18 in rms amplitude) is indicated by the dot-dashed line. From these

figures, the detection depths for all ordnance are less than 3 feet. By reducing the noise level to approximately 1.2 gamma (detection threshold of 11 gamma), these detection ranges increase to a maximum of 9 feet.

The signal amplitudes for the three UXO types are plotted to their maximum expected penetration depths in figures 19 and 20. These are (from reference 4) 2.0 feet for the 60 mm projectile, 8.5 feet for the 105 mm projectile, and 12.5 feet for the 155 mm projectile. Based on the assumptions used for this analysis (magnetic dipole strength factor, etc.), the noise levels of the STOLS would have to be reduced by approximately 37 dB in order to reliably detect the 155 mm shell at its maximum penetration depths. This analysis assumes that the detection processing consists of applying a simple threshold to the magnetometer data. Many simple techniques could be used to reduce the noise, such as adaptive filtering, match filtering, and pattern recognition techniques. This analysis also does not take into account the impact of a trained operator who is able to recognize dipole patterns on the STOLS display. All of the factors mentioned impact the detection results to varying degrees.

In order to associate probabilities of detection and false alarms with selected thresholds, the statistical distributions of both the noise and signal will have to be determined. In the previous paragraphs, the noise distribution was shown to be 90 to 98 percent Gaussian due to sensor motion-induced contamination. It is assumed that in future systems the dominating noise sources will be geophysical in nature.

5.1.1.5 **Sensor Calibration.** One final topic that must be addressed concerns the accuracy of the sensor calibrations. In estimating the size and depth of UXO, both the shape and amplitude of the magnetic signature are used. In the case of the STOLS, data from the magnetometer array are combined into a two-dimensional grid of data. The two-dimensional dipole shapes are then matched to the model functions. As occurs with nearly all sensors in the field, sensor aging, drift, and aging of the electronics, etc. cause the calibrations to change over time. Depending upon the magnitude of these changes, inaccurate estimates of the size and depth of the UXO can occur. In addition, relative inaccuracies between sensors will distort the two

Sensor Height Above Ground: 6 inches

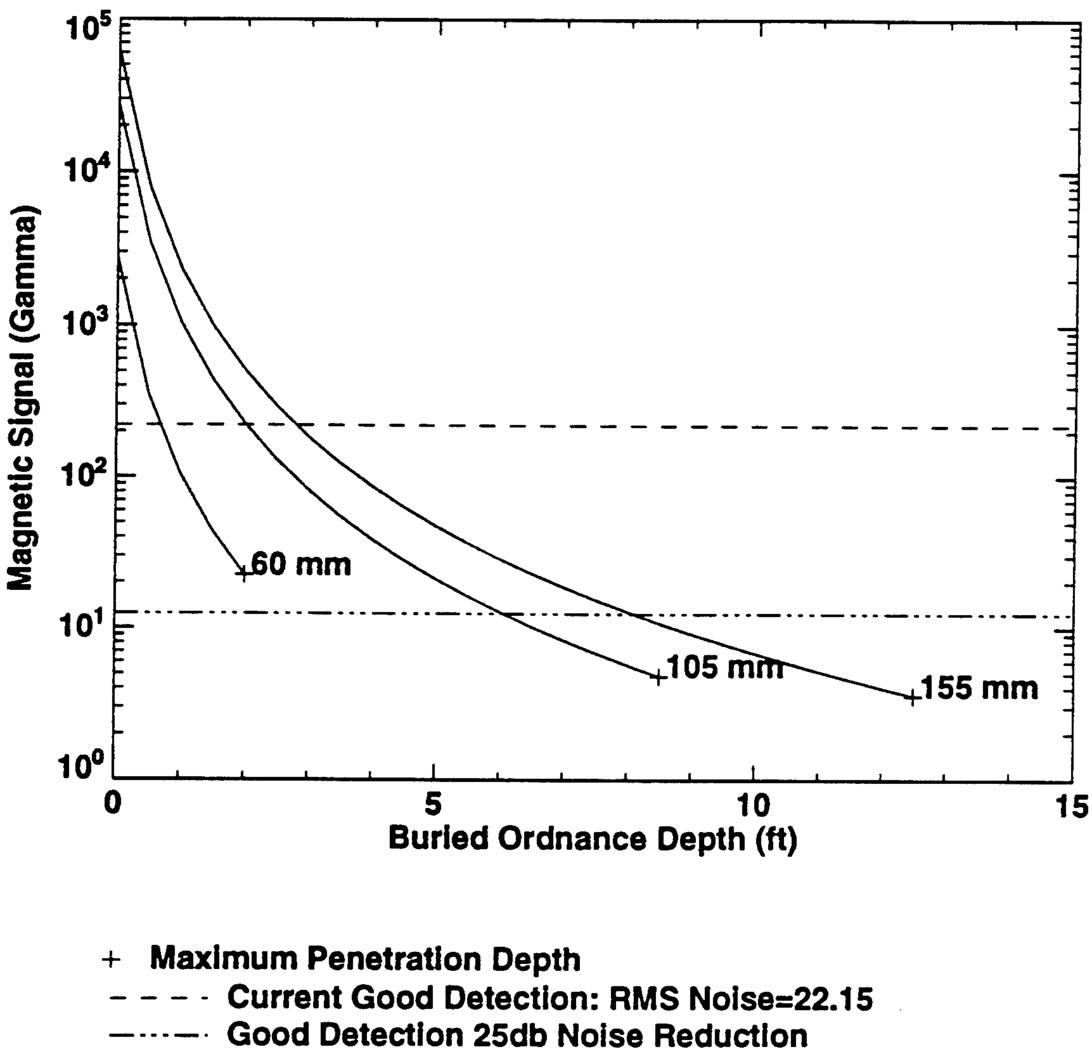

Figure 19. UXO Magnetic Signal Strength vs. Depth (Sensor Height 6 inches)

Sensor Height Above Ground: 14 inches

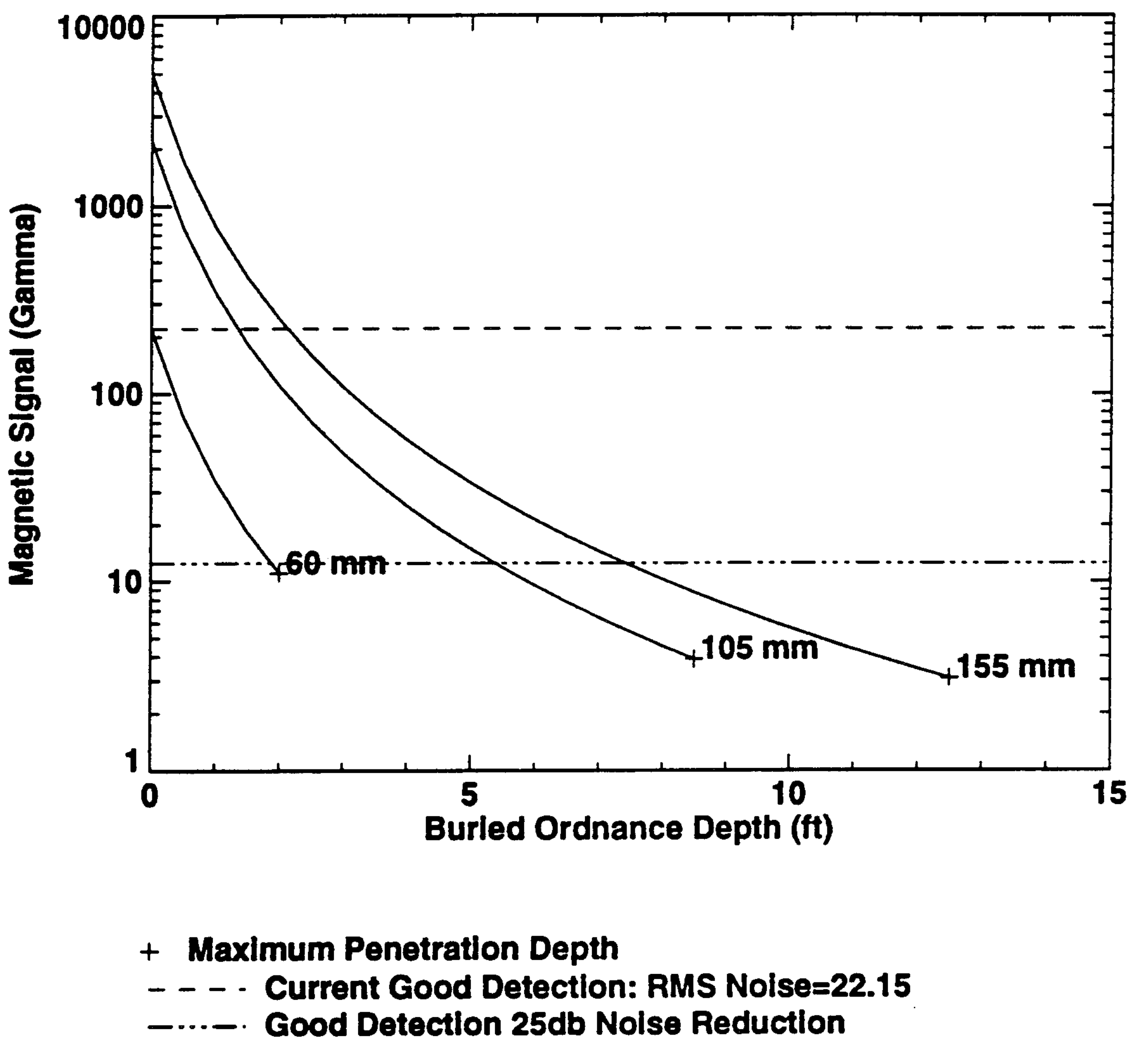

Figure 20. UXO Magnetic Signal Strength vs. Depth (Sensor Height 14 inches)

dimensional waveform causing further confusion and inaccurate estimates. Inaccurate calibration of the sensors may be one of the reasons for the relatively poor performance of the STOLS in classifying the size (50 percent correct) and in determining the depth (95 percent within $\pm$ 1.2 m).

A very simple device can be constructed to allow calibration in the field. This device, called a Helmholtz coil, consists of a tube with conducting wire wrapped around it. A constant current is passed through the wire producing a constant, known, uniform magnetic field within the coil. By placing the coil so that each of the magnetometers is within the field of this coil, a field check on the calibrations can be made at any time, thus insuring that accurate measurements are made during each survey.

5.1.2 **Localization Capability.** The STOLS localization capability is a function of the following subsystems:

a. Magnetometer Array. The magnetometer array provides the data available to the system for three- dimensional modeling of the magnetic anomaly produced by a target. If one or more of the sensors is out of calibration or inoperable, fitting the STOLS data to the correct magnetic model becomes more difficult, thus inducing inaccuracies in the solution.

b. Navigation System. The navigation system provides a position fix for the target that is used to compute target coordinates. During the MCAGCC survey, both microwave and DGPS navigation systems were used to mark targets previously detected using the microwave system. During the JPG survey, only the DGPS navigation system was used.

c. Data Processing System. The data processing system performs the initial target analysis to produce target coordinates, depth, and size classification. This analysis includes a human element that can induce unpredictable position errors; i.e., the

operator must recognize potential targets on the system display and mark them with an "area of interest" box. The size and orientation of this box can have a significant impact on the computed target position.

During the MCAGCC survey, targets were initially detected using the microwave navigation system for position data. Subsequently, 36 targets were relocated using the microwave system and validated by excavation, 50 targets were relocated using the DGPS with only 35 validated by excavation. Based on target validation results, the DGPS navigation system demonstrated better position accuracy than the microwave system. The average positional error of the DGPS under demonstration conditions at the MCAGCC was 1.1 m with a confidence level of 95 percent and a maximum error of 2 m. For the microwave system, the average error was 1.7 m, with a maximum error of 5 m. The data from the validation effort must be considered approximate because the validated positions were not accurately surveyed. The accuracy of STOLS with DGPS navigation was acceptable at the MCAGCC.

Of the 76 anomalies detected during the JPG survey, 22 corresponded to emplaced controlled targets. The STOLS was able to locate 95 percent of these targets to within a radius of approximately 5 feet (1.5 m) and a depth of 4 feet (1.2 m). Figures 21 and 22 plot CDFs of the location and depth errors, respectively. In these plots, the design goals for the location error (radius of 1 m) and depth error ($\pm$ 0.5 m) are indicated by the dotted line. As seen in these figures, a significant fraction of the reports were outside the design goals. Figure 23 shows the gross distribution of location errors at JPG in all three dimensions. Although the number of data points available is small from a statistical standpoint, the general shape of these histograms suggest a normal distribution.

5.1.3 **Classification Capability.** Classification capability is also affected by both the magnetometer array and the data processing system as described in paragraph 5.1.2. Conceptually, classification of target size and estimation of target depth are more difficult problems than estimating location in the horizontal plane. Size and depth are estimated by the STOLS by constructing a three-dimensional model of the magnetic anomaly and attempting to

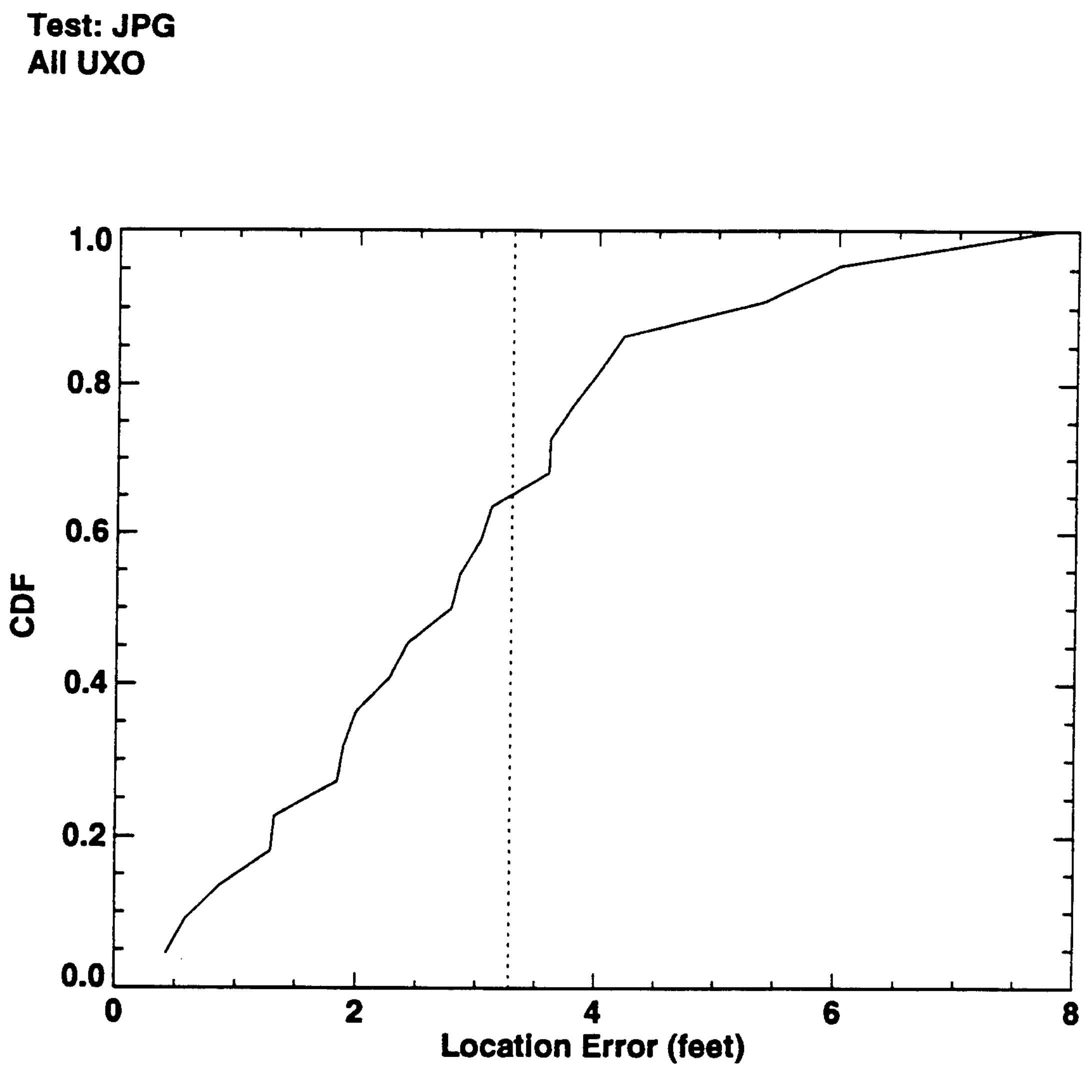

Figure 21. CDF of Location Error Radius for JPG

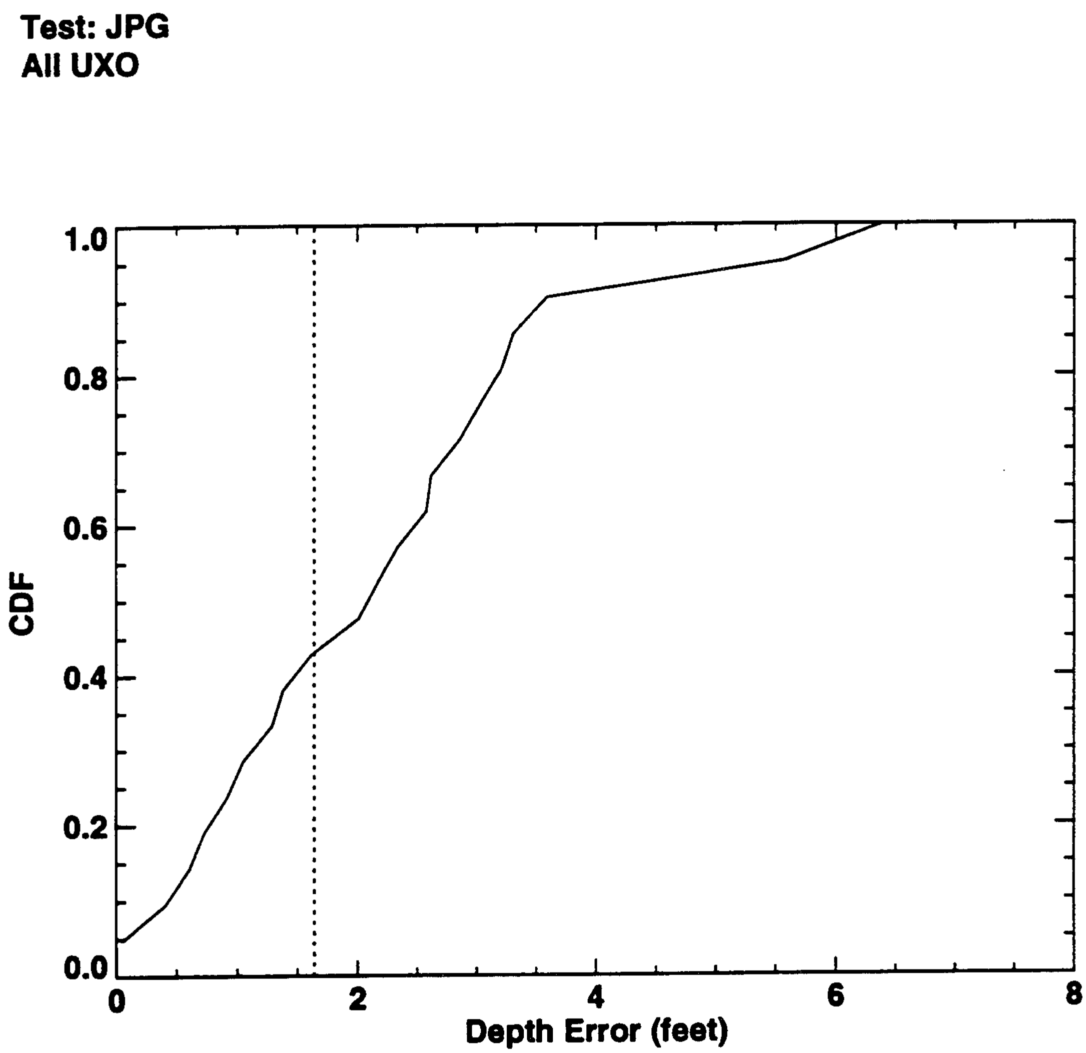

Figure 22. CDF of Depth Error for JPG

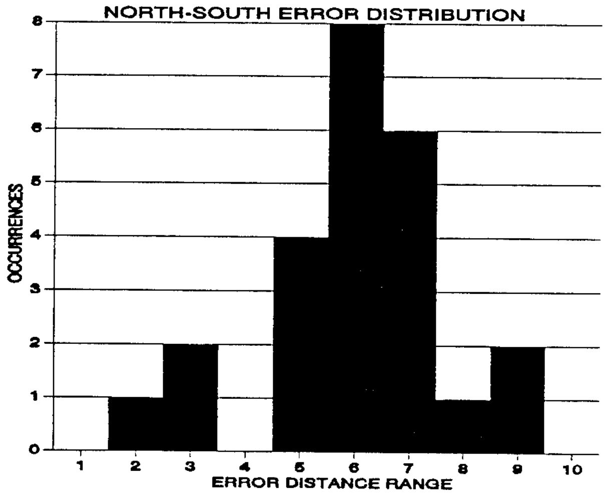

NORTH ERROR DISTANCE
(m)

Range	
1	less than -1.79
2	-1.79 to -1.42
3	-1.42 to -1.05
4	-1.05 to -0.68
5	-0.68 to -0.31
6	-0.31 to +0.07
7	+0.07 to +0.44
8	+0.44 to +0.81
9	+0.81 to +1.19
10	greater than +1.19

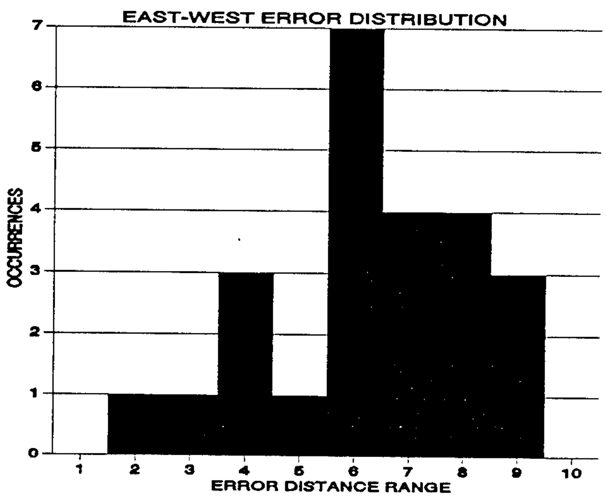

EAST ERROR DISTANCE
(m)

Range	
1	less than -1.58
2	-1.58 to -1.19
3	-1.19 to -0.82
4	-0.82 to -0.44
5	-0.44 to -0.07
6	-0.07 to +0.31
7	+0.31 to +0.69
8	+0.69 to +1.07
9	+1.07 to +1.45
10	greater than +1.45

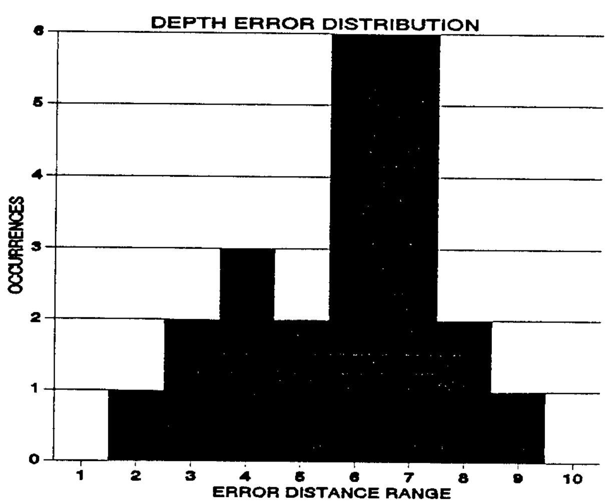

DEPTH ERROR DISTANCE
(m)

Range	
1	less than -1.71
2	-1.71 to -1.25
3	-1.25 to -0.79
4	-0.79 to -0.33
5	-0.33 to +0.13
6	+0.13 to +0.58
7	+0.58 to +1.04
8	+1.04 to +1.49
9	+1.49 to +1.96
10	greater than +1.96

Figure 23. JPG Location Error Distributions

match that model to the magnetic signature of known ordnance objects. This process is inherently sensitive to noisy, inoperable, and out-of-calibration sensors and the "target boundaries" established by the system operator during target marking.

The JPG results were used to determine how the STOLS performance varied as a function of ordnance size. Table 4 in section 4 lists the probabilities of detection and correct classification by target size using the STOLS size classifications defined in paragraph 2.3.5 (small, medium, and large). The STOLS only detected 2 of the 24 small targets emplaced in the area surveyed, while detecting all of the medium size targets and 12 of the 14 large size targets. In classifying the size, the performance of the STOLS degrades as the size decreases: 67 percent correct for large targets and 25 percent correct for medium targets. (Because only two small targets were detected, the classification result of 50 percent is not statistically significant.)

5.2 **System Characterization.** The surveys performed at the MCAGCC and JPG provide a relatively limited body of performance data for characterizing the STOLS prototype. However, the survey sites were representative of the types of terrain, vegetation, and site conditions where the STOLS might normally be deployed. Therefore, STOLS performance observed during the MCAGCC and JPG surveys can also be considered representative of STOLS performance characteristics.

5.2.1 **Usability.** STOLS usability characteristics were evaluated by assessing performance within the following performance areas:

a. Terrain Handling Ability. In general, the STOLS prototype exhibited a satisfactory ability to operate in both the flat, sandy desert terrain of the MCAGCC and the undulating, uneven terrain of JPG. The STV maintained traction and stability on up-, down-, and side-slopes in all conditions encountered during the surveys except for one extremely muddy location at JPG. The STV's self-extraction capability in that instance was not tested because of the proximity of a potentially hazardous terrain drop-off. The STV and towed platform provided

relatively stable platforms under the conditions encountered. However, the suspension characteristics result in system vulnerabilities to small (1 foot order of magnitude) terrain irregularities, which can cause fatigue failures of metal parts located away from the STV's center of gravity, and noise-inducing motion of the magnetometer array.

b. Survey Rate. During the MCAGCC and JPG surveys, the STOLS prototype did not achieve the designer's stated goal of 20 acres surveyed per day. The maximum area surveyed on any day was 15 acres, with a sustainable average rate of approximately 10 acres per day. The reduced survey rate was attributable to the realities of a field survey; i.e., a reduction in speed of advance to mitigate the effects of rough terrain, the necessity of maneuvering around terrain obstacles, and the stress on both equipment and operators caused by temperature or other climatic extremes.

c. Maneuverability. The STV provided satisfactory maneuvering capability for the site conditions at the MCAGCC and JPG. The overall length of the towed platform dictates the use of an agile vehicle to maneuver around terrain obstacles. The STOLS prototype configuration requires an overrun area of at least 20 feet at each end of the survey area to turn the system around and align it with the next survey line.

d. Human Factors. The STV and its installed data collection and navigation equipment are relatively simple to operate. STV controls were logically located. The STV suspension characteristics made sustained operation in uneven terrain fatiguing for the operator. The data processing system also exhibited operator-related problems. The target identification process requires a trial-and-error approach to setting the sensitivity of the display in order to eliminate as much background clutter as possible while retaining the desired targets. This operation should be carefully coordinated with the survey's objectives to ensure that the

UXO targeted by the search is not "squelched" in the process of optimizing the display. The prototype system was also overly reliant on the skills and experience of the operator to identify and mark potential UXO. The system required the operator to pick out anomalies from the background clutter, associate opposite-polarity anomalies that may represent a dipole, and define an area of interest box around each target, making the box large enough to provide sufficient data for model matching but as small as possible to limit processing resources required. Each of these elements introduces significant variables into the system's detection, location, and classification performance. The target processing software also exhibited a lack of error protection capability in permitting the operator to inadvertently overwrite valid data files.

5.2.2 **Reliability.** The STOLS was operated for an estimated total of 190 hours during the MCAGCC and JPG surveys. Failure rates (λ) and mean time between failures (MTBF) were not calculated for these surveys because of multiple changes in system configuration and operations that occurred during this period. In order to utilize equipment manufacturers' predicted or actual λ or MTBF, the operating environment assumed by the manufacturer would have to be known to permit comparison with the STOLS environment. The required data were not available during this study. Table 9 summarizes, by STOLS subsystem, the failures that occurred during the surveys and the total estimated down time resulting from those failures, including logistics delays. The following equipment, assemblies, and components exhibited unsatisfactory reliability characteristics: magnetometers, cabling, and the STP.

Table 9. Failure Summary by Subsystem

Subsystem	Number of Failures	Estimated Down Time (Hours)
STV (Chassis, Engine, Drive Train, Engine Electrical)	3	2.5
Microwave Navigation System	0	0
DGPS Navigation System	3	29
Data Acquisition System	1	346
Sensors	frequent	see Note 1
Towed Platform	1	4
Data Processing System	2	12

Notes:

1. Individual sensors experienced frequent failures not apparent during the survey operations, consequently no down time resulted. Refer to paragraph 5.1.1.2 for a discussion of inoperable sensors.

5.2.3 **Maintainability/Supportability.** The STV and STP were generally trouble free, preventive maintenance was easy to perform, most repairs are feasible in the field, and the necessary parts were deployed with the system. Sensor maintenance can also be performed in the field and a limited supply of parts were on hand. Most repairs to the navigation system must be performed by a qualified electronics facility. The data acquisition system is serviceable in the field; however, due to the lack of documentation, some diagnosis is time intensive and is best done at home base. The data processing system requires service by the manufacturers or their authorized repair centers.

SECTION 6 - CONCLUSIONS AND RECOMMENDATIONS

The data collected during the MCAGCC and JPG surveys were processed and analyzed to assess the performance of the STOLS. Based on the results of the analyses, the following conclusions are made:

- During the MCAGCC survey, the STOLS location accuracy was 1.7 m with microwave navigation and 1.1 m with DGPS navigation. These performance parameters cannot be compared to data from other surveys because there are two location error components involved (i.e., the location accuracy of the original target detection and the navigation error from target reacquisition), and because only 71 of the 264 potential targets were excavated.

- During the JPG survey, the STOLS demonstrated a probability of detection of only 0.48. Missing over half of the UXO constitutes unsatisfactory performance. During the same survey, the STOLS was able to locate 95 percent of these UXO to within a radius of approximately 5 feet (1.5 m), and determine the depth to within 4 feet (1.2 m). The demonstrated location accuracy was within reasonable limits; however, the depth accuracy was satisfactory only for relatively shallow targets. The STOLS was able to classify the size (small, medium, or large) correctly for only 50 percent of the detected targets, and could not distinguish between UXO and non-UXO targets. This classification capability would be unsatisfactory in a live site survey.

- The noise levels of the STOLS (19 to 28 gamma) as determined by field operations are too high to reliably detect the desired ordnance (60 mm, 105 mm, 155 mm shells) to the maximum penetration depths (2 feet, 8.5 feet, and 12.5 feet, respectively).

- The desired performance at the maximum penetration depths (155 mm shell at 12.5 feet) requires a final noise level of the processed output of 0.3 gamma, which 37 dB below the noise level during the MCAGCC and JPG surveys.

- Approximately 90 to 98 percent of the STOLS noise is due to irregular sensor motion in the earth's magnetic field while the sensor array is being towed over the ground. This motion induced noise is Gaussian in nature.

- The engine of the tow vehicle, when running, generates a positive 5 gamma increase in the magnetic field around the sensors.

- The direction of travel introduces a positive or negative shift of 5 gamma dependent on the orientation of the sensors and tow vehicle relative to the earth's magnetic field.

- The current data compression algorithm does not have sufficient dynamic range to handle noisy sensors. It may also distort very strong magnetic signals, which would impair the STOLS ability to characterize the UXO.

- The DGPS navigation system has an absolute positioning accuracy to within 1 m 95 percent of the time. The RACAL microwave navigation system has an absolute positioning accuracy to within 1.7 m 95 percent of the time.

From the conclusions above and the preceding analyses, the following recommendations are made to improve the performance of the current STOLS or future systems:

- Three axis accelerometers should be mounted on each sensor in the array and processed with some form of an adaptive noise cancellation technique to reduce the motion-induced noise from the magnetometers.

- Techniques to remove the large scale fluctuation in the magnetometers (engine induced, tow direction, background clutter, etc.) should be investigated to further reduce the noise. Some of the techniques could include adaptive mean removal filters, adaptive median filters, two dimensional filters, etc.

- More robust data compression techniques with greater dynamic ranges should be investigated, or the system should record and store the full digitized information.

- Since UXO size and depth primarily determine the strength of the magnetic signature, design goals for future system should be stated in terms of specific UXO types and maximum penetration depths of interest.

- Since estimation of the size and depth of the ordnance require accurate calibration of the magnetometer sensor array, techniques for checking the calibration of the magnetometers in the field should be developed.

This page is intentionally left blank

SECTION 7 - REFERENCES

1. "STOLS Operating and Maintenance Manual", Naval Explosive Ordnance Technology Division, September 1993.

2. "Surface Towed Ordnance Locator System (STOLS): Survey Data Analysis Report"; PRC Inc.; November 1994.

3. "Unexploded Ordnance Advanced Technology Demonstration Program at Jefferson Proving Ground (Phase I)," USAEC Report No. SFIM-AEC-ET-CR-94120, December 1994.

4. Marple, S. Lawrence, Jr.; Digital Spectral Analysis with Applications; Prentice Hall, Englewood Cliffs, NJ; 1987.

5. Stalcup, B.W., and J.P. Dugan; "Adaptive Technique for Eliminating Motion Contamination from Towed Temperature Arrays;" Journal of Atmospheric and Oceanic Technology, Vol. 7, No. 2, pages 340-348; April 1990.

6. "Detection of Unexploded Ordnance," DODESB TR-76-1, April 1976.

7. McFee, J.E., Y. Das, and R.O. Ellingson; "Locating and Identifying Compact Ferrous Objects"; IEEE Transactions on Geoscience and Remote Sensing, Vol. 28, No. 2, March 1990, pages 182-193.

8. Jackson, J.D.; Classical Electrodynamics; John Wiley & Sons, Inc., New York, NY, 1975.

9. Hersey, J., and Pennella, J.; "Ordnance locator techniques-An overview"; NAVEODFAC Technical Report TR-188, March 1978.

10. "Magnetic Techniques in the Detection of Projectiles"; NAVEODFAC Technical Report TR-239, March 1982.

APPENDIX A

MCAGCC SURVEY

A.1 Site Characteristics

The MCAGCC consists of 595,367 acres. The joint UXO project was conducted in the southwest of the area close to Deadman's Lake (dry). The general site area consists of unconsolidated sediments of undissected fill of the valleys and flood plains. Fill consists of wind blown sand, clay, and silt, alluvium, and alluvium fan gravel. The surface soil contains hematite and limonite which can exhibit significant magnetic properties when concentrated or compacted. No igneous or volcanic rock formations are close to the survey site. Sediments at the site extend down to more than 2,000 feet before reaching bedrock.

The sites to be surveyed consisted of two areas, separated by an airfield (see figure A-1). The area located to the south of the airfield was designated by the MCAGCC as area 20B, and the other area was designated as 20A. Historical data indicates that these areas have been used as ordnance/ammunition storage sites since circa 1976. See reference 2 for a listing of ordnance and ammunition known to have been stored in these areas. ASP 20B is a 74 acre triangular shaped site that has been used as a temporary field ammunition storage area. The site usually contains assorted types of aircraft mounted ordnance and munitions. ASP 20B is composed of hard packed sandy soil which is sparsely covered with desert scrub brush varying in shape and size. Figure A-2 shows the layout of ASP 20B, where the surveys documented in this report were conducted. Reference 2 contains additional site details.

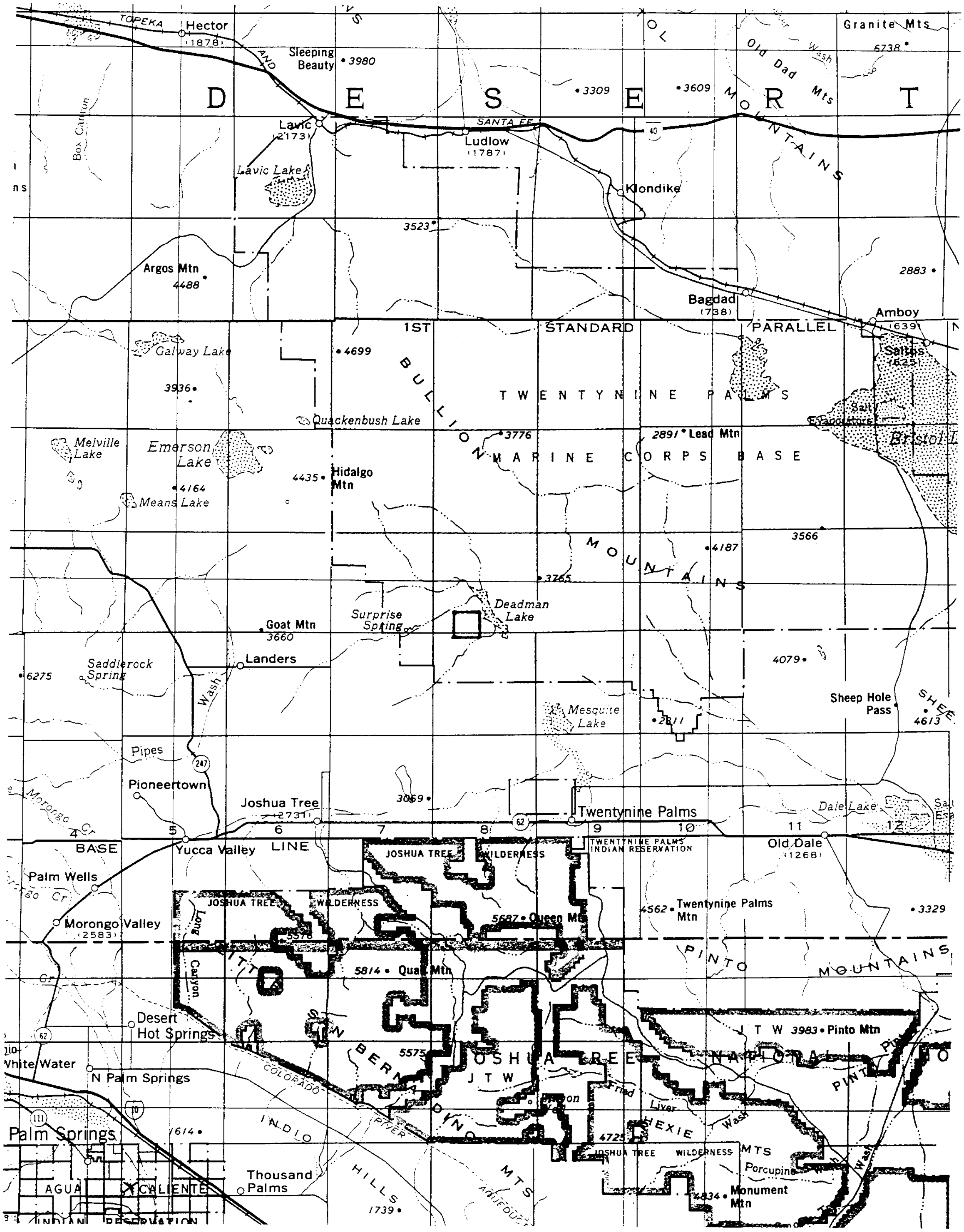

Figure A-1. MCAGCC Site Location (Sheet 1 of 2)

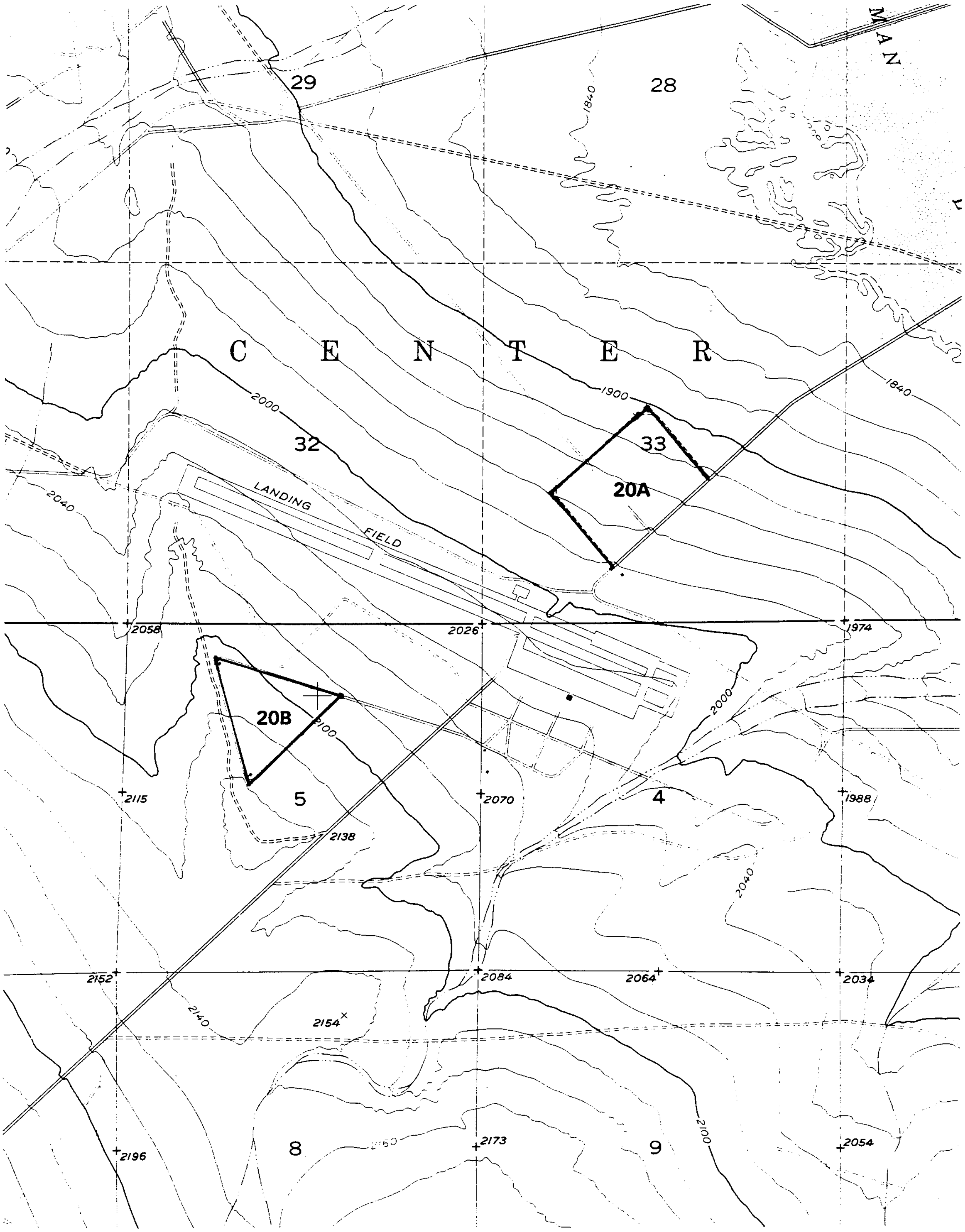

Figure A-1. MCAGCC Site Location (Sheet 2)

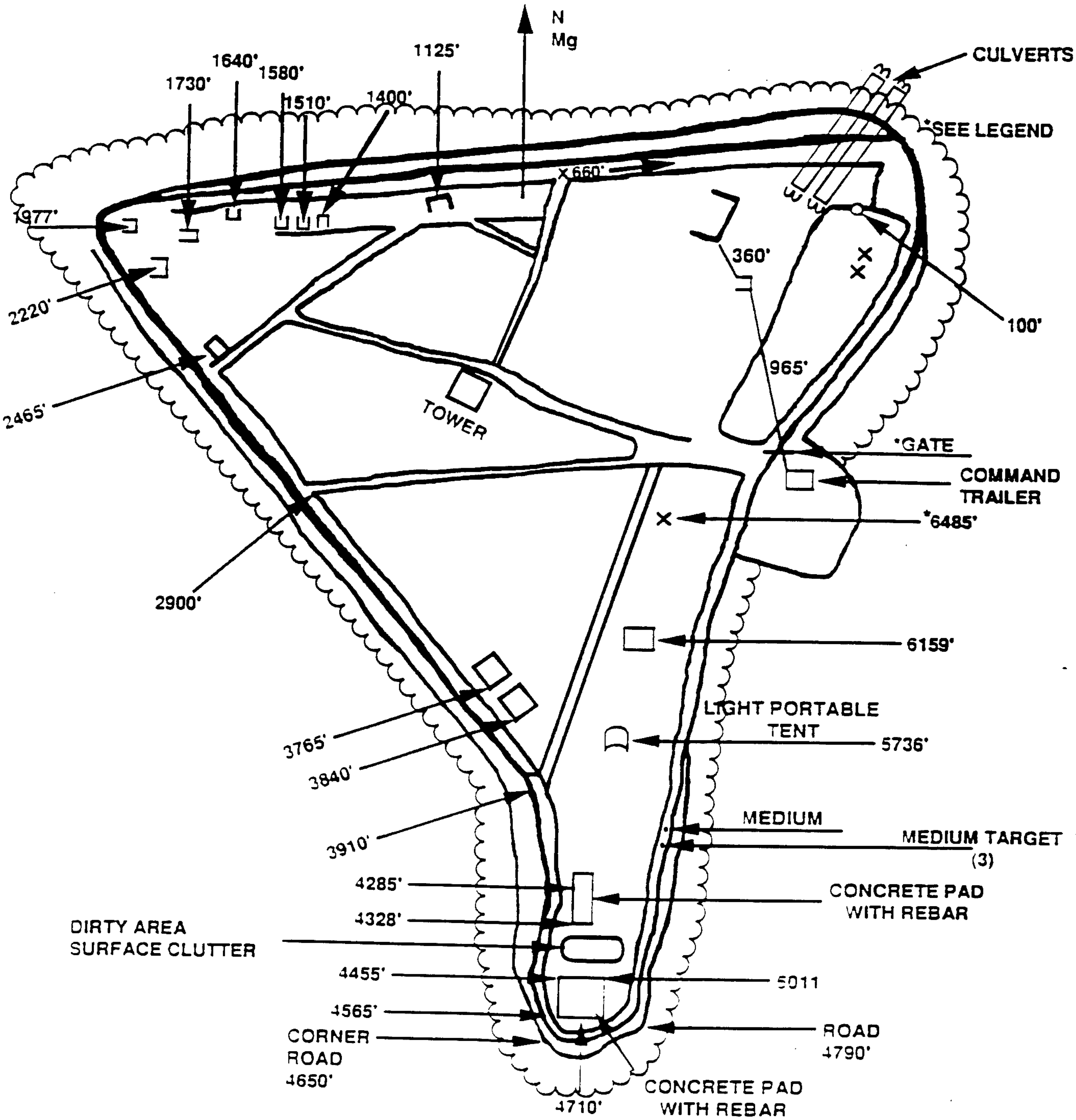

Figure A-2. ASP 20B Site Layout

A.2 Survey Operations

During both survey periods, NAVEODTECHDIV personnel had to modify survey objectives and schedules because of equipment breakdowns, software problems, the high magnetic background noise, and operational considerations. As a result, approximately 50 of the 74 acres in survey site 20B were surveyed, and no surveying was performed at survey site 20A. The MCAGCC provided survey and logistical support during both periods, including secure storage areas, generators, and a commercial backhoe for target validation. Significant events and milestones for each of the survey periods are summarized in the following paragraphs.

A.2.1 **First Survey Period (14 - 26 May 1993).** The first 2 days of this survey period were used to unpack, setup, and checkout the STOLS, command center, and navigation systems at survey site 20B. During setup the DGPS was found to be inoperable for survey operations because of a communications problem between the stationary and mobile stations. During pre-survey site clearance and rough grading of the site, two inert 2.75 inch rocket warheads and a live MK 104 fuze were found on the surface. The site was partitioned into 2 mission areas, one of 50 acres and the other 24 acres; approximately 4 acres at the southern end were determined to be unsurveyable because of reinforced concrete slabs and structures.

Survey operations commenced on 16 May using the RACAL microwave system for navigation. The magnetometer array was set at the lowest ("A") setting, 6 inches above the ground, to increase the probability of detecting small ordnance items. Surveying continued for 3 days using the microwave system; the largest area surveyed in a day was 13 acres, and 5 acres had to be resurveyed due to faulty navigation data.

Survey traverse lines were performed with a north-south orientation to optimize target position fixing. Data was collected for approximately 2 to 4 hours at a time, after which the STOLS returned to the staging area and survey and navigation data were downloaded to the command center workstation. The STOLS then returned to the site to continue the survey while

an operator began data processing in the command center. After surveying operations were halted for the day the results of the data analyses were printed out as a target report.

Relocation and marking of targets using the microwave system mounted on a utility truck began on 19 May. Survey operations using DGPS on the STOLS were conducted from 19 through 21 May. STV survey speed was slowed because the rough terrain was causing DGPS lock-on problems. On two separate occasions, STOLS software problems caused existing survey data files to be overwritten, resulting in the loss of a half day's data in each case. A DGPS failure on 22 May was ultimately determined to be unrepairable in the field and DGPS surveying was suspended. Marking of targets using the microwave system continued.

MCAGCC EOD personnel began excavation of marked targets on 20 May, using a backhoe, picks and shovels, and hand-held ordnance locators. Target locations and depths were documented by a NAVEODTECHDIV representative as a validation record for the STOLS location and classification performance.

Survey operations concluded on 26 May. The site was secured and the STOLS was prepared for storage and moved to secure storage at the MCAGCC.

Geo-Centers participation in the survey was then concluded at the end of the first survey period. The Geo-Centers functions were allocated to NAVEODTECHDIV and PRC personnel.

A.2.2 **Second Survey Period (19 July - 2 August 1993).** During the first 2 days of this survey period, the team performed preventive and corrective maintenance on STOLS equipment and set up the command center at survey site 20B. The plan was to resurvey site 20B using DGPS navigation and a higher magnetometer array setting (setting "D," the highest above the ground), and to survey the areas of that site not covered during the first survey period. However, an MCU failure on the STV prevented accomplishment of any of those planned objectives.

From 21 July through 2 August, the STV was used to mark targets in survey site 20B using DGPS navigation. MCAGCC personnel excavated and recorded target data to validate STOLS target data. Excavation operations were suspended before completing all marked targets.

On 2 August, the site was secured and all STOLS equipment was prepared for shipment and removed to a secure area to await transport.

A.3 Survey Results

Target Maps and target tables from the MCAGCC survey are provided in the following pages.

This page is intentionally left blank

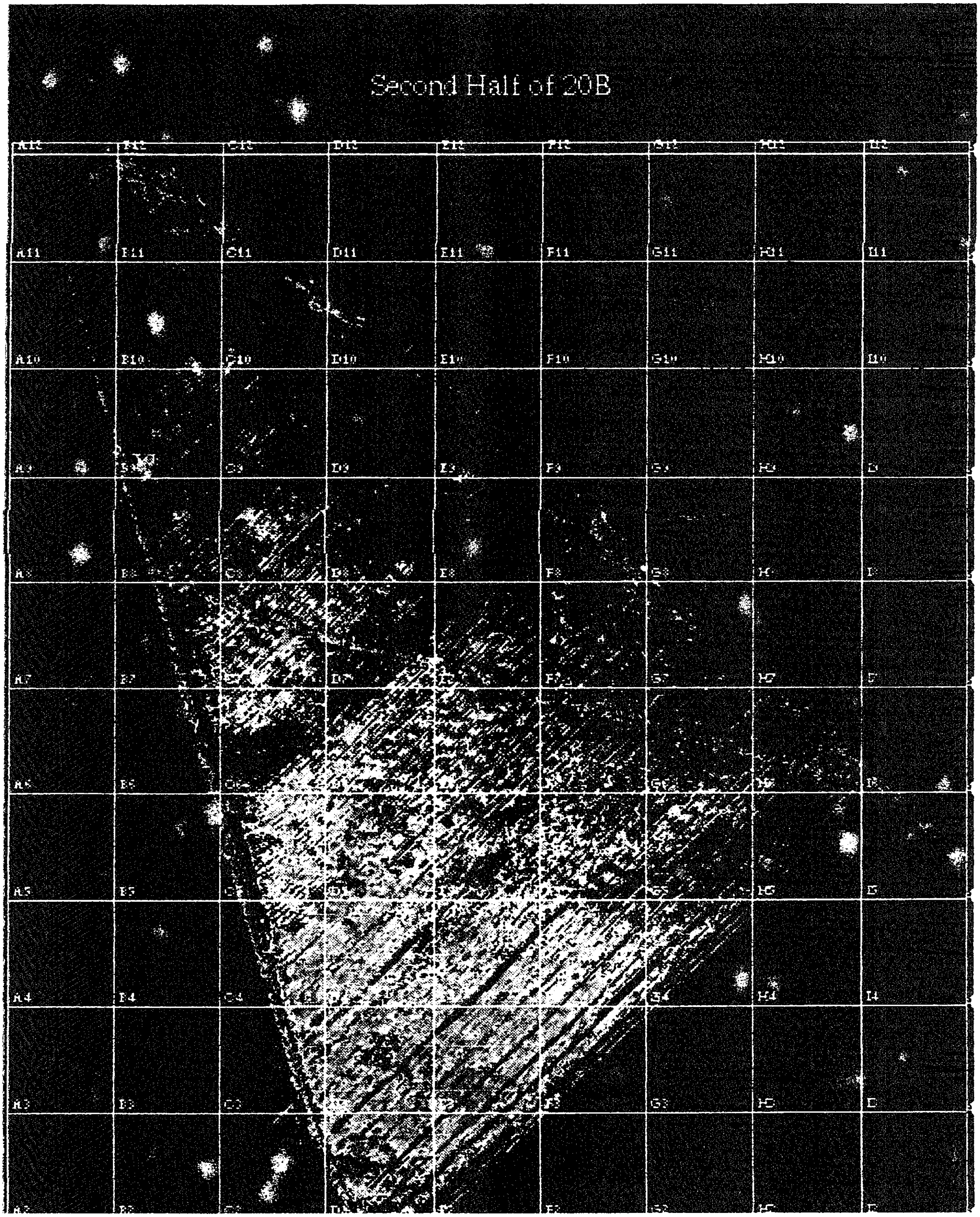

Figure A-3. MCAGCC Target Maps (Sheet 1 of 3)

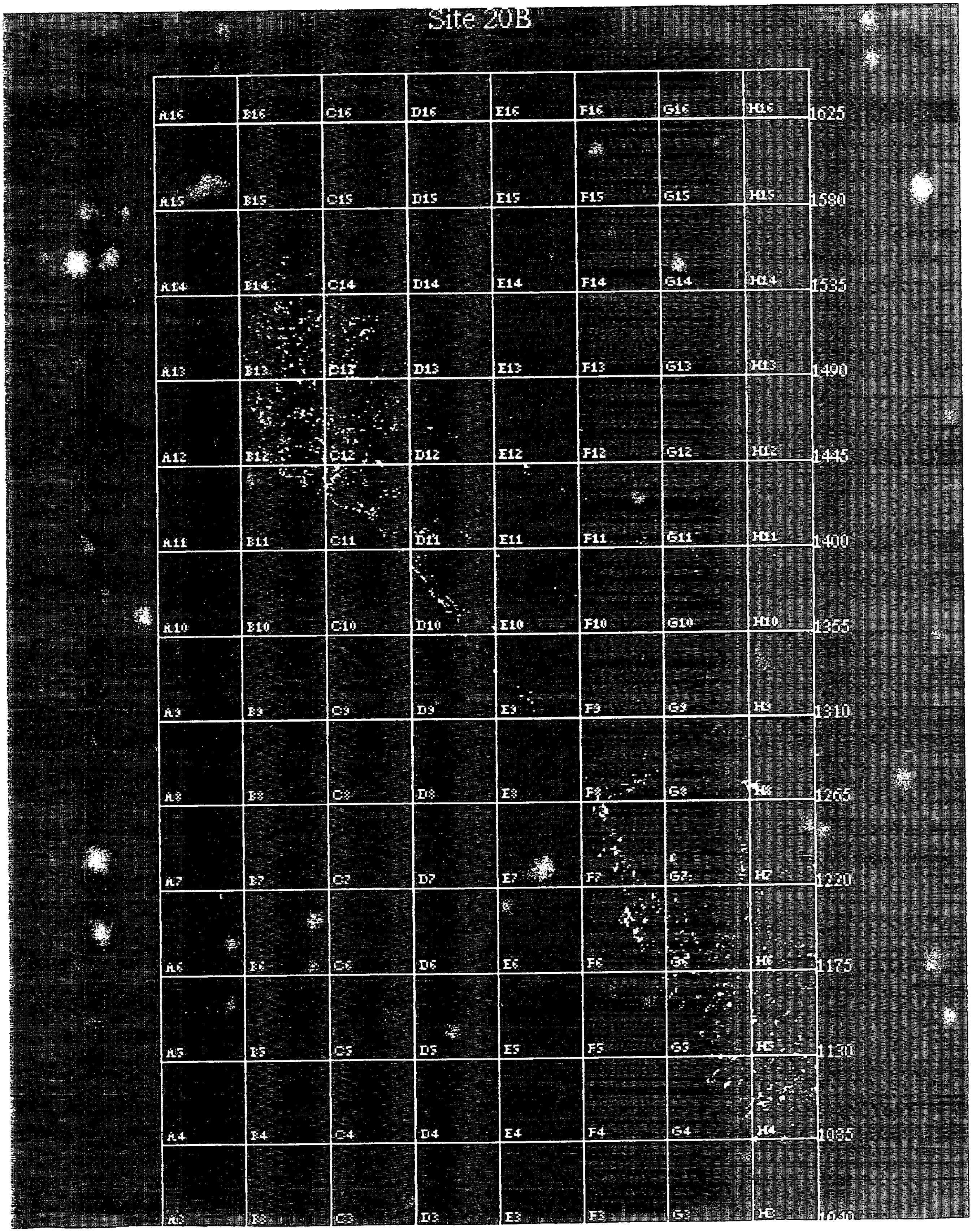

Figure A-3. MCAGCC Target Maps (Sheet 2)

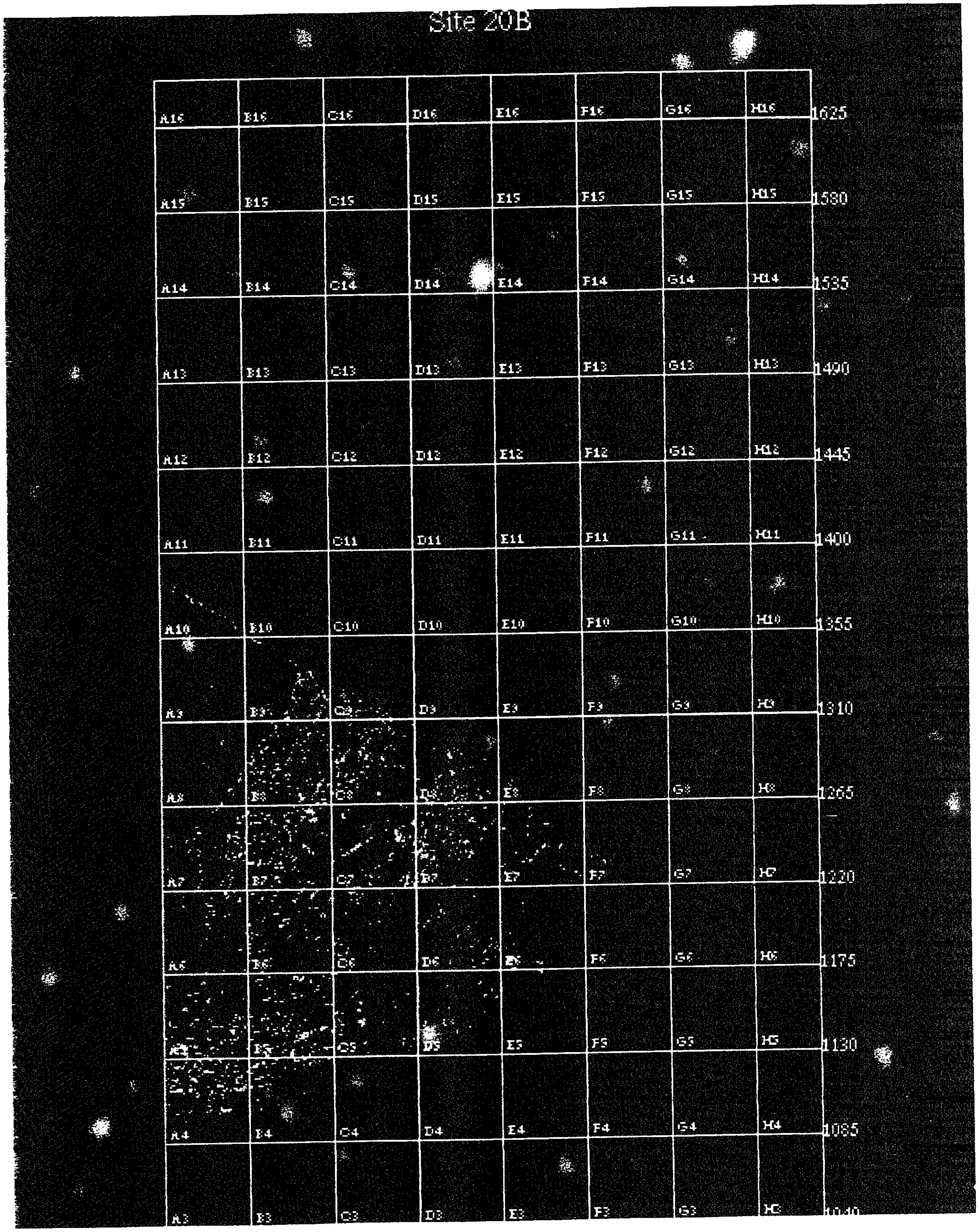

Figure A-3. MCAGCC Target Maps (Sheet 3)

This page is intentionally left blank

****

Site 20B TARGET REPORT Tue May 25 08:10:28 1993

Site ID: MCBB MISSION 1

****

Total number of targets = 248
ID number of last target found = 251
Number of targets deleted = 3

Targ ID	Quadrant	x	y	Depth(m)	Category
219	D1	1106.4	974.2	0.2	s
220	D2	1109.0	1030.9	1.6	l
221	F2	1213.8	1031.5	1.5	l
222	F2	1182.1	1020.8	1.2	s
223	F2	1202.5	1016.0	0.2	s
242	F3	1213.0	1067.9	0.3	?
243	F3	1212.2	1070.8	0.4	?
224	G3	1252.6	1065.5	0.5	s
225	G3	1221.9	1068.1	0.9	?
226	G3	1221.5	1070.4	0.9	?
227	G3	1251.5	1068.4	0.4	?
228	G3	1261.8	1071.1	0.3	s
229	G3	1255.4	1081.3	0.7	m
230	G3	1255.8	1084.3	0.7	l
231	G3	1239.9	1081.1	0.8	?
241	G3	1259.2	1072.8	0.8	s
151	G4	1254.0	1115.7	0.6	?
152	G4	1254.7	1117.0	0.1	s
232	G4	1254.3	1090.2	1.3	l
233	G4	1250.5	1092.5	0.9	l
234	G4	1254.8	1099.7	0.3	?
248	G4	1252.2	1102.9	1.0	?
249	G4	1256.6	1104.5	0.8	?
250	G4	1254.0	1107.2	0.6	m
251	G4	1240.5	1086.5	0.8	?
235	H3	1277.6	1081.3	0.3	m
236	H3	1278.6	1075.9	1.6	?
Comment: Appears Large - Depth Unknown					
240	H3	1276.6	1080.8	0.6	s
7	H4	1286.8	1092.7	0.7	s
8	H4	1288.7	1116.2	1.1	s
9	H4	1286.9	1123.6	0.4	?
185	H4	1291.8	1105.1	3.3	l
186	H4	1298.8	1114.2	0.7	s
187	H4	1286.9	1112.2	2.8	l
188	H4	1281.7	1106.6	1.1	m
189	H4	1286.4	1107.8	0.7	s
190	H4	1269.8	1109.6	0.9	?
191	H4	1266.5	1105.7	1.2	?
192	H4	1280.7	1123.6	2.0	?

193	H4	1279.4	1130.3	0.4	s
194	H4	1296.5	1111.1	0.5	?
195	H4	1293.5	1128.4	1.0	s
196	H4	1285.1	1097.8	0.6	?
197	H4	1299.0	1103.9	0.5	s
198	H4	1267.2	1107.4	0.9	s
199	H4	1295.3	1123.8	0.3	s
200	H4	1291.7	1120.5	2.2	l
201	H4	1294.3	1117.9	0.2	?
202	H4	1271.3	1104.6	0.4	s
203	H4	1282.9	1087.0	0.6	s
204	H4	1268.4	1085.5	1.1	s
205	H4	1270.2	1089.3	0.5	s
237	H4	1270.2	1088.4	0.2	s
238	H4	1266.9	1090.8	0.5	?
239	H4	1285.2	1097.9	0.8	?
244	H4	1292.6	1092.4	0.7	s
245	H4	1296.0	1093.5	0.5	s
246	H4	1295.5	1095.4	0.8	?
247	H4	1292.3	1094.2	0.5	s
129	F6	1206.9	1193.6	0.4	?
130	F6	1208.4	1208.9	0.7	s
131	F6	1202.4	1204.2	0.5	s
132	F6	1206.7	1211.2	1.7	m
133	F6	1215.9	1214.0	0.4	s
134	F7	1185.8	1263.2	1.4	?
135	F7	1192.4	1231.4	0.9	s
136	F7	1202.9	1228.0	0.7	?
137	F8	1205.8	1274.9	0.7	s
138	F8	1204.2	1279.0	0.5	s
139	F8	1201.1	1271.2	0.6	?
140	F8	1191.4	1267.2	0.4	s
153	G5	1229.1	1157.7	0.3	s
154	G6	1228.6	1194.2	0.3	s
155	G6	1229.2	1196.8	0.4	s
156	G6	1226.0	1197.2	0.4	?
157	G6	1230.7	1183.8	0.7	?
158	G6	1225.1	1185.1	0.4	?
159	G6	1222.5	1187.7	0.6	s
160	G6	1229.1	1177.5	0.2	s
28	G7	1225.4	1236.4	0.6	m
29	G7	1225.6	1239.1	1.3	l
30	G7	1225.0	1236.1	0.4	s
31	G7	1226.9	1234.5	0.7	s
161	G7	1226.8	1234.6	0.4	s
162	G7	1225.0	1236.1	0.4	s
163	G7	1224.1	1238.0	0.4	?
164	G7	1233.5	1224.8	0.1	s
165	G7	1251.6	1253.5	0.4	?
166	G8	1264.2	1269.6	0.9	?
167	G8	1262.9	1274.1	0.6	s
168	G8	1262.8	1298.5	0.3	s
206	H5	1291.2	1131.3	1.5	l
207	H5	1286.6	1143.0	0.1	s
208	H5	1293.6	1165.6	0.4	?
3	H6	1289.1	1188.0	?	?
4	H6	1295.4	1181.9	0.5	s
5	H6	1294.0	1187.0	2.3	l

6	H6	1297.3	1186.9	1.0	?
10	H6	1298.6	1186.8	0.7	m
209	H6	1296.9	1187.3	2.0	l
210	H6	1289.9	1186.6	1.5	l
211	H6	1286.6	1190.0	1.2	?
212	H7	1295.4	1234.9	0.8	s
213	H8	1265.8	1301.7	0.2	?
214	H8	1268.2	1274.6	1.4	?
35	B11	1040.0	1437.5	0.3	s
36	B11	1024.9	1439.9	0.7	s
37	B11	1036.7	1441.4	0.6	?
32	B12	1018.9	1469.2	0.4	m
38	B12	1018.9	1469.2	0.4	m
39	B12	1020.9	1474.0	0.7	?
40	B12	1011.1	1475.7	1.2	s
41	B12	1004.1	1474.3	0.6	s
42	B12	1020.7	1469.9	0.5	?
43	B12	1014.4	1448.1	0.1	s
44	B12	1022.1	1483.6	0.4	?
45	B12	1017.7	1484.1	0.2	?
46	B12	1002.2	1478.9	0.2	?
70	C11	1080.1	1423.5	0.5	s
71	C11	1083.5	1425.4	0.1	s
72	C11	1080.5	1432.4	0.7	s
73	C11	1069.2	1428.8	0.3	s
74	C11	1076.7	1409.3	1.3	m
75	C11	1072.5	1411.1	0.6	s
76	C11	1069.0	1411.4	2.9	l
77	C11	1041.9	1428.3	0.7	s
78	C11	1040.0	1437.5	0.3	s
79	C11	1041.1	1440.2	0.6	?
80	C11	1077.0	1431.2	0.5	s
81	C11	1061.4	1443.2	0.3	s
82	C11	1076.6	1412.5	1.1	s
83	C11	1046.3	1439.3	0.4	s
84	C12	1061.2	1474.0	0.3	s
85	C12	1076.6	1477.5	0.2	s
86	C12	1077.9	1478.2	0.1	s
87	C12	1055.9	1486.7	0.2	s
88	C12	1049.0	1462.9	0.3	s
89	C12	1050.0	1469.2	1.1	s
90	C12	1051.3	1475.9	0.5	s
91	C12	1051.1	1474.0	0.5	?
92	C12	1040.8	1464.9	0.4	s
100	D10	1128.0	1361.1	0.4	?
101	D10	1128.8	1358.4	0.7	?
102	D10	1128.9	1394.7	0.5	?
103	D10	1090.4	1396.2	0.3	s
104	D10	1093.1	1397.0	0.3	?
105	D11	1125.0	1419.0	0.5	s
106	D11	1118.3	1419.4	0.6	?
107	D11	1096.4	1412.8	0.6	?
108	D11	1099.2	1414.8	0.1	s
109	D11	1094.0	1406.5	0.8	s
113	E9	1141.4	1327.7	0.3	s
114	E10	1144.6	1391.1	0.4	?
115	E10	1146.7	1384.7	0.4	s

116	E10	1173.4	1374.8	0.2	s
117	E10	1170.6	1370.2	0.5	?
118	E10	1131.7	1397.0	0.5	s
119	E11	1174.7	1436.4	0.6	?
120	E11	1147.7	1442.8	2.3	l
121	E12	1155.8	1474.8	1.1	s
122	E12	1157.2	1477.3	0.6	s
123	E12	1155.2	1477.1	0.2	?
124	E12	1138.7	1464.0	0.3	s
125	E12	1136.8	1463.2	0.3	s
126	E12	1146.2	1446.1	0.1	s
127	E12	1174.2	1461.1	0.2	?
128	E12	1175.5	1462.1	0.5	?
141	F10	1201.3	1362.1	0.5	s
142	F10	1210.7	1383.0	0.4	?
143	F10	1190.6	1388.1	0.5	?
144	F11	1205.8	1402.5	0.8	s
145	F11	1216.8	1414.6	0.2	s
146	F11	1206.7	1404.6	0.4	?
147	F11	1219.6	1414.8	0.9	?
148	F11	1176.6	1439.2	0.6	s
149	F12	1176.8	1461.3	2.1	l
150	F12	1197.8	1450.3	1.6	m
169	G10	1256.8	1395.7	0.3	s
170	G10	1243.7	1364.6	0.4	?
171	G10	1260.2	1390.5	0.2	s
172	G10	1230.7	1394.0	1.7	l
173	G10	1250.0	1393.0	2.2	l
174	G10	1231.4	1390.5	3.8	l
175	G10	1235.0	1398.8	0.9	s
176	G10	1238.7	1395.4	0.2	s
177	G10	1236.9	1393.3	0.3	?
178	G11	1233.4	1411.2	0.1	s
179	G11	1240.3	1409.8	0.5	?
180	G11	1230.6	1409.5	0.5	?
181	G11	1238.9	1399.7	0.2	s
182	G11	1245.1	1427.3	0.1	?
183	G11	1236.0	1420.5	0.5	?
184	G11	1224.8	1408.1	0.3	?
215	H10	1281.2	1396.0	0.4	s
216	H10	1283.0	1398.2	0.6	s
217	H11	1272.9	1403.1	0.4	?
218	H11	1270.8	1401.9	0.2	s
33	A13	994.1	1504.0	0.1	s
34	A13	993.7	1517.1	0.2	?
11	B13	1022.6	1531.3	1.6	l
12	B13	1014.8	1528.7	0.8	m
13	B13	1017.1	1531.7	0.9	?
14	B13	1020.4	1529.0	0.2	s
15	B13	1031.8	1526.7	0.2	s
16	B13	1031.3	1517.4	0.3	s
17	B13	1024.5	1516.9	0.1	s
18	B13	1030.0	1516.4	0.4	s
19	B13	1027.7	1530.6	0.7	s
20	B13	1028.3	1532.3	0.7	s
21	B13	1020.4	1525.9	1.2	s
22	B13	1018.9	1528.0	0.4	?
23	B13	1016.7	1529.1	2.0	l

24	B13	1033.1	1526.7	0.9	?
25	B13	1032.5	1518.4	0.8	?
26	B13	1017.1	1517.9	0.4	s
47	B13	1030.7	1522.9	0.3	?
48	B13	1031.8	1526.7	0.2	s
49	B13	1020.3	1529.0	0.2	s
50	B13	1022.7	1530.8	0.1	s
51	B13	1015.9	1532.2	1.4	l
52	B13	1015.2	1529.4	1.0	l
53	B13	1011.0	1517.6	0.5	s
54	B13	1001.9	1523.5	0.4	?
55	B13	1018.8	1502.4	0.3	s
56	B13	1022.9	1497.0	0.9	s
57	B13	1032.1	1500.2	0.1	?
58	B13	1034.1	1506.8	0.3	?
59	B13	1031.1	1520.7	0.6	?
60	B13	1038.2	1523.0	1.8	m
61	B13	1036.9	1520.8	0.4	s
62	B13	1039.0	1504.8	0.5	s
63	B13	1010.7	1515.1	0.4	?
64	B13	1010.0	1512.5	0.2	s
65	B14	1015.9	1545.8	0.1	s
66	B14	1015.1	1545.1	0.1	s
67	B14	1012.8	1544.3	0.5	?
68	B14	1022.1	1540.1	0.4	?
69	B14	1018.3	1541.3	0.2	s
93	C13	1070.7	1494.5	0.4	?
94	C13	1083.4	1497.2	0.8	?
95	C13	1081.1	1507.0	0.1	s
96	C13	1058.7	1494.0	0.5	s
97	C13	1059.6	1494.6	0.8	?
98	C13	1058.1	1490.9	0.3	s
99	C13	1052.3	1510.5	0.4	s
110	D13	1108.1	1509.4	0.3	?
111	D13	1109.3	1510.4	0.5	?
112	D13	1093.8	1495.5	0.2	?

****

Site 20B TARGET REPORT Sat May 22 11:45:14 1993

Site ID: MCBB MISSION 2

****

Total number of targets = 152
ID number of last target found = 152
Number of targets deleted = 0

Targ ID	Quadrant	x	y	Depth(m)	Category
90	A7	1342.3	1238.4	0.1	s
91	A8	1332.0	1297.7	0.7	?
92	A8	1331.8	1299.0	0.1	s
93	A8	1333.1	1299.4	0.6	?
94	A8	1338.4	1296.7	0.1	?
82	B7	1379.1	1242.3	1.1	m
83	B7	1378.4	1240.8	0.6	?
84	B7	1361.4	1224.0	0.3	s
85	B7	1379.3	1263.6	0.3	?
86	B7	1365.1	1259.4	0.3	s
87	B7	1385.9	1251.4	0.5	?
88	B7	1360.2	1247.8	0.2	?
89	B7	1368.0	1251.8	0.5	s
95	B8	1379.0	1266.4	0.5	m
96	B8	1388.1	1276.7	0.6	s
97	B8	1369.7	1290.4	0.4	?
64	C7	1428.4	1251.9	2.0	l
65	C7	1429.7	1246.7	1.2	l
66	C7	1424.3	1239.6	0.9	l
67	C7	1432.7	1254.7	2.5	?
68	C7	1433.5	1237.6	0.5	s
69	C7	1434.3	1229.4	0.3	l
Comment: Large Mass					
70	C7	1400.5	1260.6	0.2	?
71	C7	1396.1	1258.1	0.3	?
72	C7	1394.8	1259.2	0.7	s
73	C7	1402.2	1223.6	1.2	s
74	C7	1406.6	1221.9	0.4	s
75	C7	1399.6	1241.1	0.8	s
76	C7	1396.3	1237.4	0.7	?
77	C7	1430.2	1263.5	0.4	?
78	C7	1430.3	1262.5	0.9	?
79	C7	1422.4	1245.1	0.1	s
80	C7	1430.6	1242.9	1.0	l
81	C7	1434.7	1252.7	0.5	s
98	C8	1421.3	1305.0	0.6	?
Comment: Possible surface trash					
99	C8	1422.8	1301.6	0.2	s
100	C8	1432.8	1276.2	0.8	s
101	C8	1434.9	1278.5	1.2	l
102	C8	1409.2	1278.7	0.3	?

103	C8	1425.6	1286.2	0.3	s
104	C8	1429.2	1284.0	0.6	?
105	C8	1427.6	1285.6	0.9	s
106	C8	1430.3	1301.2	0.4	s
107	C8	1397.9	1289.9	1.0	m
108	C8	1416.8	1271.7	0.5	s
109	C8	1406.6	1291.0	0.9	?
110	C8	1409.8	1298.3	1.2	?
111	C8	1400.5	1306.6	0.3	s
112	C8	1402.1	1307.0	0.5	s
113	C8	1397.5	1280.1	1.1	?
114	C8	1416.2	1280.9	0.7	s
115	C8	1395.0	1281.7	0.6	s
116	C8	1395.1	1276.3	0.9	s
117	C8	1393.8	1287.9	0.9	?
118	C8	1394.3	1291.1	0.5	s
119	C8	1412.2	1292.9	0.9	s
120	C8	1401.4	1300.7	0.2	?
37	D7	1444.7	1236.1	0.9	?
Comment: Possible Medium - Trashy					
38	D7	1446.4	1231.5	0.7	?
Comment: Possible Medium/Large - Trashy					
39	D7	1441.3	1249.5	0.3	m
40	D7	1476.7	1253.9	0.5	s
41	D7	1468.8	1259.0	0.9	?
42	D7	1466.0	1259.8	0.2	s
43	D7	1462.0	1259.7	0.9	?
44	D7	1444.7	1240.1	1.1	?
45	D7	1436.8	1236.8	1.0	?
46	D7	1437.8	1226.4	0.9	l
Comment: Appears Very Large					
47	D7	1452.2	1252.8	0.4	?
48	D7	1440.7	1255.1	0.7	l
49	D7	1436.2	1261.0	0.5	s
50	D7	1458.5	1244.3	0.5	?
51	D7	1465.6	1254.8	0.3	?
52	D7	1472.9	1258.1	0.5	?
53	D7	1472.7	1262.5	0.2	s
54	D7	1472.0	1250.3	0.1	s
55	D7	1471.0	1245.9	0.5	s
56	D7	1456.0	1221.1	0.2	s
57	D7	1434.8	1241.2	0.9	m
58	D7	1464.2	1239.9	0.7	s
59	D7	1440.4	1223.3	0.1	s
60	D7	1454.1	1239.6	0.4	?
61	D7	1469.3	1251.6	1.2	?
62	D7	1448.6	1257.4	0.4	?
63	D7	1434.5	1252.9	0.9	?
Comment: Possible Large					
121	D8	1455.7	1290.4	0.6	s
122	D8	1457.9	1292.6	0.8	?
123	D8	1456.0	1293.6	0.7	?
124	D8	1457.5	1295.6	0.4	?
125	D8	1471.2	1268.8	0.7	s
126	D8	1436.4	1277.2	0.6	?
127	D8	1444.4	1266.0	0.4	l
128	D8	1446.5	1278.4	0.1	s
129	D8	1462.5	1275.2	0.7	l
130	D8	1445.8	1275.4	0.1	s
131	D8	1466.4	1277.1	0.2	?

132	D8	1456.9	1277.1	0.8	?
133	D8	1448.3	1279.6	0.8	?
134	D8	1435.8	1269.9	0.8	l
135	D8	1437.6	1268.8	0.1	s
136	D8	1451.3	1274.5	1.5	?
1	E6	1492.8	1211.1	0.3	?
2	E6	1501.5	1209.6	0.2	?
3	E6	1485.4	1195.1	0.1	s
4	E6	1491.8	1193.5	0.3	?
5	E6	1482.9	1186.7	0.4	?
6	E6	1494.9	1178.9	0.3	s
7	E6	1482.7	1179.4	0.4	s
8	E6	1480.5	1200.6	0.4	?
9	E6	1498.3	1218.1	0.3	?
10	E6	1487.5	1179.9	1.4	m
11	E6	1500.8	1177.9	0.5	s
12	E6	1496.9	1181.4	0.3	?
13	E6	1493.2	1183.5	0.3	?
14	E6	1491.0	1176.3	0.6	s
15	E6	1488.0	1176.0	0.2	s
20	E7	1496.6	1261.5	0.1	s
21	E7	1498.1	1257.9	0.4	s
22	E7	1494.6	1248.3	0.5	s
23	E7	1481.8	1259.9	0.1	s
24	E7	1513.8	1231.7	0.1	s
25	E7	1514.7	1229.6	0.6	?
26	E7	1516.7	1228.8	0.2	s
27	E7	1520.6	1228.2	0.6	s
28	E7	1505.5	1252.8	0.3	s
29	E7	1502.0	1248.9	1.2	m
30	E7	1504.1	1259.7	0.8	s
31	E7	1488.1	1237.9	0.3	?
32	E7	1521.3	1233.4	1.0	s
33	E7	1519.2	1232.5	0.2	?
34	E7	1483.7	1251.5	1.7	m
35	E7	1486.9	1262.6	0.3	?
36	E7	1517.4	1248.1	0.2	?
137	E8	1487.7	1277.4	0.4	s
16	F7	1531.0	1236.7	1.1	s
17	F7	1536.6	1232.7	0.8	s
18	F7	1529.9	1228.6	1.0	?
Comment: Possible Medium Target					
19	F7	1525.9	1231.3	0.6	m
148	A10	1341.7	1358.5	0.4	?
149	A10	1339.6	1361.4	0.3	m
150	A10	1339.0	1362.5	0.4	s
151	A10	1316.1	1376.5	0.9	s
152	A10	1310.7	1382.1	0.2	?
138	B9	1358.1	1313.6	0.1	s
139	B9	1374.8	1322.1	0.3	s
140	B9	1376.5	1332.1	1.8	l
141	B9	1373.1	1331.9	0.4	s
142	C9	1416.5	1311.4	0.1	s
143	C9	1413.7	1312.1	0.5	s
144	C9	1408.4	1314.8	0.8	?
145	C9	1401.7	1320.5	0.7	s
146	C9	1404.4	1318.3	0.4	?

147	C9	1398.2	1314.0	0.2	s

****

Second Half of 20B TARGET REPORT Sat May 22 14:40:51 1993

Site ID: MCBC MISSION 2

****

Total number of targets = 279
ID number of last target found = 281
Number of targets deleted = 2

Targ ID	Quadrant	x	y	Depth(m)	Category
222	C4	6287.1	4589.3	2.2	l
223	C4	6289.6	4586.1	3.6	l
165	D1	6319.3	4451.9	0.6	l
166	D1	6313.1	4449.7	0.6	s
167	D1	6308.9	4441.2	0.2	s
168	D1	6305.5	4437.2	0.2	s
Comment: Looks Large					
169	D1	6315.9	4433.9	1.4	s
170	D1	6320.7	4440.4	1.1	s
171	D2	6317.2	4479.4	0.5	m
172	D2	6309.0	4477.6	0.2	s
173	D2	6304.5	4478.9	0.7	?
174	D2	6302.3	4478.5	1.4	l
175	D2	6295.7	4480.5	1.0	s
176	D2	6296.4	4476.5	0.2	s
177	D2	6294.6	4473.5	0.7	s
178	D2	6311.5	4493.0	0.1	s
179	D2	6315.2	4460.6	0.4	s
180	D2	6320.3	4455.5	0.7	m
181	D2	6316.0	4456.5	1.1	l
182	D2	6302.6	4460.4	0.9	s
183	D2	6322.2	4469.7	1.6	m
184	D2	6323.8	4462.6	1.1	l
185	D2	6305.9	4490.4	1.8	m
186	D2	6326.8	4479.5	2.1	m
187	D2	6317.4	4475.4	1.6	m
188	D2	6314.2	4484.7	0.4	s
189	D2	6314.3	4455.9	3.0	?
190	D2	6320.2	4479.0	1.4	s
191	D3	6308.4	4515.7	0.3	s
192	D3	6300.8	4515.0	0.7	?
Comment: Appears Small					
193	D3	6305.7	4522.9	0.3	s
Comment: Missed Area - Possible Large					
194	D3	6311.8	4523.2	0.5	m
195	D3	6314.3	4521.1	1.0	?
196	D3	6319.3	4528.3	0.5	s
197	D3	6318.3	4531.3	0.6	m
198	D3	6312.3	4531.6	0.3	m
199	D3	6332.5	4518.2	0.6	?
200	D3	6322.3	4517.4	2.4	l
201	D3	6326.0	4513.3	1.8	m

202	D3	6331.4	4510.7	0.4	?
203	D3	6299.5	4508.2	0.1	s
204	D3	6288.3	4528.2	0.3	?
Comment: Missed Area - Possible Medium/Large					
205	D3	6332.4	4521.5	0.2	s

128	E2	6358.3	4476.9	0.1	?
Comment: Smeary Nav.					
129	E2	6341.2	4473.9	0.9	s
130	E3	6335.3	4518.3	0.5	s
131	E3	6339.6	4506.0	0.3	s
132	E3	6345.9	4508.5	0.4	?
133	E3	6348.4	4527.6	0.5	s
134	E3	6360.1	4515.3	2.2	?
Comment: Maybe Large/Medium					
135	E3	6337.2	4519.3	0.8	?
136	E3	6347.4	4519.9	1.0	?
137	E3	6348.1	4517.9	0.4	s
138	E3	6380.2	4508.3	0.2	s
139	E4	6362.9	4550.1	0.6	s
110	F3	6391.7	4512.7	0.7	s
111	F3	6395.7	4533.7	1.0	?
Comment: Looks Medium					
112	F3	6387.5	4514.5	1.1	s
113	F3	6385.8	4513.7	1.1	s
114	F3	6395.6	4513.2	0.6	s
115	F3	6389.7	4508.6	2.0	?
116	F3	6380.0	4508.2	0.2	s
117	F3	6398.3	4537.1	1.0	s

251	B5	6244.5	4630.8	1.0	s
252	B6	6245.0	4677.7	1.1	?
253	B6	6244.8	4679.6	1.2	?
254	B6	6237.2	4660.8	0.3	s
255	B6	6233.5	4661.3	1.1	s
256	B6	6236.4	4655.4	1.3	m
257	B7	6244.0	4680.0	0.8	m
258	B7	6236.2	4720.0	0.6	s
259	B7	6234.3	4720.4	1.1	s
260	B7	6236.2	4723.2	0.1	s
261	B7	6219.3	4721.9	0.7	s
262	B8	6227.5	4757.2	2.0	l
263	B8	6220.7	4730.4	0.9	s
264	B8	6217.6	4726.9	0.6	s

224	C5	6275.7	4622.2	1.5	s
225	C5	6258.3	4627.7	1.9	m
226	C5	6251.6	4628.8	2.6	l
Comment: Very Large					
227	C7	6285.0	4690.5	1.4	s
228	C7	6278.0	4693.4	0.8	s
229	C7	6279.7	4696.3	0.3	s
230	C7	6283.4	4703.2	0.9	s
231	C7	6279.2	4704.9	1.6	m
232	C7	6275.0	4702.8	2.4	l
233	C7	6268.3	4720.0	0.5	s
234	C7	6265.0	4706.4	1.2	s
235	C7	6259.6	4707.5	1.8	m
236	C7	6282.2	4701.6	2.9	l
237	C7	6261.9	4708.6	2.5	l

238	C7	6250.4	4720.5	1.0	s
239	C7	6269.4	4723.5	0.2	s
240	C7	6276.3	4682.2	0.6	s
241	C7	6247.4	4716.2	0.9	s
242	C7	6266.1	4717.9	0.2	s
243	C7	6268.5	4718.6	0.4	s
244	C7	6264.0	4721.4	0.1	s
245	C7	6263.3	4719.6	0.2	s
246	C7	6276.6	4708.7	0.9	s
247	C8	6278.3	4744.0	1.0	s
248	C8	6254.9	4755.0	2.0	?
Comment: Faint - Possible Medium/Large					
249	C8	6256.6	4758.1	2.3	m
250	C8	6258.6	4745.4	2.2	m
206	D5	6308.9	4633.2	2.2	l
207	D5	6301.1	4630.9	0.8	s
208	D5	6300.0	4597.3	2.9	?
Comment: Appears Large					
209	D5	6298.6	4619.0	0.6	s
210	D7	6321.2	4717.6	2.9	l
211	D7	6323.7	4692.6	1.5	s
212	D7	6299.9	4682.2	4.5	l
213	D7	6303.0	4698.7	0.9	s
214	D7	6308.9	4696.6	0.5	s
215	D7	6319.9	4692.5	1.3	s
216	D7	6293.1	4701.5	1.5	s
217	D8	6320.2	4735.1	2.4	m
218	D8	6317.8	4728.0	0.5	s
219	D8	6302.1	4728.7	1.3	s
220	D8	6304.4	4727.7	0.4	s
221	D8	6317.0	4736.3	0.2	?

1	E5	6353.0	4604.7	1.3	l
2	E5	6358.8	4605.8	2.4	l
140	E5	6370.4	4596.9	0.5	s
141	E5	6345.1	4629.5	0.6	s
142	E5	6359.9	4609.1	1.3	m
143	E5	6337.6	4591.8	0.7	s
144	E5	6343.4	4596.5	0.7	s
145	E5	6376.7	4596.1	0.1	s
146	E5	6346.1	4613.0	0.7	s
147	E5	6337.2	4613.7	0.8	s
148	E5	6359.9	4601.6	1.6	l
149	E5	6350.3	4634.7	1.1	s
150	E5	6336.8	4597.2	0.4	s
151	E5	6363.6	4606.5	0.9	s
152	E6	6339.4	4637.5	0.4	s
153	E6	6347.7	4660.7	0.3	s
154	E6	6376.9	4677.6	0.9	s
155	E6	6374.4	4678.1	0.8	s
156	E7	6374.3	4707.6	0.6	s
157	E7	6354.0	4701.8	0.8	s
158	E7	6363.4	4703.3	0.6	?
159	E7	6341.5	4688.4	1.5	s
160	E8	6350.7	4752.5	1.0	s
161	E8	6379.7	4756.8	0.2	?
162	E8	6373.6	4748.3	0.3	?
118	F5	6424.1	4626.4	0.4	s
119	F5	6421.8	4628.8	0.1	s
120	F5	6391.7	4596.6	0.2	s

121	F6	6401.8	4672.9	1.6	m
122	F6	6407.1	4677.4	1.1	m
123	F6	6411.4	4673.9	1.6	m
124	F6	6412.6	4671.8	1.1	m
125	F6	6417.8	4665.6	1.1	s
126	F6	6384.1	4677.8	1.3	m
127	F6	6415.8	4662.7	0.7	s
3	F7	6392.1	4701.5	0.6	s
4	F7	6421.3	4701.7	0.7	s
6	F7	6406.2	4697.3	0.8	s
7	F7	6396.5	4690.6	1.4	m
41	F7	6390.4	4721.9	3.1	l
42	F7	6392.1	4701.4	0.6	s
43	F7	6396.5	4690.5	1.4	m
44	F7	6401.1	4694.5	1.0	s
45	F7	6406.2	4697.3	0.7	s
46	F7	6408.4	4695.9	0.6	s
47	F7	6415.5	4691.9	0.7	s
48	F7	6418.8	4696.3	1.2	s
49	F7	6418.5	4725.0	0.9	s
50	F7	6415.4	4723.5	1.5	m
51	F7	6418.7	4718.1	1.4	s
52	F7	6412.4	4684.4	1.3	s
53	F7	6409.4	4681.8	0.9	s
54	F7	6421.0	4713.2	0.8	s
55	F7	6412.1	4696.4	0.3	s
56	F7	6418.4	4699.2	0.3	s
57	F7	6414.8	4688.9	0.3	s
28	F8	6409.4	4747.8	1.2	s
29	F8	6403.9	4757.7	1.7	m
30	F8	6410.7	4733.9	4.4	l
31	F8	6401.6	4747.2	1.6	s
32	F8	6392.2	4739.9	1.2	s
33	F8	6417.8	4727.9	0.8	s
34	F8	6418.6	4725.0	0.7	s
35	F8	6415.2	4724.5	2.2	l
36	F8	6418.2	4733.1	1.5	m
37	F8	6416.0	4742.6	0.7	s
38	F8	6389.9	4752.2	0.3	s
39	F8	6385.1	4756.9	0.1	?
40	F8	6387.6	4739.2	0.2	?
-------	-------	-------	-------	-------	-------
106	G5	6440.9	4604.4	0.5	s
107	G5	6459.5	4604.8	3.8	l
108	G5	6460.3	4595.4	0.3	s
109	G5	6466.0	4596.5	0.6	s
82	G6	6458.0	4638.6	0.3	s
83	G6	6427.7	4665.0	0.5	s
84	G6	6456.5	4658.4	0.8	?
85	G6	6454.5	4656.5	0.1	s
86	G6	6444.5	4664.5	0.5	s
87	G6	6431.0	4678.5	1.6	l
88	G6	6429.6	4666.5	0.8	s
89	G6	6440.4	4655.6	1.5	m
90	G6	6446.1	4658.5	0.8	s
91	G6	6426.9	4674.1	0.6	s
58	G7	6444.2	4711.8	0.3	s
60	G7	6434.7	4700.2	1.2	s
61	G7	6438.2	4701.0	0.9	s
62	G7	6444.6	4702.5	1.2	s

63	G7	6443.0	4702.4	0.5	s
64	G7	6440.9	4710.5	0.8	s
Comment: Nav Smear - Appears Large					
65	G7	6430.3	4690.7	0.3	?
66	G7	6432.6	4691.0	0.4	s
67	G7	6427.1	4694.7	0.6	s
68	G7	6436.7	4681.6	1.0	s
69	G7	6435.3	4684.1	0.5	s
163	G8	6426.9	4728.1	0.1	s
164	G8	6426.7	4729.6	0.3	?
103	H5	6499.7	4624.6	0.6	s
104	H5	6477.1	4620.5	0.5	s
105	H5	6509.2	4622.2	1.0	l
Comment: Appears Very Large					
70	H6	6491.4	4669.2	2.9	l
71	H6	6481.0	4677.4	0.4	s
72	H6	6486.6	4672.5	1.3	s
73	H6	6492.2	4672.3	0.4	s
74	H6	6504.4	4662.5	1.1	l
75	H6	6514.6	4638.8	0.4	s
76	H6	6510.8	4643.8	0.6	?
77	H6	6472.6	4657.2	0.4	?
78	H6	6477.9	4649.7	0.9	s
79	H6	6500.1	4638.4	1.4	s
80	H6	6504.8	4639.6	0.7	s
81	H6	6498.9	4662.1	0.3	s
92	I5	6541.6	4628.5	1.9	l
93	I5	6547.8	4619.5	2.7	l
94	I5	6550.9	4616.6	0.6	?
95	I5	6538.4	4625.4	0.8	?
96	I5	6531.3	4635.5	0.1	s
97	I5	6538.0	4627.8	0.2	?
98	I5	6537.8	4629.7	0.1	?
99	I5	6543.5	4623.6	0.1	s
100	I5	6542.8	4622.9	1.9	m
101	I5	6553.4	4615.1	0.2	?
102	I6	6515.3	4641.5	0.5	s
281	A10	6183.0	4832.4	0.4	?
279	A11	6195.4	4900.8	0.9	s
280	A11	6197.5	4902.9	0.9	s
265	B9	6214.1	4781.0	3.6	l
266	B11	6214.1	4887.3	0.6	?
267	B11	6212.3	4886.5	0.7	?
268	B11	6212.4	4888.3	0.5	?
269	B11	6210.4	4891.8	0.6	?
270	B11	6209.2	4892.5	0.4	?
271	B11	6221.3	4889.7	1.7	m
272	B11	6234.7	4877.0	1.3	s
273	B11	6213.4	4884.0	1.3	m
274	B11	6204.0	4895.0	1.0	s
275	B11	6216.5	4878.8	0.7	s
276	B11	6228.1	4873.4	0.2	s
277	B11	6210.3	4903.0	2.0	m
278	B11	6202.6	4899.3	1.0	s
8	C10	6285.4	4838.7	5.8	l
Comment: Large Deep Target					
9	C10	6283.3	4835.8	4.0	l

Comment: Large Deep Target

16	C11	6252.1	4867.7	1.1	m
17	C11	6258.3	4870.0	0.7	s
10	D10	6303.5	4838.3	2.1	m
11	D10	6297.1	4841.9	0.3	s
12	D10	6291.2	4841.4	1.9	m
13	D10	6302.6	4833.8	0.5	?
14	D10	6321.4	4835.4	0.4	s
15	D10	6297.1	4841.8	0.3	s
18	E9	6367.4	4778.9	0.1	?
19	E9	6339.1	4774.5	0.6	?
20	E9	6352.1	4798.4	1.8	m
21	E9	6341.6	4808.1	0.5	s
22	E9	6351.6	4801.4	0.9	s
23	E9	6349.4	4803.1	0.9	s
24	E9	6344.3	4806.2	0.3	s
25	E9	6372.1	4785.1	0.2	?
26	E9	6370.7	4783.5	0.2	?
27	E9	6341.1	4796.4	0.3	s

This page is intentionally left blank

APPENDIX B
JPG SURVEY

B.1 Site Characteristics

JPG is located about 5 miles north of Madison, Indiana, in Jefferson, Ripley, and Jennings Counties (see figure B-1). The facility covers nearly 55,265 acres and includes firing lines, impact areas, buildings, roadways, and other structures. Within the facility property two areas have been selected for use as UXO detection technology demonstration areas. A 40 acre area located in the northwest quarter of Section 36, T6N, R10E, was designed for demonstration of UXO detection technologies that are portable by manpower or that can be towed across the site's surface. An 80 acre area located at the center of Section 14, T5N, R10E, was designed for demonstration of airborne UXO detection systems. The 40 acre area (see figure B-2) was used for the STOLS prototype demonstration.

Both areas are located on the access road along the east side of the facility. Both areas have only sparse forestation. These areas are not known to contain residual UXO, hazardous substances, or hazardous wastes. Drainage at the 40 acre site is to the west into Big Creek. Drainage at the 80 acre area is to the east into West Fork Creek.

The unconsolidated materials on the 40 acre area vary in thickness from approximately 22 feet in the center to 5 feet in the west. The surface soils have been mapped as belonging to the Avonburg, Cobbsfork, and Rossmoyne soil series. These soils developed on a thin mantle of wind blown silt (loess) atop glacial drift. The Cobbsfork series is found on the uplands, is poorly drained, and has slow permeability. This soil tends to be a hydric with water content near saturation much of the year. The Avonburg series has developed on either gently sloping or nearly level topographic features. The Rossmoyne series developed on the hill sides with 0 to 2 percent slopes. Below the surface soils is a fragipan that inhibits the vertical migration of water within the soil horizon. The fragipan and the remaining unconsolidated materials are remnants of the Illinoian age glacial drift. Below the drift is varying thickness of residual clays with

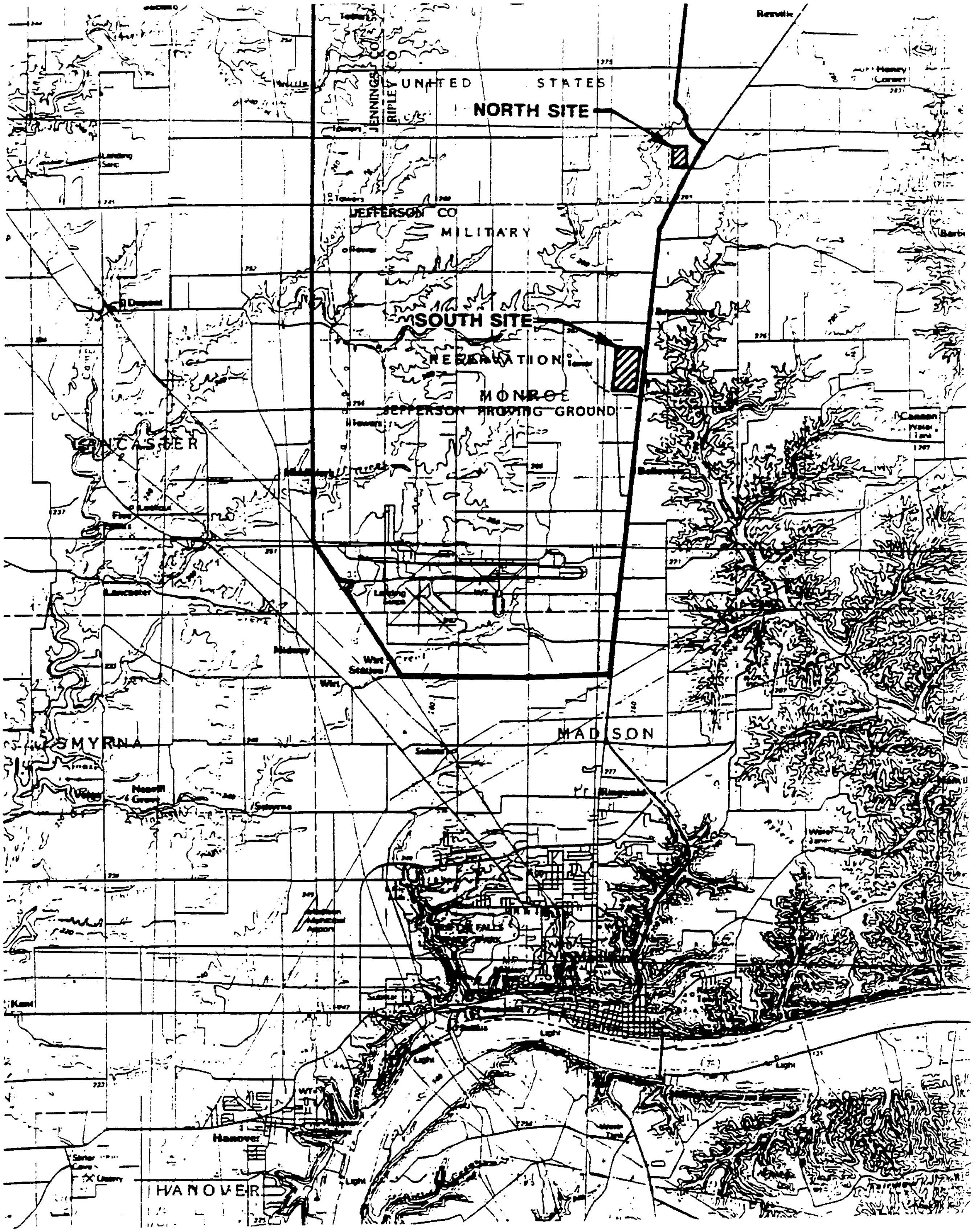

Figure B-1. JPG Site Location

Figure B-2. JPG 40-Acre Site Layout

abundant chert fragments, developed from the weathering of surfacial bedrock. The bedrock surface below each site is fairly flat lying with valleys and solution channels eroded into the surface. The bedrock is either limestone or shale depending on the amount of dissection of the rock surface.

The hydrogeology of the two areas is the product of the various geologic materials. The upper soil horizons tend to be wet due to the fragipan inhibiting the downward migration of water. This in turn allows for water to be drained out of the drift materials by the underlying limestone bedrock. The drift has a low moisture content and is generally not saturated above the bedrock. The exception to this is where the bedrock is shale which allows even less migration of water than the fragipan. In these areas the drift may be saturated above the bedrock. Generally, however, aside from the wet surface soil, there is very little groundwater above the bedrock.

Geophysical investigations consisting of total magnetic field (TMF) and vertical electric sounding (VES) surveys were performed at the 40 and 80 acre test sites located at JPG. The purpose of the investigation was to provide a characterization of the respective test sites prior to locating targets for the upcoming technology demonstration.

The TMF measurements at both sites were collected at the four corners of grid stations with a spacing of 100 feet. The magnetic readings were collected using a Geometric G-856 proton precession memory magnetometer. A base station was established to determine the background magnetic field, record diurnal variations in the field, and to detect possible magnetic storm activity. The TMF measurements were corrected for diurnal variation to achieve a 1-gamma resolution for each grid station. Isomagnetic contour maps were constructed to locate anomalous areas at the respective test sites. A preliminary data review indicates that total magnetic field measurements at the respective test sites are within 30 gammas of the magnetic background established at the base station. Variations in the magnetic field primarily appear to be caused by ferro-magnetic debris associated with previous farming activity at the test sites.

The VES surveys were performed at the respective test sites using a Wenner electrode arrangement. Electrode spacings of 3, 5, 7, and 10 feet were used at each VES station. The VES surveys were used to indicate the range of apparent resistivity with depth and between respective VES stations. Preliminary review of VES data indicates minimal variation in apparent resistivity between stations.

The sites were believed by JPG personnel to be free from UXO and contained vegetation that is desirable for the planned use. Vegetation 4 inches or less in diameter was cut to a height of approximately 3 inches. The sites were divided into 100 foot by 100 foot grid cells in accordance with the Area Layout Plan. The grid corner on the northeast is the point of origin (A-1). Subsequent grids along the northern boundary of the site progress westward alphabetically. Grids along the eastern boundary progress to the south numerically. The site dimensions of the north (40 acre) site are 1,320 feet along the northern edge by 1,320 feet along the eastern edge (40.0 acres), and contains 3 permanent surveyor's monuments.

B.2 Survey Operations

The STOLS survey of JPG began on March 7, 1994 and ended March 16, 1994. The 40 acre grid was divided into rectangular sections (820 feet N-S, 200 feet E-W). It was decided to survey around the perimeter of each section and move inward instead of running STOLS in a N-S direction. The reason for this decision was because there was no way to turn STOLS around at the south perimeter due to the tree line. There did not appear to be any problem with moving STOLS in a circular (clockwise) direction around each rectangle.

At the beginning of the survey, two magnetometers gave failure indications. These two magnetometers were moved to the outside of the array so that overlapping survey tracks would compensate for the loss of data from these sensors.

Survey operations began in the southwest corner of the site, but were shifted to the northeast corner because of rough terrain. STOLS appeared to be operating reliably until grid

cell G1, where the background gamma increased dramatically, especially when traveling in the southward direction. Throughout the survey of the northwest corner, background gamma readings continued to be higher when moving southward than when moving northward. During the survey the welds holding the magnetometer array broke off, causing the cables to break away from the magnetometers. This occurred just prior to the onset of high gamma readings. However, this was not believed to be the cause of the high background gamma readings, since later demonstrators on this site also experienced high background readings in that area.

B.3 Survey Results

The actual target data produced by this survey have been omitted to prevent disclosure of emplaced target locations at the controlled test site. The survey results have been summarized in the body of the report.

APPENDIX C

DETECTION PROCESSING AND ASSESSMENT TECHNIQUES

C.1 Introduction

In this appendix, the specifics of the standard processing techniques used to assess the detection performance of the STOLS in sections 4 and 5 are presented in detail. In assessing the detection performance of any system, the characteristics of both the noise and the signal must be considered. This aspect is important in understanding the current level of performance as well as in recommending improvements to future systems in the areas of processing and system/sensor design. To this end, data from both surveys as well as models for the magnetic anomaly signatures will be analyzed to characterize the noise and signals as measured by the STOLS system. The approach of this assessment, the tools used in this assessment, and a brief tutorial on interpreting their respective outputs are presented in this appendix.

C.2 Methodology

The following approach was used to analyze STOLS sensor data and assess the system's detection capability:

a. Sensor data files were plotted to visually identify any files that appeared to contain anomalous or improbable data. Statistical means and variances were then computed.

b. Sensor data were analyzed to characterize noise components and identify possible noise sources.

c. STOLS system noise was compared to magnetic anomaly models for typical ordnance items to assess the system's detection capability.

C.2.1 **Statistical Means and Variance.** The noise of the STOLS sensor array was examined using the data from the MCAGCC and JPG surveys. Raster plots of the magnetometer readings (vs. time) were examined for inoperative sensors or any anomalous responses that might contaminate the analysis results. The mean and standard deviations of the noise were then produced for each sensor from each recorded data file. These statistics are tabulated in Section 4. Figure C-1 shows an example of a raster plot of the STOLS magnetometer data from a MCAGCC survey data file. In the figure, the magnetometer data from each sensor are plotted as a function of time. Prior to plotting, the mean for each sensor was removed. The mean and standard deviation of the noise from each sensor are listed to the right of each sensor plot.

C.2.2 **Noise Characterization.** The recorded data from the surveys, as well as observations from special tests during the field surveys, were examined to determine characteristics of the noise from the sensors and to identify possible sources of the noise. To accomplish this, the frequency content of the noise from each of the sensors was examined using plots of the PSD functions (i.e., noise power vs frequency). From these plots, the frequency extent of significant noise contributions can be identified as well as their possible sources. The extent to which these noise sources are coherent across the sensor array was then identified using spectral coherence plots. Finally, the underlying distributions of the noise were examined by producing PDFs and CDFs of the noise from each sensor. From these analyses, significant contributors to the magnetometer noise were identified, and techniques to reduce or eliminate them can be proposed.

C.2.2.1 **Power Spectral Density.** The PSD function is useful in determining the spectral content (power vs frequency) of a specific data series (reference 4). An example PSD from the MCAGCC is shown in figure C-2. In this figure, the PSD is seen to decrease as the frequency increases. This type of PSD is often referred to as a "red" spectrum since lower frequencies have higher energies. The small peak around 2 Hz is probably due to sensor motion in the earth's magnetic field. The spectrum continues to decrease until it reaches a floor at around 8 Hz. This floor is probably due to the internal sensor and electronic sensor noise. (A flat spectrum is referred to as a "white" spectrum.)

In this report, all PSD's were computed in the following manner. Sections of data 1024 points in length (approximately 51 seconds) were extracted from each of the magnetometer sensors. The local mean was removed from each of these segments, and a Hanning spectral window was applied to the data to reduce spectral leakage of strong spectral signals into adjacent frequency bands. Then, a Fast Fourier Transform (FFT) of the data was computed, and the squares of the complex amplitudes (normalized by the sampling frequency/1024) were plotted as a function of frequency (figure C-2).

C.2.2.2 **Spectral Coherence.** Spectral coherence quantifies the coherence of spectral energy in a particular frequency band between two time series. An example from the same data (sensors 2 and 3) plotted in figure C-2 is displayed in figure C-3. In this figure, the energy levels in the low frequencies (less than 0.5 Hz) are coherent (greater than 0.8). The energy within these bands is probably due to the large scale environmental magnetic fluctuations. The other peak in the coherence function around 2.0 Hz is due to the vertical motion of the magnetic sensors in the earth's magnetic field.

C.2.2.3 **Probability Density and Cumulative Distribution.** The PDF and CDF are useful in determining the statistical distribution (or distributions) contained in the data. The probability density function, p(x), at a value "x," times Δx is defined as the probability that a value randomly drawn from the distribution is within Δx of x. The cumulative distribution function CDF at a value x, F(x), is:

$$F(x) = \int_{-\infty}^{x} p(\tau)\, d\tau$$

The CDF at a particular value x represents the probability that any random value drawn from the distribution of x's will be less than or equal to x.

A sample PDF and CDF are displayed in the bottom and top panels of figure C-4, respectively. This data came from a single magnetometer during a portion of the MCAGCC survey. To compute these functions, the data were first sorted in ascending order to obtain the

x values. The CDF is then just the location of the value within the ordered series normalized by the total number of points. To compute the PDF, the CDF is differentiated with respect to x, since:

$$p(x) = dF(x)/dx.$$

In figure C-4, the distributions of the data are represented by solid lines. A Gaussian (or normal) distribution that was fit to the data is indicated by the dashed lines. The Gaussian distribution, which requires a mean and standard deviation, was fit to the magnetometer data in the following manner. The mean was assigned by selecting the value associated from the 50th percentile of the CDF. The standard deviation was determined from the slope of the CDF around the mean. Using standard probability axes, Gaussian distributions are indicated by straight lines in the CDF plots. In this figure, approximately 98 percent of the magnetometer data can be characterized by a Gaussian distribution in that it closely follows the dashed line from around 0.01 to 0.99. Results of the statistical and spectral analyses are presented in section 5.

C.2.3 **Detection Capability.** The expected magnetometer signals from the buried UXO were examined using a standard model for the induced magnetic field caused by a ferric object (buried UXO) placed in a magnetic field (earth's). From reference 7, the three-dimensional magnetic field seen by a magnetometer is the vector sum of the local earth's magnetic field and the induced magnetic field from a ferrous object, which can be represented by the standard magnetic dipole equation (reference 8):

$$\mathbf{B}_s = \mathbf{B}_e + \frac{\mu_0}{4\pi} \frac{3\mathbf{n}(\mathbf{n}\cdot\mathbf{m}) - \mathbf{m}}{|\mathbf{x}|^3}$$

where

$\mathbf{B}_s$ = the magnetic induction vector at the sensor

$\mathbf{B}_e$ = the earth's local magnetic induction vector

$\mathbf{x}$ = the distance vector from the object to the sensor

$\mathbf{n}$ = a unit vector in the direction of $\mathbf{x}$

$\mathbf{m}$ = the magnetic dipole strength vector of the object

μ_0 = the magnetic permeability constant

$= 4\pi \bullet 10^{-7}$ weber/amp-m

Assuming a local B_e = 60,000 gamma with an inclination of 70° from the vertical and a spherical object, the above equation provides a peak magnetic signal due to the anomaly B_p of:

$$B_p = \frac{m}{d^3} \text{ gamma}$$

where

m = 0.0403 [ferrous mass(in kg)]$^{1.2}$ (from references 9 and 10)

d = burial depth of object + sensor height above ground (in meters)

Using the above equation, the peak signal seen by the STOLS magnetometers can be estimated and then compared with the observed noise levels to assess the expected detection performance.

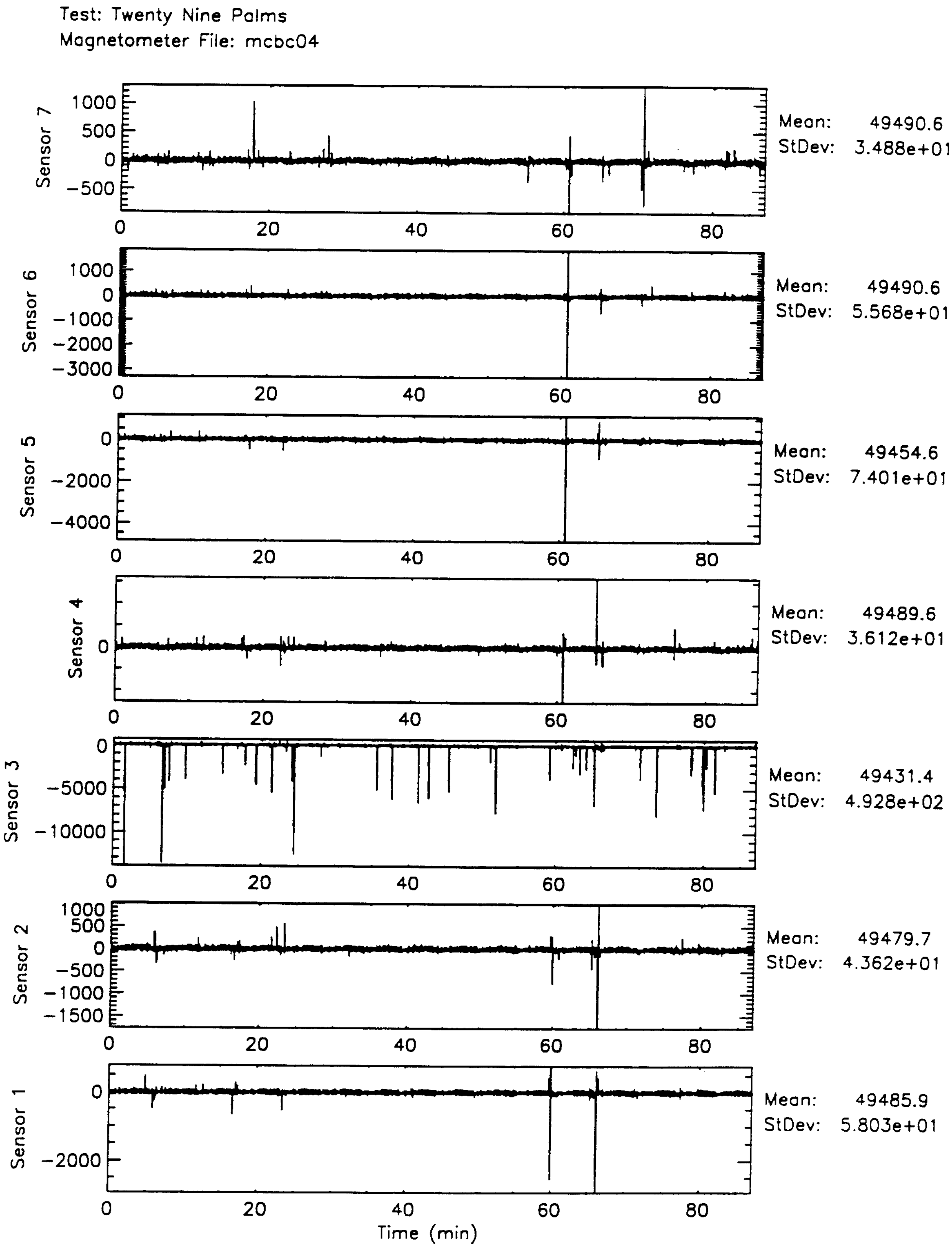

Figure C-1. Magnetometer Raster Plots (MCAGCC File 04)

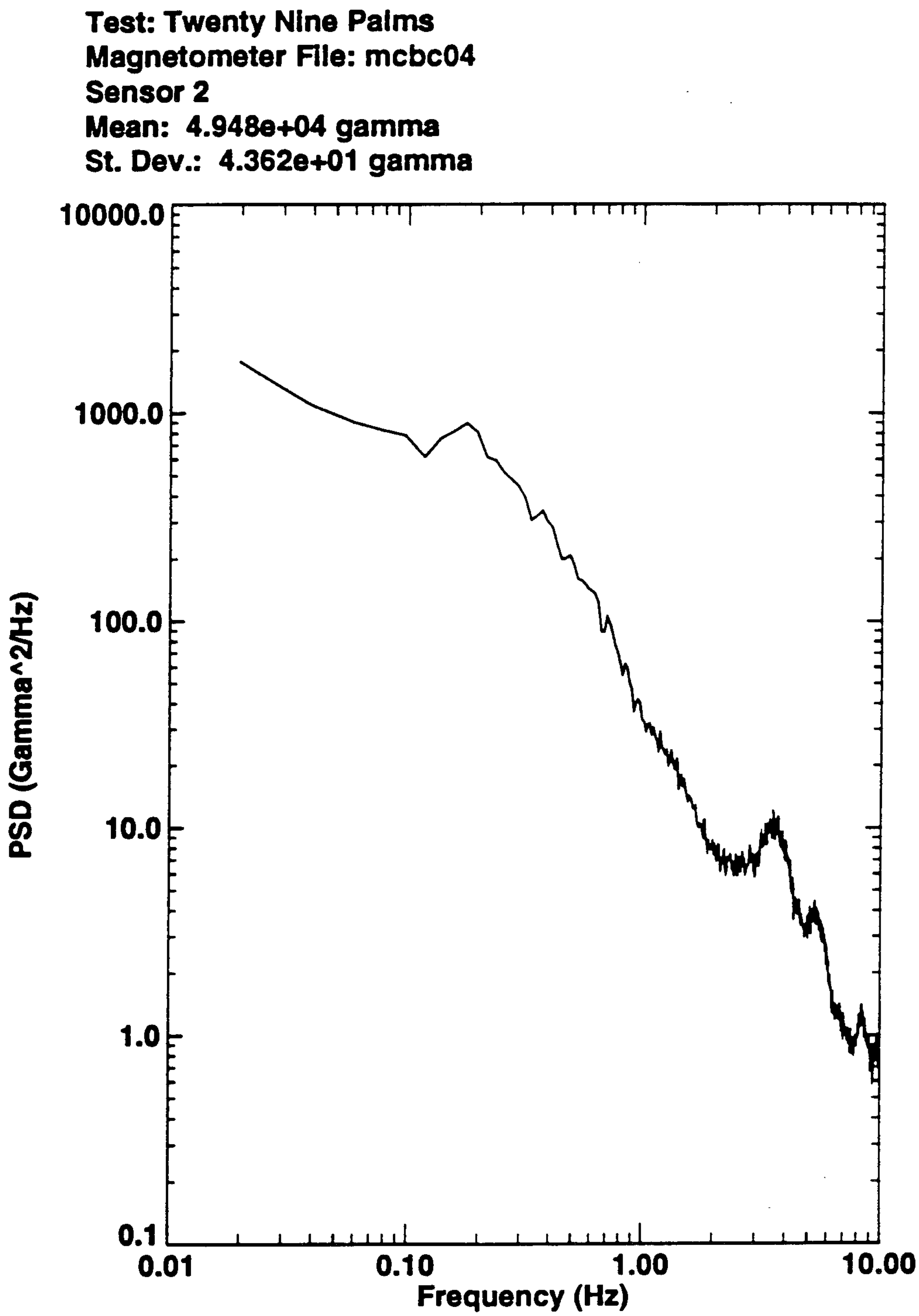

Figure C-2. Magnetometer Power Spectral Density, Sensor 2 (MCAGCC File 04)

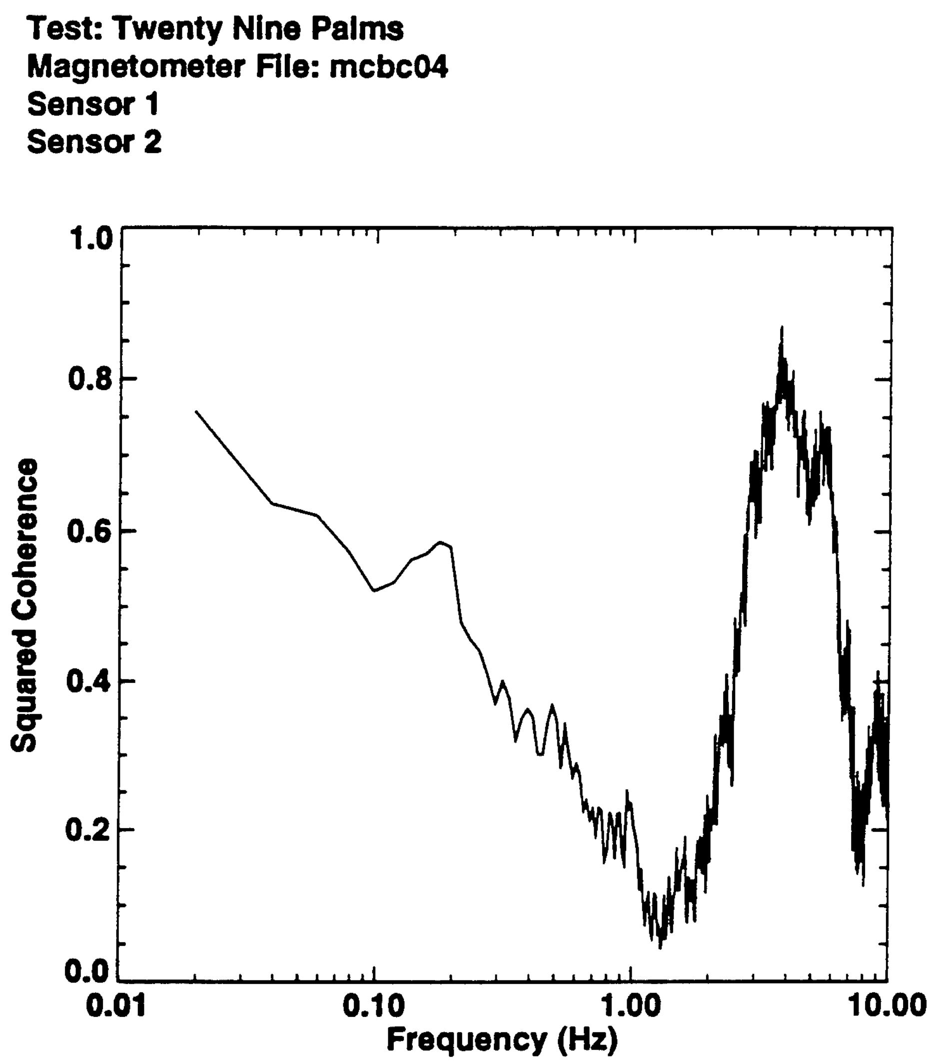

Figure C-3. Magnetometer Squared Coherence, Sensors 1 and 2 (MCAGCC File 04)

Test: Twenty Nine Palms
Magnetometer File: mcbc04
Sensor 2
Chi Square Statistic: 5.658e+01
K-S Statistic: 0.0276
Degrees of Freedom: 100203

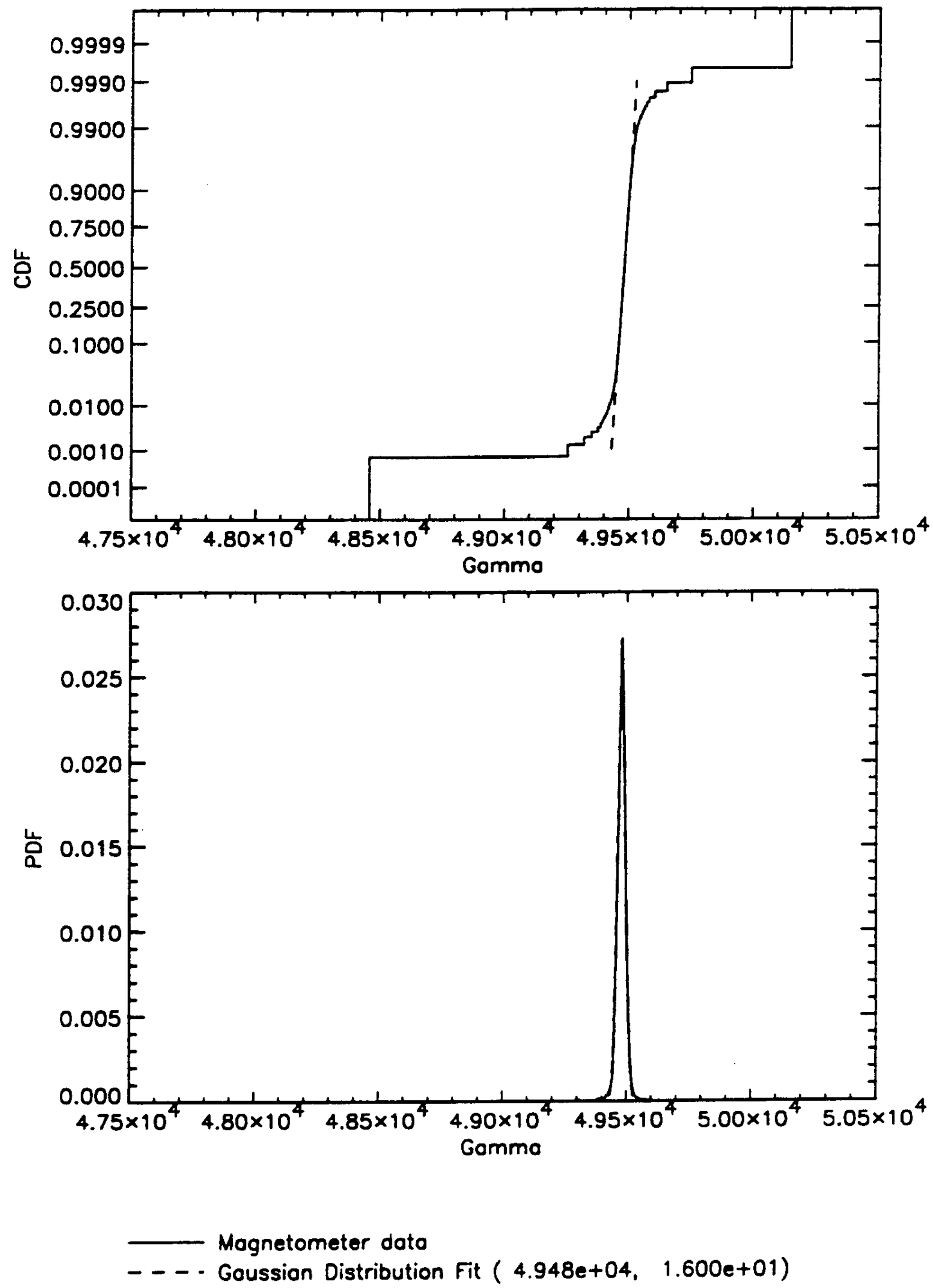

Figure C-4. Magnetometer PDF and CDF, Sensor 2 (MCAGCC File 04)